Laboratory Column Studies on Geochemical Transformation During Artificial Storage And Recovery

Wong Kong Chue

School of Civil & Environmenal Engineering

A thesis submitted to the Nanyang Technological University
in fulfilment of the requirement for the degree of
Master of Engineering

2006

ACKNOWLEDGEMENTS

I am indebted to my supervisor Associate Professor Shuy Eng Ban, School of Civil and Environmental Engineering, Nanyang Technological University, for his guidance and advice during the course of this study. I also appreciate his patience, help, and guidance throughout my research at the university.

I would like to extend my gratitude to Dr. Lloyd Chua Hock Chye, A/P Tan Soon Keat, A/P Edmond Lo, Assist Prof. Lim Teik Thye for their valuable advices and guidance.

I would like to thank the members of the Clean Water Programme's project group for their advice and help:

- Dr Mzila Ngodnizashe, Mr Yee Woon Kang, Mr Leong Chorng Min for their companionship and invaluable advice on research issues.
- Dr Lim Tok Hoon, Dr Chow San San , Miss. Tan Lai Heng, Miss Xie Shuang, Mr. Chen Yue Hua, Miss Hu Chengqi and Mrs. Ke Jin Xia for there their much appreciated support, encouragement and help throughout the research.

I also appreciate the help and support I received from the laboratory staff of the Environmental Laboratory especially Mrs. Phang-Tay Beng Choo, Mrs. Lim-Tay Chew Wang, Mr. Aw Wah Beng and Mr. Tan Han Khiang, for their assistance during this research.

TABLE OF CONTENTS

SUMMARY

Since the 1960s, extensive land reclamation works have taken place along the shallow coastal areas around Singapore. The reclaimed land is filled with granular material of high porosity with depths of 10 to 15m. This provides a potential for the sub-surface treatment, storage and recovery of advanced treated wastewater.

In this project, laboratory and field studies were carried out to investigate potential geochemical effects during artificial storage and recovery (ASR). A short term column study was carried out to quantify the response of the aquifer when the first pore volume of reverse osmosis (RO) effluent was passed through the column saturated with native groundwater. RO effluent was chosen due to its purity and aggressiveness, and hence would represent the worst case scenario in geochemical transformation. RO effluent would also cause minimal contamination to the groundwater system. Promising laboratory results prompted a similar field scaled study to be carried out at the Changi reclaimed land in order to verify the laboratory findings. The results show conclusively that carbonate dissolution and ion exchange reaction did take place during the recharge process.

Nevertheless, artificial recharge using RO effluent is not practical due to the high cost of RO treatment. As a result, feasibility studies using secondary effluent (SE) and ultra-filtered (UF) effluent were carried out in batch studies. Mineralogy studies were also carried out to complement the water quality studies. A better understanding of the mineral assemblage would provide an explanation to the existence of certain contaminants in the effluent. In addition, the mineral composition could be used as an input to the numeral solution in order to predict the aquifer response in the long run.

Another column study was also carried to investigate the long term aquifer response to artificial recharge. SE, UF and RO influents were recharged through a sand column separately over a period of 4 months each. An average of 400 exchanges of pore volume passed through the column and the extent of geochemical effect was assessed. The dominant geochemical effect was found to be carbonate dissolution. Ion exchange effect was not as significant as in the short term column and field experiments, as a "washing out" effect on major heavy metals was observed in the first 20 exchanges of pore volume. Therefore, column studies were inferior to batch studies in verifying the long term effect of leaching. However, column studies did provide useful information on the kinetics of geochemical transformation.

This study confirmed that geochemical effect was significant in artificial groundwater recharge. Long term carbonate dissolution could lead to collapse of the aquifer matrix and the consequences are severe. A possible solution will be to adjust the pH of the recharge water to higher than 8.0 as this will reduce the extent of carbonate dissolution.

LIST OF TABLES

LIST OF FIGURES

LIST OF ABBREVIATIONS

AEC	Anion Exchange Capacity
ALK	Alkalinity, also Carbonate Alkalinity
ASR	Aquifer Storage & Recovery
BS	British Standards
CEC	Cation Exchange Capacity
CMT	Continuous Multi-channeled Tubing
CPT	Cone Penetration Test
CWP	Clean Water Programme
DIC	Dissolved Inorganic Carbon
DO	Dissolved Oxygen
DOC	Dissolved Organic Carbon
EC	Electrical Conductivity, also Conductivity
EC	Electrical Conductivity
ESR	Exchangeable Sodium Ratio
FSW	Fully Screened Well
FULLPAT	Full Pattern Quantitative Analysis Program for XRD
GDP	Gross Domestic Product
IAP	Ion Activity Product
IC	Ion Chromatograph
ICP	Inductively Coupled Plasma
K_{so}	Solubility product, or Solubility constant
MCL	Maximum Contaminant Level
MF	Micro-Filtered Permeate/ Effluent
ML	Multi-level well
MSL	Mean Sea Level
NPOC	Non-Purgeable Organic Carbon
NTU	Nanyang Technological University
ORP	Oxidation Reduction Potential
pH	Negative log concentration of hydrogen ions
PUB	Public Utilities Board
PV	Pore Volume
RO	Reverse Osmosis Permeate / Effluent
SAR	Sodium Adsorption Ratio
SAT	Soil Aquifer Treatment
SE	Secondary Effluent
SEM	Scanning Electron Microscope
SI	Saturation Index
TDS	Total Dissolved Solids
TOC	Total Organic Carbon
TSS	Total Suspended Solids
UF	Ultra-filtered Effluent
USEPA	United States Environmental Protective Agency
UVA	Ultra-Violet Absorbance
WHO	World Health Organisation
XRD	X-Ray Diffraction

LIST OF SYMBOLS

ΔG°	standard free energy change (kJ / mol)
ΔH°	standard enthalpy change (kJ / mol)
γ	activity coefficient
α_1	ionization fraction for carbonic acid
α_2	ionization fraction for bicarbonate ion
α_3	ionization fraction for carbonate ion
ΔH_r°	change in enthalpy of formation (kJ / mol)
K_{θ}	equilibrium constant at particular temperature θ
P_{CO_2}	partial pressure of carbon dioxide (atm)
(aq)	subscript: in water solution
(g)	subscript: gas
μg	microgram
μm	micrometer (micron)
μS	micro Siemens
a	Activity (pure number)
A	wetting area (m^2)
atm	atmosphere
C_g	coefficient of gradation
cm	centimeter
C_u	uniformity coefficient
d_{50}	mean particle size with 50% passing through
g	gram
G_s	specific gravity (pure number)
h	head difference (m)
I	ionic strength
K	equilibrium constant
k	hydraulic conductivity (m/day)
L	liter
L	length (m)
M	moles/L
m^3	cubic meter
meq	milli-equivalent unit
mg	milligram
mgd	million gallon per day
m_i	concentration of component i (mol/L)
M_i	molar concentration (moles/L)
min	minutes
mm	millimeter
mS	milli Siemens
NTU	Nephelometric Turbidity Unit
°C	degree Celsius
ppb	part per billion
ppm	part per million
ppt	part per thosand
Q	flow rates (m^3/day)

R	universal gas-law constant ($J/(mol \cdot ^\circ C)$)
T	temperature, Kelvin (°C + 273.15)
W	weight (g)
X	percentage fraction
z	ionic charge (pure number)

1 INTRODUCTION

1.1 Background

The demand for potable water has always been a challenging problem all over the world, as a result of rapid growth in population and economic development. In Singapore's context, it has always been one of the most important national strategies to secure sufficient long term water resources in order to sustain growth. In 1948, the average daily water consumption was about 140,000 m^3, of which about 64,000 m^3 came from Johor. By 1958, this had increased to 270,000 m^3 per day. The daily demand exceeded one million m^3 by the late 1980s. The current demand is approaching 500 million m^3 per year (Mzila, 2003). Water demand will continue to rise, with a projected long term population of 5.5 million as well as with the economy continuing to expand with gross domestic product (GDP) growing by more than 7 % in year 2004. With the two water supply agreements with Malaysia expiring in 2011 and 2061 respectively, serious attention is required to address this problem. Continuous efforts have been made expand the surface impounding capacity of reservoirs, increasing surface runoff collection in new housing estates, recycling wastewater in the form of NEWater, desalinating seawater and carrying out research studies on new water resources or storage mechanisms.

1.2 Water sources

1.2.1 Background

The demand for drinking water in Singapore will continue to rise in the coming decades. Thus, there is a pressing need to search for new water resources to meet the nation's long-term needs. Both conventional and non-conventional sources of water have been exploited. One notable innovation is in wastewater reclamation, in which NEWater is produced. NEWater, together with natural precipitation, imported raw water and desalinated water, form the four national water taps of Singapore as shown in **Figure 1.1**. The two non-conventional sources, though accounting for less than 10% of

Singapore's current water demand, would gain prominence as the production cost is made more affordable due to advancement in membrane technology.

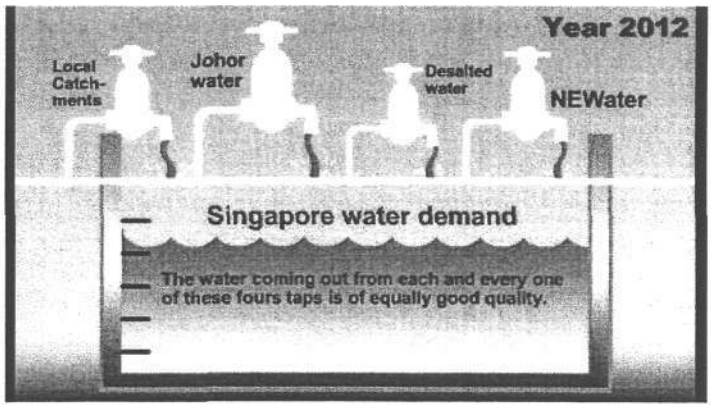

Figure 1.1 The Four national taps

1.2.2 NEWater

The NEWater project was initiated in 1998 as a joint initiative between the Public Utilities Board (PUB) and the Ministry of the Environment and Water Resources. NEWater is treated used water that has undergone stringent purification and treatment process using advanced dual-membrane treatment, i.e. ultra-filtrating (UF) and reverse osmosis (RO), and ultraviolet disinfection. The NEWater Factories at Bedok and Kranji Water Reclamation Plants were commissioned at the end of 2002 and had since supplied NEWater to wafer fabrication plants for non-potable use. The total capacity of the three existing NEWater factories, including the Seletar NEWater factory, which was commissioned in 2004, was 92,000 m3/day or 20 million gallons per day (mgd). At present, PUB had introduced 3 mgd of NEWater, which is about 1% of total daily water consumption, into the raw water reservoirs. The amount will be increased progressively to about 2.5% of total daily water consumption by 2011.

1.2.3 Desalinated water

Two pilot desalination plants will be completed by the year 2005. The two plants will supply a total of about 30 mgd of potable water. Desalination involves converting seawater, which is plentiful around Singapore, into drinking water. The cost of

desalination is higher than conventional water treatment, but it guarantees the future supply of water for Singapore's needs.

1.2.4 Groundwater

1.2.4.1 Background

Due to the geologic nature of Singapore, groundwater has never presented itself as a potential option for water supply in Singapore as there are no viable natural aquifers. In addition, groundwater pumping has been made illegitimate since 1890s to prevent groundwater contamination by poorly designed wells.

Due to scarcity of land area in Singapore, shallow coastal areas around the island have gradually been reclaimed since the 1960s. This has expanded Singapore's land area by about 1/6 of its original area. The two largest pieces of reclaimed lands are at Tuas located at the west coast, and at Changi along the east coast. As the reclaimed lands were filled with medium to coarse sand of high porosity, man-made aquifers with fill depths up to 15m or more were un-intentionally created. They provide a potential for sub-surface storage and recovery of water. With abundance of high quality treated wastewater currently being discharged into the sea, it is possible to use the reclaimed land as an underground storage reservoir by recharging the reclaimed wastewater into the ground. In addition, naturally occurring microorganisms in the sandy aquifer could provide further treatment for the recharged tertiary treated effluent. This treatment process is generally referred to as soil aquifer treatment or SAT.

1.3 Groundwater Quality

The original water in the ground after completion of reclamation is residual seawater and hence brackish. However, with an average yearly rainfall of 2,400 mm, the original seawater has been replaced by the natural rainwater over the years, and the background salinity value has since dropped to around 0.5 ppt compared with the value for seawater of 25-30 ppt. Nonetheless, there is still an underlying layer of saline water

of 18-20ppt salinity, probably trapped by the uneven original sea bed topography. This layer will take a longer time to be flushed out by the rain water.

In order to better understand the quality of the existing groundwater, an extensive network of water sampling points were established, from which water samples were collected from continuous multi-channelled tubings (CMT), Multi-level sampling tubes, piezometers and fully screened wells. Typical results obtained from Corner 2 (as shown in Figure 1.4) of the Nanyang Technological University's (NTU) test plot are presented in **Table 1.1**. Many of the parameters met the drinking water standards laid down by the US Environmental Protective Agency (USEPA) and the World Health Organisation (WHO) with the exception of arsenic. There is an increasing awareness towards arsenic concentration in drinking water as it has been linked circulatory system problems and increased the risk of getting cancer. As a results, the maximum contaminant level (MCL) for arsenic has been revised downwards to 0.01 mg/L.

Table 1.1 Comparison of existing groundwater quality against USEPA and WHO drinking water standards

Parameters	***Units***	***Groundwater @ Corner 2 (15^{th} Sept 2004)***	***USEPA Drinking Water Standards***	***WHO Drinking Water Standards***
pH		8.21	6.5-8.5	-[1]
Electrical Conductivity	mS/cm	2.073	-	-[1]
Sodium	mg/L	246.54	-	200
Potassium	mg/L	39.26	-	-[1]
Calcium	mg/L	33.09	-	-[1]
Magnesium	mg/L	54.64	-	150
Chloride	mg/L	304.50	-	250[1]
Sulphate	mg/L	257.59	250	250[1]
Nitrate	mg/L-N	0.644	-	50
Dissolved Inorganic	mg/L-C	75.42	-	-[1]

Carbon (DIC)				
DOC	mg-C/L	3.894	-	-
Iron	mg/L	0.026	0.3	0.3
Aluminium	mg/L	0.256	0.05-0.2	0.2
Copper	mg/L	0.015	1.3	2
Zinc	mg/L	0.006	5	3
Arsenic	mg/L	0.035	0.01[2]	0.01(P)[3]
Lead	mg/L	n.d.[4]	0.015	0.01
Manganese	mg/L	0.124	0.05	0.5

[1]Not of health concern at levels found in drinking-water

[2]With Effect on 23rd January 2006

[3]Provisional guideline value, as there is evidence of a hazard, but the available information on health effects is limited

[4] Not Detectable

1.4 Changi Reclaimed Land

The Changi reclamation project involved the reclamation of more than 2,000 hectares of land, carried out in four phases over a period of seven years. **Figure 1.2.** shows the location of the site. The fill material consisted of sand dredged from the seabed, from two offshore islands near Singapore (Tan *et al.*, 2004). A photo taken at the reclamation site is shown in **Figure 1.3**. The reclaimed land was filled to +3.77 m above the mean sea level (MSL) and the groundwater table is typically 0.8 – 2.0m below the ground surface, varying with the antecedent natural precipitation. The total volume of sand fill is estimated at approximately 206 million m^3. Assuming an average porosity value of 0.35, the potential saturation storage capacity of the Changi reclaimed land is in excess of 70 million m^3. This is higher than the largest impounding reservoir in Singapore, which has a capacity of 34 million m^3 (Mzila, 2003).

A preliminary study had been carried out in 1998 to examine the feasibility of developing the Changi reclaimed land into an aquifer for storage and recovery. Preliminary findings were positive which lead to the implementation of the Clean Water Programme (CWP). The CWP was to conduct detailed studies on the

groundwater hydraulic and geochemical characteristics of the artificial aquifer through oth field and laboratory experiments.

Figure 1.2 Singapore map showing the location of Changi reclaimed land

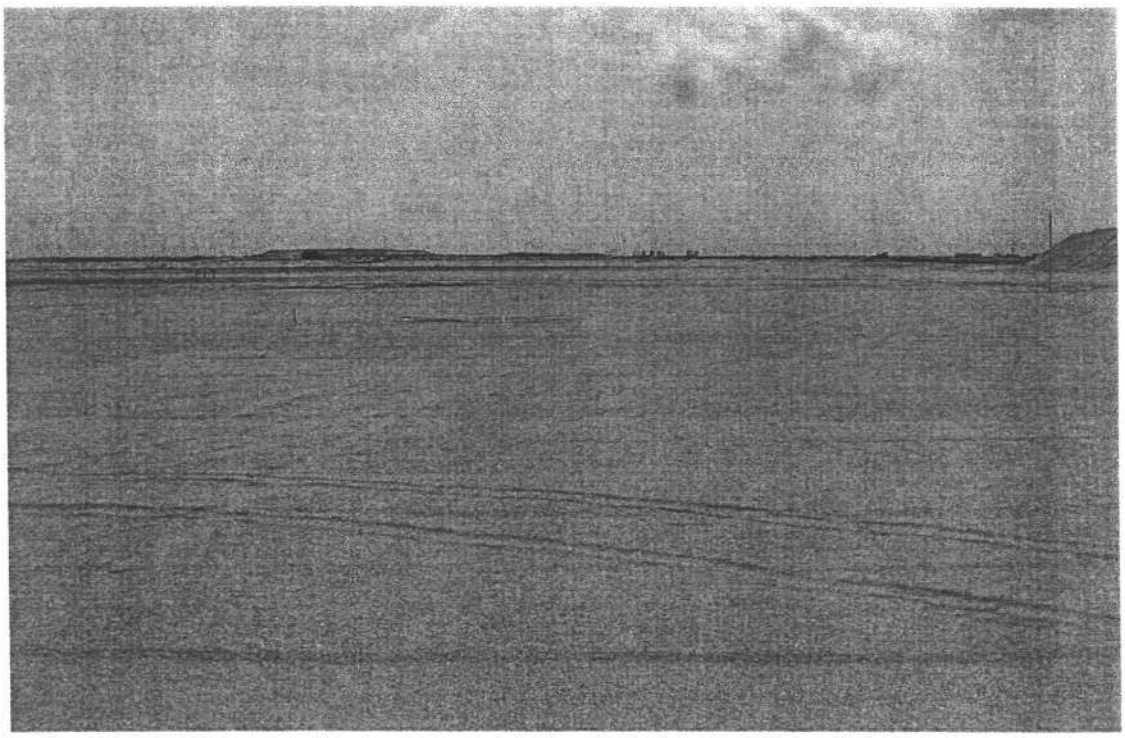

Figure 1.3 Photo of Changi reclaimed land

1.5 Objectives of Study

The primary objective of this study is to quantify the geochemical characteristics during artificial recharge using the different types of influent water through batch, column and field tests. The specific objectives include:

- To quantify the physical and chemical characteristics of the sand media;
- To determine the quality of existing groundwater, rain water and various potential recharge waters;
- To investigate the short term and long term geochemical effects during aquifer storage and recovery (ASR);
- To examine the effect of adsorption/desorption of heavy metal;
- To examine the extent of clogging and "wash-out" phenomenon during long term artificial recharge;
- To verify the potential of soil aquifer treatment (SAT) under a short retention time;

1.6 Scope of Study

This thesis presents the results of a three pronged approach to quantify the effects of geochemical transformation in a sandy aquifer. Firstly, the geochemical effects in a one dimensional sand-filled column during recharge of reverse osmosis (RO) water were investigated. Secondly, two related studies were carried out in the field to verify the results obtained from the laboratory column studies. RO effluent was chosen as the recharge water in these tests as it was the most aggressive among other possible feed waters; so as to represent the worst potential geochemistry effects. Finally, more laboratory columns were set up to investigate the medium to long term effects, i.e. >400 pore volumes (PV) (8 hours per PV, in which 400PV is equivalent to 33 years of continuous recharge on a field scale), on geochemical transformations using different types of recharge water. In this study, secondary effluent (SE), ultra-filtered (UF) and reverse osmosis (RO) water were allowed to pass through the column for more than 400 PVs. These allow the geochemical effects during recharge of different types of influents to be investigated.

1.7 Organisation

This thesis is organised into five chapters. **Chapter 1** gives an overview of the motivation for the study, and outlines the scope of the study. **Chapter 2** gives a brief introduction on geochemistry and reviews previous experiences by other researchers in the field of tracer studies, column studies and geochemical transformation. In addition, some previous studies on the Changi reclaimed land are also presented. In **Chapter 3**, the equipments and methodologies used in this study are discussed in depth. **Chapter 4** presents and discusses the results obtained. **Chapter 5** concludes the findings and discusses the potential future developments in this area of study.

2 LITERATURE REVIEW

2.1 Introduction

Since the 1960s, extensive land reclamation works have taken place along the shallow coastal areas around Singapore. This has increased the total land area of Singapore by about 1/6. The reclaimed land is filled with granular material of high porosity with depths of 10 to 15m. This presents a potential for the sub-surface treatment, storage and recovery of advanced treated wastewater. In this chapter, the author reviews some basic knowledge on geochemistry that is essential for the present research. A three pronged approach will be adopted to study the minerals and the solution individually, as well as the reactions that could take place when the two come into contact. In the later part of this chapter, previous experiences by other researcher on laboratory column studies and field scale recharge tests on geochemical transformations.

2.2 Fundamental Chemistry

2.2.1 Equilibrium Constant

In geochemistry studies, equilibrium constant is an important parameter in the understanding of the processes responsible for the formation of minerals and mineral assemblages. It provides a background in solving problems related to weathering, sedimentation, diagenesis, metamorphism and hydrothermal and magmatic processes. Equilibrium constant is highly dependent on variations in temperature and pressure. As a result, the composition of minerals and solution changes as the equilibria shifts in tandem with a change in pressure-temperature conditions (Krauskopf, 1995). For a chemical reaction of the form:

$$aA + bB \Leftrightarrow xX + yY$$

where a, b, x, y= molar constant

A, B= reactants

X, Y= products

The equilibrium constant, K, can be written as in **Equation 2.1**.

$$K = \frac{[X]^x[Y]^y}{[A]^a[B]^b} \quad (2.1)$$

where K= equilibrium constant

[X, ... etc]= activity of the respective chemical

It is difficult to obtain a good estimation of K in view of the difficulty in determining the equilibrium point. As a result, an exact formulation of the equilibrium constant based on thermodynamic principles is used instead. The values could be obtained from **Equation 2.2.**

$$\log K = \frac{-\Delta G^o}{2.303RT} \quad (2.2)$$

where ΔG^o = Standard free Gibbs energy

R= reaction constant

T= temperature in Kevin's scale.

2.2.2 Temperature Compensation

The equilibrium constant, which could govern the values for pH and partitioning of carbonate minerals, etc, can vary even over a small range of temperature. As a result, it is necessary to adjust data collected at different temperatures to a standardised temperature, either 20°C or 25°C, for analytical purposes. The equilibrium constant can be corrected using the Van't Hoff's equation as shown in **Equation 2.3.**

$$\log_{10} K_\theta = \log_{10} K_{25} - \frac{\Delta H_r^0}{2.303R}\left(\frac{1}{T_1} - \frac{1}{T_2}\right) \quad (2.3)$$

where K_θ= equilibrium constant at the desired temperature (Kevin's scale)

ΔH_r^0= enthalpy of formation

The enthalpy of formation in **Equation 2.3** could be computed using **Equation 2.4**, with published values available from the literature.

$$\Delta H_r^0 = \sum \Delta H^0_{products} + \sum \Delta H^0_{reactants} \quad (2.4)$$

2.2.3 Ionic Strength

Ionic strength provides a simple indication of the amount of ions present in a solution. It differs from the sum of molar concentration in a complex solution by emphasising the effect of higher charges of multivalent ions. Ionic strength could be computed as shown in **Equation 2.5**.

$$I = \frac{1}{2}\sum m_i z_i^2 \qquad (2.5)$$

where I= ionic strength

m_i= molar concentration in moles/L

z_i=charge of the ions

2.2.4 Activity

Water molecules tend to neutralise atoms that dissolve into solutions to form ions. However, some residual forces of attraction will remain, and prevent the ions from acting as completely independent particles in solution. These residual forces are known to be a function of the concentration of the solute. The more dilute the solution, the lesser the residual forces and the solutes behave like they are completely ionised. In a more concentrated solution, the inter-ionic spaces are smaller, and there existed higher residual forces which prevent the complete ionisation of the ions. In this situation, there is a difference in the true concentration of solute determined from an analysis and an apparent concentration, in which the apparent concentration is known as the activity of the solute. The relationship is as shown in **Equation 2.6**.

$$\gamma_i = \frac{a_i}{M_i} \qquad (2.6)$$

where γ_i= activity coefficient

a_i= activity

M_i= molar concentration

The activity coefficient is also related to the ionic strength in the Davies' equation as shown in **Equation 2.7**.

$$\log_{10}\gamma = -Az^2\left(\frac{\sqrt{I}}{1+\sqrt{I}} - 0.2I\right) \qquad (2.7)$$

where A= function of temperature and dielectric constant of the solvent
approximately 0.51 in water at 25 °C

Therefore, using the concentration of the ions found from laboratory analysis, the activity coefficient and the activity can be derived (Evangelon, 1998).

2.2.5 Carbonate Equilibrium

Inorganic carbon that dissolved in fresh water and sea water has its origin in minerals and the atmosphere. Carbon dioxide from the atmosphere provides an acid that reacts with the bases in the rocks. The water may also lose dissolved carbon to the sediments by precipitation reactions. Dissolved carbonate species participate in homogeneous and heterogeneous acid-base and exchange reactions with the lithosphere and atmosphere. Such reactions are significant in regulating the pH and the composition of natural waters.

The distribution of $CO_2, H_2CO_3, HCO_3^-, CO_3^{2-}$ is highly dependent on pH and the amount present will affect the buffer intensity of the water. By considering a simple aqueous carbonate solution, the nature of the equilibrium concentration of the six solute components ($CO_2, H_2CO_3, HCO_3^-, CO_3^{2-}, H^+$ and OH^-) can be described by a system of six chemical reactions. The appropriate set of equations comprises four equilibrium relationships:

$$H_2CO_3 \Leftrightarrow CO_{2(aq)} + H_2O$$
$$H_2CO_3^* \Leftrightarrow H^+ + HCO_3^-$$
$$HCO_3^- \Leftrightarrow CO_3^{2-} + H^+$$
$$H_2O \Leftrightarrow H^+ + OH^-$$
Where $[H_2CO_3^*] = [CO_{2(aq)}] + [H_2CO_3]$

And two other equations describing a concentration and an electro-neutrality or proton condition:

$$CaCO_3 + CO_{2(aq)} + H_2O \Leftrightarrow Ca^{2+} + 2HCO_3^-$$
$$CaCO_3 \Leftrightarrow Ca^{2+} + CO_3^{2-}$$

These equations provide the important equilibrium constants for further computation, as shown in **Equation 2.8-2.11**:

Hydration constant for CO_2, $K_H = \frac{[CO_{2(aq)}]}{[H_2CO_3]}$ **(2.8)**

First acidity constant, $K_1 = \frac{[H^+][HCO_3^-]}{[H_2CO_3^*]}$ **(2.9)**

Second acidity constant, $K_2 = \frac{[H^+][CO_3^{2-}]}{[HCO_3^-]}$ **(2.10)**

Ion product of water, $K_W = [H^+][OH^-]$ **(2.11)**

With total inorganic carbon, C_T, analysed using the TOC analyser, represented as in **Equation 2.12**:

$$C_T = [H_2CO_3^*] + [HCO_3^-] + [CO_3^{2-}] \quad \textbf{(2.12)}$$

it is possible to fractionise each of these three components into the following relationship (**Equation 2.13-2.15**):

$$[H_2CO_3^*] = C_T\alpha_0 \quad \textbf{(2.13)}$$

$$[HCO_3^-] = C_T\alpha_1 \quad \textbf{(2.14)}$$

$$[CO_3^{2-}] = C_T\alpha_2 \quad \textbf{(2.15)}$$

By rearranging the equations, the individual ionisation fractions can be obtained as follows:

$$\alpha_0 = \left(1 + \frac{K_1}{[H^+]} + \frac{K_1K_2}{[H^+]^2}\right)^{-1} \quad \textbf{(2.16)}$$

$$\alpha_1 = \left(\frac{[H^+]}{K_1} + 1 + \frac{K_2}{[H^+]}\right)^{-1} \quad \textbf{(2.17)}$$

$$\alpha_2 = \left(\frac{[H^+]^2}{K_1 K_2} + \frac{[H^+]}{K_2} + 1 \right)^{-1} \qquad (2.18)$$

where $\alpha_0 + \alpha_1 + \alpha_2 = 1$

$\alpha_0, \alpha_1, \alpha_2$ = ionisation fraction

The percentages of the activities of the un-dissociated carbonic acid and the hydrogen carbonate and carbonate species can be plotted against pH as shown in **Figure 2.1**. The diagram indicates that over the usual pH range of groundwater (6-8), CO_2 occurs mainly as hydrogen carbonate ions and un-dissociated carbonic acid; while in the acid range (<pH 6), un-dissociated carbonate species (H_2CO_3); and in the alkaline range (>pH 10), carbonate ions are dominant (Hem, 1970).

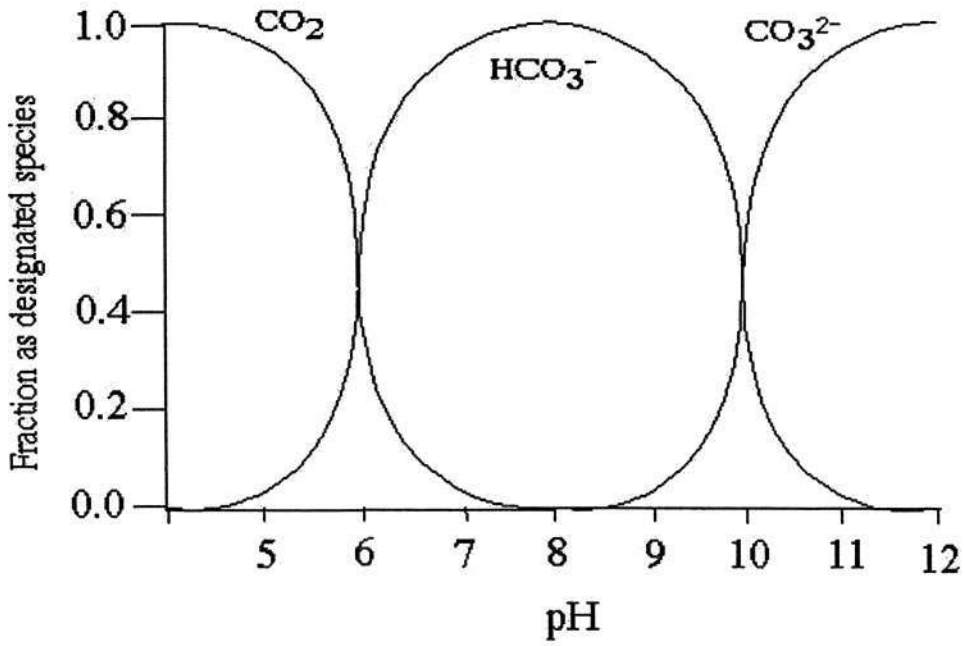

Figure 2.1 Ionisation fractions of carbonate species against pH

2.3 Geochemistry

2.3.1 Background

Groundwater chemistry is a dynamic system for which a single determination is not necessarily representative of the conditions prevailing over a period of time. Apart from variations of groundwater quality in the time domain, large variations could be observed over a short distance within the same aquifer (Barcelona *et al.*, 1989; Bjerg and Christensen, 1992; Mathess, 1982; Ronen *et al.*, 1987; Schulmeister *et al.*, 2004).

The two fundamental information required to analyse groundwater are to understand the reaction that take place among minerals and groundwater, as well as the speed of these reactions. Hence chemical equilibrium and kinetics are very important in this study (Evangelon, 1998). Due to the reactivity of groundwater, e.g. carbonate equilibrium which takes place swiftly, the only way to extract geochemical information from the aquifer is by collecting a representative and unavoidably, a substantial amount of samples (Farnharm et al., 2003). As a result, sampling scheme has to be designed carefully for geochemistry studies. In addition, parameters such as temperature, pH, redox potential (ORP), dissolved gases, major cations/anions, trace elements, and organic compounds are needed to characterise the quality of groundwater. Solids may be reactive such that they dissolve or precipitate in the aquifer; or they may participate in ion exchange; or adsorption/desorption reactions, resulting in a change in water quality (Deutsch, 1997). In this section, works that had been done by other researchers would be reviewed with the aim to establish a list of concerned parameters that would portray a complete picture on geochemistry. A summary of parameters of interest, analytical methods and equipment is tabulated in **Table 2.1**.

2.3.2 Temperature

Geochemical properties such as gas and mineral solubility are temperature dependent; an accurate measurement of aquifer temperature is hence necessary to interpret the chemical data in terms of interactions between the water, gaseous and solid phases.

Temperature should be measured on site if not in situ, so as to minimize contact with the atmosphere (Deutsch, 1997).

Table 2.1 Methodologies and equipments for water characterisation tests

Characterization Test	*Method Used*	*Instruments Used*
Turbidity	2130A Nephelometric Method	Hach portable turbidity meter
Colour	2120C Spectrophotometric Method	Shimadzu UV-1201V UV Spectrophotometer
Total Suspended Solids (TSS)	2540D TSS	-
Total Dissolved Solids (TDS)	2540C TDS	-
Total Alkalinity (ALK)	8203 Phenolphthalein and Total Method	HACH digital titrator
Temperature, pH, Conductivity	2510 Conductivity, 2520B Electrical Conductivity Method, 4500-H+ pH VA	Thermo-Orion multi-parameter meter
Dissolved Oxygen (DO)	4500-O G. Membrane Electrode Method	Thermo Orion DO meter
Oxidation Reduction Potential (ORP)	2580BORP	Horiba pH/ion meter with platinum ORP probe
Total Organic Carbon (TOC) Analyzer - Non-Purgable Organic Carbon (NPOC) - Dissolved Inorganic Carbon (DIC)	5310 B High-Temperature Combustion Method	Shimadzu TOC-V_{CSH} TOC-analyzer with Shimadzu ASI-V auto-sampler
Inductively Coupled Plasma (ICP) Spectroscopy - Cations: Na^+, K^+, Ca^{2+}, Mg^{2+} - Trace heavy metals	3120 B ICP Method	Perkin Elmer - Optical Emission Spectrometer Optima 2000DV
Ultra Violet Absorbance (UVA) at 254 nm	-	Shimadzu 1601 - UV/VIS spectrophotometer (path length 1cm)

2.3.3 pH

An accurate measurement of groundwater pH is essential because many of the solution processes, water and rock interactions, gas solubility, and biochemical reactions are pH sensitive. The activity of hydrogen is measured by pH of the water, defined as in **Equation 2.19.**

$$pH = -\log_{10}[a_{H^+}] \qquad (2.19)$$

where $[a_{H^+}]$ = activity of hydronium ion

A variation in the water pH may have a major effect on the solubility of minerals. Metal hydroxide minerals are usually less soluble at higher pH values and may also precipitate in the same sample bottle if they become over saturated, hence samples are usually acidified to pH of 2 for preservation, so that metals would not precipitate from the solution and would be available for measurement by the solution analytical technique. In addition, partial pressure of CO_2 and oxidation-reduction can also be affected by the pH of the water (Deutsch, 1997).

2.3.4 Electrical Conductivity (EC)

Specific conductance is a measure of the sample's ability to conduct electricity and it provides a measure of the total quantity of ions in the solution corrected to 25 °C. The measurement is approximate because the specific conductance of a fluid with a given total dissolved solids (TDS) content varies depending on the ions present (Deutsch 1997). For an estimate in TDS, it was sufficient to multiply the specific conductance of the water by 0.65 (Mathess, 1982). Nonetheless, a better estimation can be obtained easily by measuring the density of the targeted water sample.

2.3.5 Dissolved Oxygen (DO)

In geochemistry analysis, dissolved oxygen is the only gas being routinely measured. The oxygen content of the water is important because of its impact on oxidation-reduction reactions, and its use as a qualitative indicator of the redox potential. Water in contact with an atmospheric oxygen concentration will have a DO concentration that varies from 4.7 to 7.0 mg/L over the temperature of 0 to 35°C (Deutsch, 1997). It is necessary that the oxygen content of groundwater samples be measured with minimal contact with air. Therefore, in line DO measurement is necessary. This leads to the development of some sophisticated on-line DO instruments or to a lesser extent, a fabricated flow through cell.

2.3.6 Oxidation-Reduction Potential (ORP)

ORP can be defined as a redox reaction and involves a transfer of electrons from one element to another, hence changing the valence or oxidation number of the elements.

Oxidation refers to the removal of electrons from an atom, forcing a change in the oxidation number of an element. Reduction is the addition of an electron to lower the oxidation number. Redox reactions transfer electrons from a reductant (electron donor) to an oxidant (electron acceptor), resulting in no free electrons. A high positive potential will favour the more oxidizing valence state of an element, while a lower potential will favour the more reduced valence state.

Redox influences the mobility of metal ions in solution, the concentration of the metal found in the metal ion state (mobility), or in the precipitate state (immobility), and the toxicity of certain elements is dependent on the redox state. With a more complex system, pH could be affected as well because the hydrogen ion is part of the oxidation-reduction reaction (Deutsch, 1997).

A redox condition in groundwater is controlled by oxygen-consuming reactions, involving a breakdown of organic substances and the oxidation of reduced substances. Oxygen consumption begins with the presence of organic and inorganic compounds. Incomplete decay leads to enrichment in organic material below the surface. With increasing oxygen deficiency, decay products would accumulate in the subsurface (Schoeller, 1962, Hartog et al., 2004).

2.3.7 Alkalinity/Acidity

Alkalinity is the measure of the total acid-neutralizing capacity of the water, and is determined by titration with sulphuric acid to an end-point of about pH 4.5. Alkalinity and acidity represent the cumulative reactions that consume hydrogen as acid is added to the solution, or that released hydrogen as a base is added to the solution respectively. Alkalinity is expressed in mg/L of $CaCO_3$ and is more commonly determined for groundwater since most of the alkalinity in groundwater is due to the amount of inorganic carbon ions present in the solution. In addition, its measurement could be used to determine the bicarbonate and carbonate concentration of the groundwater (Deutsch, 1997). However, the accuracy and effectiveness of analysing alkalinity depend on how fast the analysis could be carried out as well as the amount of samples

required for analysis. It is usually carried out on site (Cronin et al., 2005) and requires a sample of 500 ml for triplicate analysis for the range of 20-100 mg/L of $CaCO_3$ (Chae et al., 2004). As a result, dissolved inorganic carbon (DIC) is usually analysed instead of alkalinity. DIC and alkalinity are interrelated and can be converted using **Equation 2.20**.

$$[DIC] = \frac{\{[Alkalinity] + [OH^-] - [H^+]\}}{\alpha_1 + 2\alpha_2} \qquad \textbf{(2.20)}$$

where $\alpha 1$, $\alpha 2$: as ionisation fraction

2.3.8 Major Cations and Anions

2.3.8.1 Background

These ions are primary contributors to ionic strength, which reflect the effective concentrations of all dissolved species. The major ions form strong solution complexes with each other and with the trace elements, thereby affecting their mobility and reactivity. These major cations and anions concentrations would facilitate the computation of ion balance which act as a fundamental check for accuracy in geochemistry analysis.

2.3.8.2 Calcium and Magnesium

Calcium and Magnesium originate from soils and rocks that contain limestone, dolomite, and gypsum (Heath, 1983). Rocks with equivalent ratio Ca/Mg closed to unity are classified as dolomites.

Calcium originates either as cyclic salt from seawater or from the dust of calcareous rocks and industrial emissions. In the presence of higher CO_2 content in the ground air, more $CaCO_3$ could be dissolved. In groundwater, it is expected that with sufficient residence time in the subsurface, the calcium carbonate-carbon dioxide equilibrium could be established. However, Back (1963) had discovered otherwise in Eocene limestone, Florida, despite years of contact.

Magnesium occurs as a constituent of salt deposits of marine origin. The solubility of magnesium carbonate is much harder to determine than that of calcium carbonate. However, the solubility of magnesium carbonate in pure water and in the presence of CO_2 is greater than that of Calcium Carbonate (Mathess, 1982).

2.3.8.3 Sodium

Sodium originates from seawater through primarily sea spray, or original sea water that is trapped during reclamation. It is common to find high concentrations of sodium ion, >200 mg/L, in groundwater. Excessive sodium content can cause swelling of clayey material.

2.3.8.4 Sulphate and Chloride

Sulphate originates from gypsum, pyrite and other rocks containing sulphur compounds. Chloride originates from inland areas, primarily from seawater trapped in sediments at time of deposition, and they are not retained in permeable rocks (Heath, 1983). Considerable amounts of Sulphate are also added to the hydrologic cycle with the precipitation from the atmosphere primarily from dried sea spray as a cyclic salt (Mathess, 1982).

2.3.8.5 Carbonate Speciation

Carbonate, or inorganic carbon, appears in numerous speciation with respected to pH. It can be in any of the following complexation, e.g. H_2CO_3, HCO_3^-, CO_3^{2-}, $CO_{2(aq)}$, $CaCO_3^0$ or $CaHCO_3^+$ in the case of calcite equilibria (Krauskopf, 1995).

The total CO_2 content in water is usually subdivided into free and bound CO_2. Free bound CO_2 comprises dissolved carbon dioxide and the undissociated H_2CO_3. Bound CO_2 includes the hydrogen carbonate and carbonate ions. Free carbon dioxide is produced by anaerobic or aerobic oxidation of organic substances.

Hem (1970) plotted the percentages of the activities of the undissociated carbonic acid and the hydrogen carbonate and carbonate species against pH. The diagram indicated that over the usual pH range of groundwater (6-8), CO_2 occurred mainly as hydrogen carbonate ions and un-dissociated carbonic acid. In the acid range (<pH 6), undissociated carbonate species, and in the alkaline range (>pH 10) carbonate ions were dominant (**Figure 2.1**).

In the unsaturated zone, the partial pressure of CO_2 gas is increased by factors of 100 or more compared with atmospheric air values as a result of the oxidation of organic matter. This reaction reduces organic matter and oxygen. It also raises the carbon dioxide gas level. As the soil vapour partial pressure of CO_2 increases, the total amount of dissolved inorganic carbon (DIC) also increased to maintain equilibrium between the gas and solution phases (Kehew, 2001). Since DIC is a function of both pH and partial pressure of CO_2, a relationship could be used to calculate the P_{CO_2} in equilibrium with groundwater using in-field measured values for pH and alkalinity. The relationship is shown in **Equation 2.21**.

$$P_{CO_2}(atm) = \frac{\left(\gamma_{CO_3^{2-}}\right)\left(10^{-pH}\right)^2 Alkalinity(mg/L CaCO_3)}{10^{-18.2}\left(2+\frac{10^{-pH}}{10^{-10.3}}\right)\left(5\times10^4\right)} \quad (2.21)$$

where P_{CO_2} = partial pressure of carbon dioxide

$\gamma_{CO_3^{2-}}$ = activity coefficient of CO_3^{2-}

2.3.8.6 Manganese

In a case study at Chesapeake, Virginia, geochemical assessment had discovered the presence of manganese bearing minerals in the storage zone. Recharge water with a pH below 8.0 had mobilised the manganese so that after a few weeks of storage, recovered water had unacceptably high manganese concentration. In order to remediate this problem, pH of the recharge water was adjusted to about 8.4 for several months. As a result, the manganese concentration during recovery was less than 0.01 mg/L (David

and Pyne, 2000). Therefore, the move to restrict the mobility of heavy metals had shown it potential in the prevention of groundwater contamination by heavy metals.

2.3.8.7 Arsenic

Much attention has been directed to the public health significance of arsenic in drinking water in recent years. USEPA has reduced drinking water standards for arsenic with effect from 23rd January 2006. However, not much work has been done regarding arsenic removal during ASR (David and Pyne, 2000).

2.3.8.8 Other ions

Other ions such as potassium, iron, aluminium, chromium, lead, nickel, zinc, barium, selenium, copper, nitrate, nitrite, ammonium and ammonia are equally important in water quality analysis (Deutsch, 1997; David and Pyne, 2000).

2.3.8.9 Ions Balance

Sodium, potassium, calcium, magnesium, chloride, sulphate, nitrate, carbonate and bicarbonate ions contribute to more than 95% of the ionic strength of a typical groundwater sample. Therefore, the total amount of cation and anion in the water should be equal if other ions are deemed to be present in negligible amount. Based on this argument, ions balance can be computed to reflect the accuracy of the analysis. The ions balance could be computed with **Equation 2.22**. An analysis can be classified as acceptable for having a ±10 % deficiency in ion balance.

$$IonsBalance = \frac{TotalCation - TotalAnion}{TotalCation + TotalAnion} \times 100\% \qquad \textbf{(2.22)}$$

where all concentrations are in meq/L

2.3.9 Sorption

When a mineral is placed in an aqueous solution, the process in which its solute ions, complexes or molecules accumulate onto the surface of the solid material is called sorption. Sorption has a strong influenced on the mobility and uptake of metals and organic compound in groundwater, and could eventually lead to the formation of a new

mineral (Krauskopf, 1995). Quantification of sorption is not straightforward and laboratory batch test is usually applied to identify the sorption kinetics.

Column studies had been carried out to investigate the effect of pH changes in the acidic range on the sorption characteristics of heavy metals. The findings showed that the sorption characteristics were controlled by the variations of volumetric water content, time of wetting, soil pH and the influent heavy metal concentration (Elzahabi and Yong, 2001).

2.3.10 Mineral Precipitation and Dissolution

A mineral in contact with groundwater represents a geochemical system consisting of a solid and a liquid phase. Disequilibria between the two phases occur when precipitation or dissolution of the mineral takes place in the solution. Solution concentration of the components of any mineral can be used to calculate whether the solution is in equilibrium with that mineral. This can be done by comparing the ion activity product (IAP) of the mineral with the equilibrium constant of the mineral, which is actually the product of the activity of individual ion in the mineral (Deutsch, 1997; Metz *et al.*, 2002). For example, the IAP of calcite could be calculated as in **Equation 2.23**:

$$IAP_{calcite} = \left(a_{Ca^{2+}}\right)\left(a_{CO_3^{2-}}\right) \qquad \textbf{(2.23)}$$

where IAP= ion activity product

a= activity

The equilibrium condition of a solution with respect to a mineral can be calculated using the equation for Saturation Index (SI), as shown in **Equation 2.24**.

$$SI = \frac{IAP_{\text{min eral}}}{K_{sp,\text{min eral}}} \qquad \textbf{(2.24)}$$

where SI = 1; mineral is in equilibrium with solution
SI < 1; mineral is under saturated
SI > 1; mineral is over saturated

When water is under saturated with respect to a mineral, dissolution would occur as long as the mineral is available. On the other hand, if the solution was over saturated, precipitation would take place in order to restore equilibrium.

2.3.11 Ion Exchange

Ions that accumulated on mineral surfaces are held by forces that range from weak to very strong, depending on the kind of mineral and the kind of ions. Those adsorbed as outer-sphere complexes are easily replaced by other ions in the solution. If a mineral with one kind of ion adsorb on its surface is added to an electrolyte solution containing different ions, some of the original ions will be set free in the solution and some of the new ions will be adsorbed in their place. This phenomenon is called ion exchange. Ion exchange in groundwater usually involves solid material of high surface area and electro-negativity, e.g. clay, silt. Cation in the solution with higher oxidation number and larger atomic radius tends to exchange readily with its counterpart adsorb onto the solid with lower oxidation number and smaller atomic radius. Typical reaction can be written as follows:

$$Na - X + Ca^{2+} \Leftrightarrow Ca - X + 2Na^{+}$$

The reaction is reversible if a very pure solution, e.g. RO effluent, is passed through the filled material. This process is called reverse ion exchange.

Major cation exchange reactions are very common in groundwater systems. They could considerably alter the chemical compositions as groundwater moves through an aquifer, affecting not only the exchanging ions but also other species, especially via dissolution/precipitation reactions. The attenuation of some pollutants, e.g. NH_4^+, is mainly through the process of ion exchange. In addition, ion exchange could be used in indicating the flow history of a groundwater system, especially where it is uncertain what has been the dominant historical flow direction (Carlyle *et al.*, 2003).

In the process of ion exchange, cations that are being released into the groundwater system will experience saturation over time. Any excess releases through ion exchange will cause the cation to precipitate. The fine particle will crystalline/cementing and

bound with the natural solid material within the environment, causing clogging of flow channel as well as decreasing the capacity of holding pore fluid. This phenomenon is known as clogging or plugging.

However, none of the currently operational ASR systems in the United States (U.S.) has experienced plugging or water quality problems due to ion exchange between the recharge water and native water. The best documented example of ion exchange plugging was at Norfolk, Virginia, during a U.S. Geological Survey injection well recharge investigation conducted in 1971-1972. The storage zone was a clayey sand aquifer containing brackish water. Recharge was with treated drinking water. During the first three test cycles, clay dispersion was shown to cause uniform plugging of the storage zone throughout the whole length of the screen interval, with 94 % reduction in specific capacity of the well (Brown and Silvey, 1977).

2.3.12 Sodium Adsorption Ratio (SAR) and Exchangeable Sodium Ratio (ESR)

SAR is a measure of the proportion of Na^+ present, with respect to other major ions, and has been used to account for the ion exchange process as well as sodium hazard to crops. The SAR (**Equation 2.25**) expresses the relative amount of Na^+ in the water (Stumm, 1992) and is used as an indicator of clogging tendency. When the Na^+ concentration is high, it tends to adsorb onto the clay minerals, displacing calcium and magnesium ions. This phenomenon results in a soil with poor drainage and hence restricted circulation of air and water (Collins and Jenkins, 1996; Saleh et al., 1999). For a SAR value greater than 6 to 9, the recharge water could be expected to cause a permeability problem on the shrinking and swelling types of clayey soils. In addition, an empirical indicator, ESR (**Equation 2.26**) is used to predict the possibility of clay swelling when it is in excess of 15%.

$$SAR = \frac{[Na^+]}{\left(\frac{[Ca^{2+}]+[Mg^{2+}]}{2}\right)^{1/2}} \qquad \textbf{(2.25)}$$

where *SAR*= sodium adsorption ratio

$$ESR = 1.58 \times SAR \quad (2.26)$$

where *ESR*= exchangeable sodium ratio

2.4 Mineralogy

2.4.1 Physical Characteristic

From the literature, the particle size, degree of compaction, permeability etc., all played a part in determining the performance of SAT in aquifer storage and recovery (ASR), in which the storage capacity, flow rate and the ease of clogging are dependent on these physical parameters. The ASTM's standards for soil investigation are adopted for the following analysis.

2.4.2 Chemical Characteristic

The types of minerals and its proportionate quantity in the soil are critical in establishing potential reactions in the subsurface environment where water-solid interactions took place (Pavelic et al., 2001). The British standards are adopted to analyse the chemical composition of the sand, for the analysis of the geochemical data. The methodologies adopted are shown in **Table 2.2.**

Table 2.2 Methodologies for soil characterisation

Characterization Test	***Method Used***
Determination of soil pH	BS ISO 10390:1994 Soil quality
Determination of carbonate content : Volumetric method	BS ISO 10693:1995 (E) Soil quality
Determination of organic and total carbon after dry combustion (elementary analysis)	BS ISO 10694:1995 (E) Soil quality
Extraction of trace elements soluble in aqua regia	BS ISO 11466:1995 (E) Soil quality
Determination of cadmium, chromium, cobalt, copper, lead, manganese, nickel and zinc in aqua regia extracts of soil	BS 7755 3.13.1998 Soil quality; Flame and electrothermal atomic absorption spectrometric methods
Determination of effective cation exchange capacity and base saturation level using barium chloride solution	BS ISO 11260:1994 (E) Soil quality
Determination of the potential cation exchange capacity and exchangeable cations using barium chloride solution buffered at pH	BS ISO 13536:1995 (E) Soil quality

= 8.1	

2.4.3 X-Ray Diffraction (XRD)

XRD analysis provides a description of the clays and minerals present in a soil sample. The relative abundance and types of clays provide an important indicator for potential geochemical or physical plugging (David and Pyne, 2000; Johnson et al., 1999). However, direct output from the XRD machine only shows the type of elements but not quantitatively. There are several methods of quantitative analysis that can be used to obtain the composition of the mineral by comparing with a base reference. Full Pattern Quantitative Analysis Program for XRD (FULLPAT) (Chipera et al., 2002) is a freeware that serves this purpose. FULLPAT is based on the principle that patterns for each individual phase in a mixture can be added in the correct proportions to reproduce the observed pattern. It varies the proportions of individual pure components using least squares minimisation to produce the best fit between an observed pattern and the simulated pattern produced by summing together patterns of individual pure components This quantitative analysis is facilitated by first adding a known amount of aluminium oxide (Al_2O_3) internal standard to both library standards and the unknowns. Then all individual library patterns are normalised on an equal-Al_2O_3 basis so that the Al_2O_3 in each library standard is at the same intensity as the Al_2O_3 in the observed pattern. The amount of Al_2O_3 used in the standards and unknowns is identical at 20% by weight. Therefore, each analysis is reduced to scaling and matching the Al_2O_3 normalised library patterns with the patterns of those phases in the observed pattern.

The amount of a phase in the unknown mixture is equal to the amount the library standard that has to be scaled to match that phase's portion in the unknown sample pattern. This is represented by **Equation 2.27**,

$$I_{phase} = I_{std} \times X\% \qquad \textbf{(2.27)}$$

where X% is directly translated to be the abundance of the phase in the sample. The least square minimisation is done by the Solver toolbox within Microsoft Excel.

2.4.4 Scanning Electron Microscopy (SEM)

SEM images are very useful in providing a direct assessment of potential geochemical reactions, if the image is reasonably representative of the remainder of the sample. Typically, the images are provided at a series of magnifications, such as 50x, 200x, 500x and 2000x. Porous materials such as fragments of shells, corals, diatoms, remains of sea living creature can be observed with ease. Specific minerals can be identified if details of the surface structure are available (David and Pyne, 2000).

2.5 Geochemistry Studies on ASR

Water scarcity is going to be a major challenge in the coming decades. As a result, artificial recharge with treated water or excess surface water is gaining popularity as a method to replenish the depleting water resources (Bouwer et al., 1990). However, little effort has been carried out to investigate the nature and significance of abiotic geochemical processes that occurs during artificial recharge, though these reactions may have a major impact on the success of ASR (David and Pyne, 1995). Nonetheless, several detailed characterisations of aquifer geochemistry had been carried out in the delineation of recharge sources, the determination of remediation strategies as well as monitoring the efficiency of a remediation operation. Detailed characterisation of aquifer geochemistry had been found to be important to describe stream–aquifer interactions (Cirmo and McDonell, 1997), salt water intrusion (Whittemore, 1995; Ortega-Guerrero, 2003; Snyder et al., 2004; Anderson et al., 2005; Klein-BenDavid et al., 2005; Sivan et al., 2005), rock-groundwater interaction (Edmunds et al., 2003; Cipolli et al., 2004), coastal shallow groundwater aquifer (Tesoriero et al., 2004), rainfall/groundwater interaction (Saleh et al., 1999; Wang and Guo, 2004), geothermal aquifer in volcanic region (Bianchini et al., 2005) and monitoring the efficiency of a remediation operation (Roberts et al. 1982; Wiedemeier et al., 1998; Azadpour-Keeley et al., 2001; Brun and Engesaard, 2002; Norris, 1999; Fram et al., 2003; Chae et al., 2004). Unfortunately, the inorganic chemical data essential for such efforts are often

obtained as supporting information during experiments designed for other purposes such as remediation (Schulmeister et al., 2004; Vanderzalm et al. 2002).

In an ASR operation, it is common to find naturally occurring, easily leachable contaminants in the soil that would contravene with drinking water quality if leached. Naturally occurring arsenic, chromium, fluoride and total dissolved solids could make groundwater unsuitable for drinking as in a study by Baker et al. (1998) in Arizona. In addition, various reactions, including chemical precipitation, dispersion of clays, caused by the replacement of adsorbed divalent cations by sodium ion, swelling of expandable clays upon wetting, and soil plugging caused by dissolution of cementing materials will all lead to a drop in infiltration rate (Houston *et al.*, 1988). Therefore, it is important to quantify the groundwater origin and flow, hydrochemical evolution and solute transport. This information is critical for the evaluation of long term hazardous waste containment, protective natural covers and geochemical transformation (Ortega-Guerrero, 2003). All these potential problems should be addressed in the laboratory prior to the implementation of a large scale ASR scheme. Batch leaching studies and column experiments are useful for assessing the possible outcomes in an actual recharge operation.

2.5.1 Batch Studies

Batch test provides a cheap and fast way for evaluating dissolution, ion exchange, and other reactions that could occur during ASR. The fill material and recharge water are thoroughly mixed and then subjected to a progressive series of leaching test. The results obtained will provide considerable insight into the expected water quality and geochemical response to ASR. However, batch test results are not very useful for directly evaluating aquifer hydraulics response. Chesapeake, Virginia, had applied these methods to monitor the leaching of heavy metals in order to compare with results obtained through column test in their ASR studies (David and Pyne, 2000).

Johnson *et al.* (1999) had conducted batch studies with RO, Micro-filtered effluent (MF) and river water collected from Colorado River with 30 days of retention time and solid/water ration of 1 to 5. As expected, leaching was greatest with RO water. Equilibrium was achieved with respect to several carbonate minerals for RO batch test. In essence, batch studies were a fairly good screening test to determine whether certain contaminants were likely to be leached. Contaminants that were leached at measurable concentrations in the column study were also leached in the batch study and vice versa. Nonetheless, batch experiments are less useful than the columns in representing the dynamics of contaminant behavior.

2.5.2 Column Studies

Column studies simulate the actual flowing condition similar to a field scale recharge scheme, but eliminate the heterogeneities and uncertainties that will be faced in the field. A carefully conducted column study can ensure that the assumption of one dimensional plug flow condition is correct up to a certain extent. This assumption would support the validity of the Darcy's equation and help avoid the complexity of irregular flow. Nonetheless, the heterogeneity of the fill material makes this assumption basically invalid. As a result, column test results usually do not match well with the result obtained from the field. Therefore, the results from column test should represent an optimum operational scheme as most of the favourable assumptions made in the laboratory may not be true in the field.

Geochemistry column studies in ASR were not well reported in the literature and only several related cases had been published in recent years. Johnson *et al.* (1999) had conducted experiments with laboratory columns to investigate the geochemical transformation during ASR with three types of water, namely RO, MF and Colorado River water. Soils were collected from 3 depth interval in two pilot recharge wells. The columns, 25 cm in height, 5 cm in diameter, were packed with each soil types with an assume porosity of 0.33. Each of these columns was operated in the up flow mode at a rate of 0.17 L/day for 100 days which corresponded to 100 exchange of pore volume. Washout effect was observed where the saturation index of several carbonate minerals

(e.g. calcite, aragonite, magnesite) decrease from equilibrium to highly under-saturated level (Johnson *et al.*, 1999).

In another study, Delgado *et al.* (1997) had set up six columns, 50 cm in height , 7.3 cm in diameter, packed with <2 mm sieved sand. These columns were operated in a gravity flow mode in which water was dripped from the top and allowed to flow through the column under controlled flow rate. The experiment attempted to examine the performance of the soil during recharge of artificial cattle slurry. The results had shown that the sodium concentration in the effluent was higher than the influent due to ion exchange effect. However, the concentration of sodium dropped against time probably due to the exhaustion of exchangeable ions in the soil. In addition, it had highlighted the problem of packing irregularity due to the heterogeneity of the soil, causing ambiguity to the experiment's findings.

Over at Cardiff, U.K., column studies were carried out to determine the retention capability of three types of estuarine alluvia collected adjacent to a landfill site. The columns were made of Plexiglas, 125 mm in height, 115 mm in diameter and packed with the collected sand at maximum dry density. Leachate was collected from a municipal solid waste landfill and spiked with heavy metals of Pb, Cu and Zn. The results had shown that >99.99% of the heavy metals were retained in the column for the first 5 PV. This was due to both ion exchange reactions as well as precipitation with carbonate and amorphous materials. The column also showed good buffering capacity of the soil against very acidic (pH 1.5) leachate (*Yong et al.*, 2001).

In Kuwait, Mukhopadhyay et al. (1998) conducted a series of flow through column test with core samples collected from the Dammam Formation Aquifer, a dolomitic limestone formation. The studies were on the recharge of desalinated water into the aquifer using it as a temporary reservoir. Primary investigation suggested that except for some dissolution of the carbonates and movements of fines in the pore space, there is no significance geochemical transformation during the injection of desalinated water. Qualitative examination of the core samples under SEM did not reveal any change in

the texture and porosity structures. Therefore, it was concluded that the injection of desalinated water into the Dammam aqufer might not result in significant changes in the aquifer characteristic.

2.5.3 Field Studies

Although, both batch and column studies were useful as screening studies that could identify potential water quality problems before costly field-scale recharge projects wee built, neither column nor batch experiments were sufficient to make quantitative predictions of water quality changes that would occur during recharge through the vadose zone. It is prudent to operate pilot-scale projects accompanied by monitoring wells to determine the potential for water quality changes before implementing full-scale recharge projects (Johnson *et al.*, 1999).

Field scaled geochemistry study during ASR is even rarer in the literature. Lloyd *et. al. (2004)* had carried out a small scaled geochemistry study at Changi, Singapore, in which a 1 m diameter RO slug was injected into the ground. The soil was basically medium to coarse sand with high quartz and carbonate content. The geochemistry effect was monitored at 1 m away from the injection point through a multi-level sampling well. The results had indicated both carbonate dissolution and ion exchange reaction to be dominant in such a sand media.

Guo and Wang (2004) reported that the natural recharges into the shallow aquifer at Datong Basin, China, had encountered both dissolution and ion exchange effect amid in different regions. Groundwater migration from bedrock fractures and joints into the basin aquifer, had increased the alkalinity of the groundwater due to dissolution of carbonate and hydrolysis of aluminosilicate minerals. Rainfall recharge to the shallow aquifer, meanwhile, removed the calcium and magnesium ions in the groundwater by exchanging with sodium ion adsorbed on the clay minerals.

A study on alluvial groundwater of an agricultural area in Korea was geochemically investigated. Water samples were collected from the evenly distributed irrigation wells

and the results indicated that the water quality of these samples which were categorized into different geochemical zones, were consistent with the geology of the respective area. Generally, iron, manganese, calcium, magnesium and nitrate were found to be an important indicator of the subsurface geological conditions. It was concluded that the water chemistry data could be use to assess groundwater contamination susceptibilities (Chae et al. 2004).

2.6 Soil Aquifer Treatment (SAT) Studies

SAT is essentially the treatment of recharge water as it percolates down the column of soil through the vadose zone, and mixes with the native groundwater. Nitrogen species, dissolved organics and pathogens present in the recharge water are removed or transformed during percolation and storage. Dissolved organic matter is removed by a combination of chemical, physical and biological processes in the vadose zone and aquifer. Most of the treatment is achieved during percolation through the vadose zone (Quanrud *et al.*, 1996).

Laboratory column studies are commonly used to simulate the change in recharge water quality in a SAT system. Soil columns of higher hydraulic retention time (HRT) are more appropriate compared to batch tests for the determination of DOC removal efficiency, as this test system provides continuous structural changes of generally poorly degradable organic compounds during SAT (Drewes *et al.*, 1999). Besides DOC, UVA at 254 nm was also measured as the other primary indicator of the effectiveness of SAT.

Several other research studies had shown significant DOC removal during the recharge of wastewater effluent in SAT systems, as shown in Table 2.3.

Table 2.3 Reduction in dissolved organic carbon (DOC) during SAT

Authors	*Reduction (%)*	*DOC (mg/L) in Recharge*	*Sediment Thickness (m)*
Nellor et al, 1984	66	10	2.4
Bouwer et al, 1974	73	10-30	3.3
Amy et al, 1993	50	10.7-12.0	6.1
Bouwer and Rice, 1984	70	10.2-11.7	18
Drewes and Fox, 1999	72	5.7	20
Idelovitch and Michail, 1984	82	18	25
Wilson et al, 1995	90	12	37

2.6.1 Dissolved Organic Carbon (DOC)

The total organic carbon (TOC) is the primary surrogate parameter for the measurement of natural organic matter in water supplies. The dissolved organic carbon (DOC) on the other hand is operationally defined by filtration through a 0.45 μm membrane filter. The DOC results used in this study are actually non-purgeable dissolved organic carbon, but referred to as DOC for simplicity sake.

The DOC in treated municipal sewage effluent comprises a complex mixture of organic carbon compounds which include humic substances, proteins, polysaccharides, carbohydrates, and amino acids. During biological wastewater treatment of the sewage effluent, it is expected that volatile organics are essentially eliminated and DOC would comprise the total sum of dissolved organic matter present in the effluent.

In a report by Grady *et al.* (1972), the majority of dissolved organics in effluent following activated sludge treatment consisted of by-products of microbial metabolism. These by-products were usually recalcitrant to further removal, but were reported to be partially removed by SAT process. However, without identifying these by-products, DOC values are used as the indicator parameter to evaluate the organic removal efficiency in this study.

2.6.2 Ultraviolet Light Absorbance at 254nm

Ultraviolet light absorbance at 254nm (UVA) is a gross measurement of humic-like constituents with an aromatic characteristic (e.g. humic and fulvic acids). It is generally used to describe the type and characteristic of the organic carbon whereas the TOC defines the quantitative aspect.

Organic compounds that have aromatic or conjugated unsaturated bonding structures were primarily responsible for ultraviolet adsorption in the wavelength of 200-300 nm (Michail and Idelovitch, 1981). The polymer-like molecules of fulvic and humic acids contain substituted aromatic rings, saturated and unsaturated alkyl groups, carboxyl groups, and heterocyclic compounds derived from the decay of biomass (Maier and Conroy, 1981). Residual organics in sewage effluents generally comprise of 40 to 50% or more of humic substances (Rebhun and Manka, 1971). Humics are generally resistant to biodegradation, but due to their hydrophobic character, they may be more amenable to removal by sorption.

The presence of humic substances in the recharge water is of concern because they can combine with free chlorine during the disinfection process to produce disinfection byproducts (DBPs), such as trihalomethanes (THM) and halo-acetic acids. Singer *et. al.*, 1981 found a strong correlation between UVA and THM formation potential in drinking water. Reckhow and Singer (1984) concluded that UV254 was a good surrogate parameter for organic halide precursors. Singer (1999) reinforced the findings that humic substances were precursors for potentially harmful DBP.

3 MATERIALS & METHODOLOGIES

3.1 Background

The quality of an analysis could never be better than the quality of the samples itself. Hence, it was important to establish correct sampling and analytical procedures that complied with recognised standard methods. This chapter discusses the various methodologies that have been used throughout the course of the present studies. It includes discussions on sand characterisation; water samples analytical methods; laboratory column studies and field RO injection test.

3.2 Characterisation of fill material

3.2.1 Collection

Sand was collected from the Changi reclaimed land for column packing. Two types of sand samples were collected. Surface sand was collected for the short term column and subsurface sand was collected for the medium term geochemistry column. The top 30 cm soil was scraped off before the collection of surface sand samples. Approximately 400 kg of sand was collected in one exercise. As for subsurface sand, a contractor was employed to bore holes to a depth of 3.5 m and samples were collected using a modified sand catcher at every 0.5 m interval up to maximum 8.5 m below ground. Approximately 20 kg of samples was collected at each depth. Sand was collected in sealed plastic bags to prevent loss of moisture, and transported back to the laboratory within the day of collection. Care was taken to prevent contamination of the samples via air or by dust. Samples with dust-like consistency should be handled with caution, as part of it might be lost through transportation and this might alter its physico-chemical properties (BS ISO, 1994).

3.2.2 Pre-treatment

A sand sample had to be treated before it was used for further analysis. The sand had to be dried in an oven at a temperature not higher than 40°C until the loss in mass of the soil sample was not greater than 5 g per 24 hour. Crushing was done when there were

clods of sand samples. Care must be taken to minimise the loss of fines. The dried sand sample was then sieved through 2 mm aperture sieve to remove shell fragment and stone (BS ISO, 1994).

3.2.3 Physical Characteristics

3.2.3.1 Sieve analysis

Particle size distribution was carried out by sieving the sand through sieves ranging in sizes from 4.75 mm to 75 μm. The weight of sand retained in each sieve is weighed and a graph of percentage of sand passing through versus the opening of the sieve is plotted. The sand is then classified based on United Soil Classification System (ASTM, 2000; Lunne, 1997).

3.2.3.2 Specific Gravity

Specific gravity (S.G) is an important parameter for the determination of porosity. In the case of highly uniform, poorly graded sand collected from Changi, the S.G. values obtained from the literature was about 2.7. 15 g of sand was first transferred to the specific gravity bottle; filled to the brim with distilled water and connected to a vacuum pump for 24 hours. This was to purge out the trapped air. The specific gravity could then be computed by dividing the weight of sand over the weight of distilled water that occupied the same volume of sand.

3.2.4 Mineralogy

3.2.4.1 Soil pH

The soil pH is one of the most fundamental parameter to predict the geochemical effect during solid-liquid interactions. As the type of extraction solution would have different effects on the soil pH, it was always presented in 3 values using different extraction solutions. Ultra pure water, 1.0 M potassium chloride solution and 0.01 M calcium chloride solution were used to extract the sand with a ratio of solid/liquid of 1/5 volume by volume. The mixture had to be stirred vigorously for at least 2 hours, but not more than 24 hours before analysing with a pH probe (BS ISO, 1994).

3.2.4.2 Metal Digestion

Aqua regia was a mixture of three parts concentrated nitric acid and one part concentrated hydrochloric acid. The mixture could dissolve gold in which individual acid could not. Initially, 3.0 g of sand sample was transferred into a 100 ml glass beaker. 30 ml of concentrated nitric acid and 2.0 ml of concentrated hydrochloric acid (HCl) were added to the beaker. The mixture was heated without reaching the boiling point. Additional 1.0 ml of concentrated HCl was added each time until no further effervescence was observed. The mixture was then filtered through 0.45 mm Nylon membrane filter and rinsed with 10 ml of ultra pure water. The filtrate was transferred into a 100 ml volumetric flask and filled to mark. The final solution would consist of all the metal ions in the sand with the exception of silica. Concentration of individual cation was measured using inductively coupled plasma (ICP-OES) (BS ISO, 1995).

3.2.4.3 Carbonate Content

Carbonate is dissociated when it comes into contact with acid as CO_2 is released into air, as shown in the following chemical reactions:

$$MetalCO_3 + 2H^+ \Leftrightarrow (Metal)^{2+} + H_2CO_3$$
$$H_2CO_3 \Rightarrow H_2O + CO_2$$

The test was carried out by adding 1.0 ml of 0.1 M hydrochloric acid to 10 g of sand sample. Additional 1.0 ml of HCl was added to the mixture until no effervescence was observed. The mixture was then filtered through a weighed filter paper (W1) and rinsed with ultra pure water. The residue was subsequently dried at 40 °C in order to obtain the weight of the dried residue (W2). The carbonate content could then be calculated by **Equation 3.1** (BS ISO, 1995; Langford, 2004).

$$\text{Weight of residue, } W_3 = W_2 - W_1$$
$$\text{Weight of carbonate, } W_c = 10 - W_3$$
$$\text{Carbonate Content, } \%Carbonate = \frac{W_c}{10} \times 100\% \qquad \textbf{(3.1)}$$

3.2.4.4 Organic Content

Strong oxidation agent could oxidise the majority of the organic content to CO2, though it might not be as accurate compared to the combustion method where organic content would be combusted in a furnace heated to more than 800 °C. Nonetheless, the accuracy was deemed to be sufficient for hydrogeology studies. 10 g of sample was first transferred to a 100 ml glass beaker prior to the addition of 30 ml of ultra pure water. 1 ml of 30% hydrogen peroxide was added each time until no effervescence was observed. The final mixture was then heated at 90 °C for an hour. The mixture was then filtered through a weighed filter paper (W1) and rinsed with ultra pure water. The residue was subsequently dried at 40 °C in order to obtain the weight of the dried residue (W2). The organic content could then be calculated with the following formulas (**Equation 3.2**) (BS ISO, 1995; Langford, 2004).

$$\text{Weight of residue, } W_3 = W_2 - W_1$$

$$\text{Weight of organic content, } W_o = 10 - W_3$$

$$\text{Organic Content, } \%Organic = \frac{W_o}{10} \times 100\% \qquad (3.2)$$

3.2.4.5 Cation and Anion Exchange Capacity

Cation exchange capacity (CEC) is a measurement of the maximum capability of a soil to adsorb a particular cation. Anion exchange capacity (AEC) is a measurement of the maximum capability of a soil in exchanging an anion. Cation exchange is a well-known phenomenon in aquifers containing fines content and the significance of it in changing groundwater quality was well documented in both field and laboratory experiments (Nadler et al., 1980; Mercado, 1985; Sivan et al., 2005). It was found that cation exchange was likely to occur in sandy-carbonate aquifer with pH higher than 6 during water/solid interaction (Appelo and Postma, 1996).

CEC and AEC of the soil at pH 8.1 were determined using a buffer salt extraction method. The procedure generally involved three major fractions. First, the soil pH was pre-stabilized at 8.1 so that it would not fluctuate significantly when the ion exchange test was performed. The soil was then saturated with Ba^{2+} as well as Cl^- by adding 0.2

M barium chloride. The excessive Ba^{2+} and Cl^- were removed by multi-fraction rinsing using ultra pure water. Next, the total Ba^{2+} and Cl^- adsorbed were then displaced by adding 0.2 M magnesium sulphate ($MgSO_4$) solution to the $BaCl_2$-saturated soil. The total concentration of Na^+ displaced into the solution was measured in the solution using ICP-OES, whereas the total concentration of Cl^- in the solution was measured using flow injection analysis. The CEC and AEC values are computed as follows (**Equation 3.3** and **3.4**):

$$CEC(cmol/kg) = \frac{[Ba^{2+}] \times V}{M_s \times Ar.Ba} \quad (3.3)$$

$$AEC(cmol/kg) = \frac{[Cl^-] \times V}{M_s \times Ar.Cl} \quad (3.4)$$

where $[Ba^{2+}]$= barium concentration in mg/L

$[Cl^-]$= chloride concentration in mg/L

V= volume of solution in L

M_s= mass of sand in g

$Ar.Ba$= atomic weight of barium

$Ar.Cl$= atomic weight of chloride

3.2.4.6 X-Ray Diffraction (XRD)

XRD provides a simple solution to qualitatively analyse the mineral content in the soil sample. However, there were several methods in the literature that had successfully obtained quantitative results through XRD. In this study, these methods were reviewed and verified in order to identify the best method to analyse the sand samples obtained from Changi. The Bruker AXS Diffractometer D8, as shown in Figure 3.1, was used for the XRD analysis. Sand sample had to be pre-treated as described in section 3.2.2. Sand sample had to be grinded and sieved through a 150 μm sieve. The retained sand sample was to be further grinded

and sieved. This process was repeated until 95 % by weight of the sample had passed through the sieve. Sieved sand sample had to be homogenised. Next, the sample was mixed with a reference mineral, i.e. aluminium oxide (Al_2O_3) in the ratio of 8 parts to 2 parts by weight. The sample was then ready for analysis. Ethanol was used to clean the sample dish to prevent cross contamination before applying a thin layer of sample onto it. The surface of the sample was smoothened before inserting the sample into the diffractometer. **Figure 3.2** showed a typical output produced by XRD.

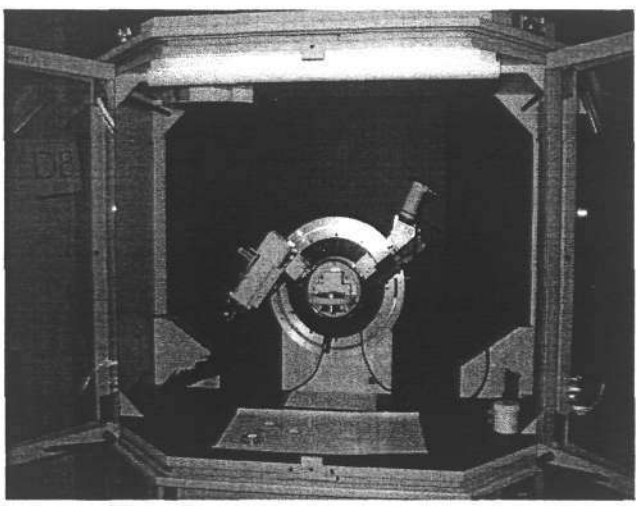

Figure 3.1 X-Ray Diffractometer

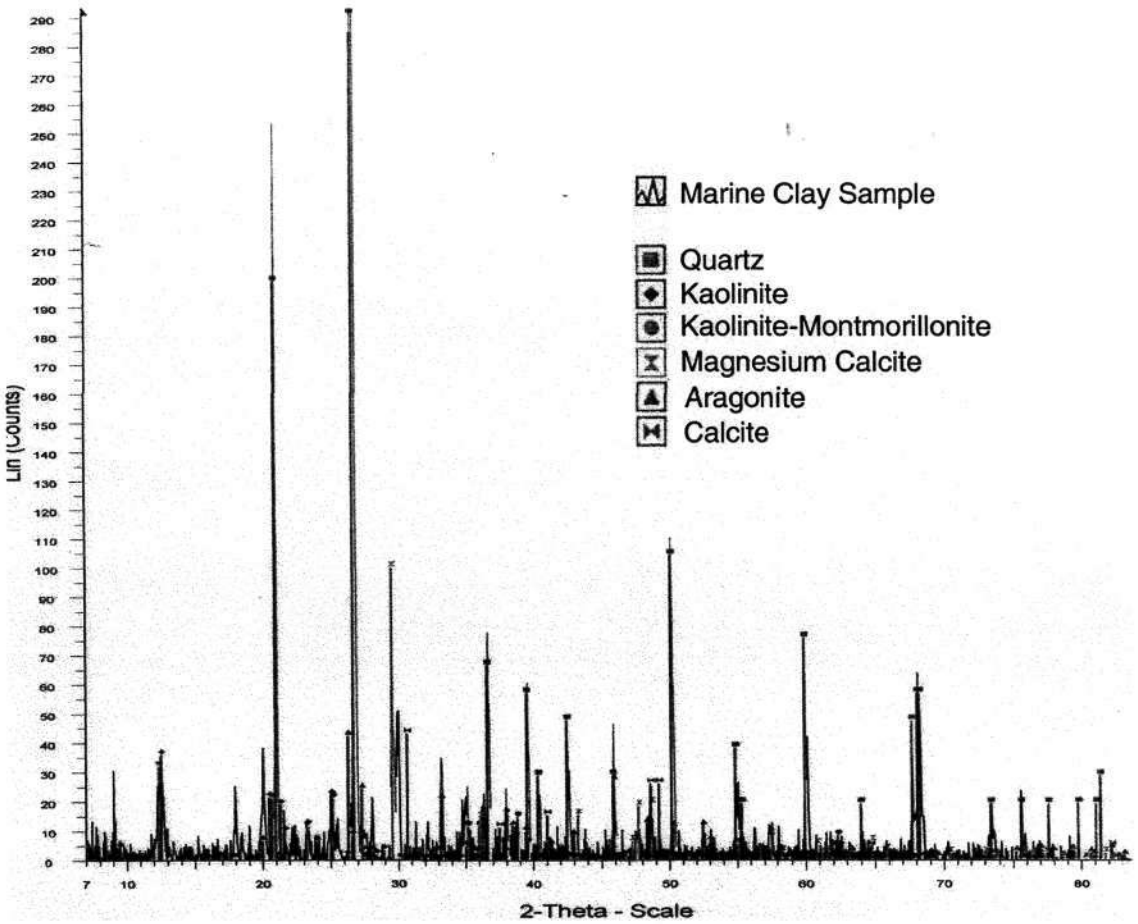

Figure 3.2 Typical XRD output file

3.2.4.7 Scanning Electron Microscope (SEM)

SEM was used to capture the image of calcareous fragments in the sand. As the sand was dredged from the sea bed, there was a fairly large amount of sea shells presented in the sand. This study was to identify the presence of these highly porous material, e.g. diatoms etc.

3.3 Water Quality Analysis

3.3.1 Samples collection

3.3.1.1 Field samples from CMT and ML wells

Field samples were collected using Masterflex L/S economy pump drive coupled with Masterflex L/S cartridge pump head. Masterflex silicone (peroxide cured) L/S 14 tubing was used. The pump tubing used was of 1.6 mm internal diameter and connected

to the sampling well directly. Flow rate was maintained low in order to prevent short circuiting between sampling ports which were adjacent to one and the other along the CMT and ML wells. For each sample, 100 ml was collected excluding flushing. The samples were filtered through 0.45 mm membrane filter and separated into three 40 ml amber glass bottles. Samples were kept at 4 °C until analysis.

3.3.1.2 Laboratory samples from batch and column tests

Laboratory samples were collected in excess of 100 ml excluding flushing. The samples were filtered through 0.45 mm nylon membrane filter and separated into three 40 ml amber glass bottles. Samples were kept at 4 °C until analysis.

3.3.2 Temperature, pH, EC

These parameters were measured using the Thermo Orion model 555A benchtop meter with Thermo Orion pHuture MMS Pentrode 617500. pH was calibrated against calibration solutions of 4.01, 7.00 and 10.01 respectively (Clesciri et. al., 1998). The Orion meter had a temperature compensation coefficient of 2.1% and was automatically corrected to 25 °C for both pH and EC. EC was calibrated using NaCl standard solution prepared to 100, 1,413 and 12,900 µS/cm (Clesciri et. al., 1998).

3.3.3 Oxidation-Reduction Potential (ORP)

ORP is an estimate of the oxidation-reduction status which indicates whether the soil conditions are oxidizing or reducing. The ORP of the soil was measured potentiometrically using a standard platinum electrode (HORIBA redox potential meter), and reported to the nearest millivolt (mV) relative to Ag/AgCl. ZoBell's solution was used to check the performance of the electrode (Clesciri et. al., 1998).

3.3.4 Dissolved Oxygen (DO)

DO is an important parameter to determine whether the aquifer is aerobic, anoxic or anaerobic. The Thermo Orion 850A+ basic dissolved oxygen meter and the Orion 083005D DO electrode were used for both field and laboratory measurements. As DO value would change as soon as the samples came into contact with air, a flow-through

cell was designed to solve this problem. The DO electrode was slotted into the flow-through cell where samples would pass through the internal chamber without coming into contact with air. **Figure 3.3** illustrates the working principle of the flow-through cell.

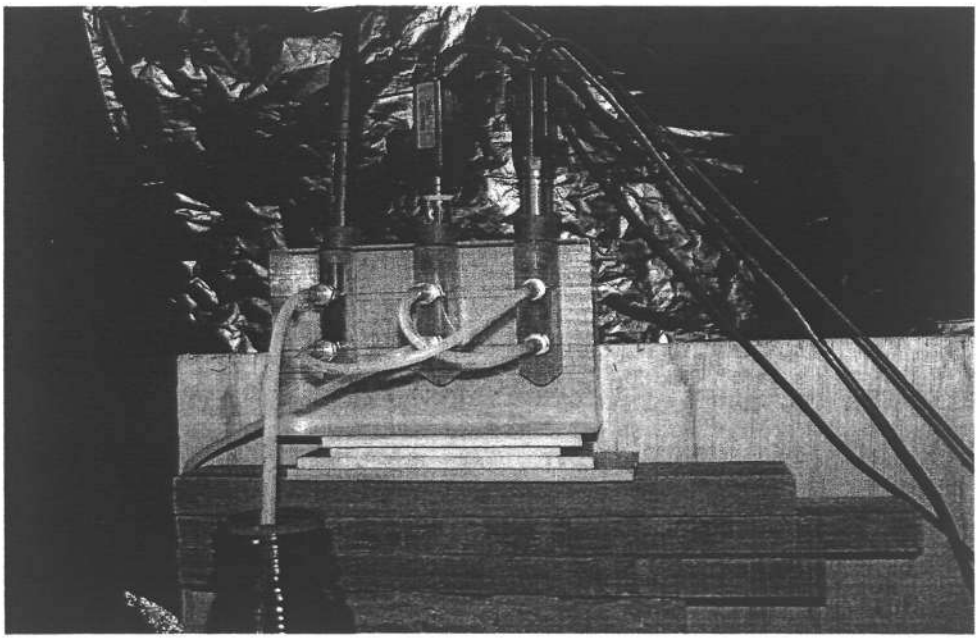

Figure 3.3 Flow through cell

3.3.5 Turbidity

The HACH's portable turbidity meter was used for both field and laboratory measurements. In accordance to the 2130A Nephelometric Method, samples had to be agitated prior to testing. The standard solutions used were stabilized formazin at 0.1, 20, 100, 800 NTU (Clesciri et. al., 1998).

3.3.6 Dissolved Organic Carbon (DOC) or Non-Purgeable Organic Carbon (NPOC)

DOC samples were collected in 40 ml amber glass bottles and acidified to pH 2 after filtering through 0.45 μm Nylon membrane filter. The Shimadzu TOC-V CSH total organic carbon (TOC) analyser and Shimadzu ASI-V auto-sampler, as shown in **Figure 3.4**, were used for DOC analysis with a 7-point calibration performed weekly. Each DOC sample was analyzed in triplicates. Standard solutions of potassium hydrogen phthalate (KHP) as organic carbon source were also analyzed as calibration checks

during each analysis to ensure the validity of results obtained. When samples were injected into the analyser, it is being acidified and sparged before passing through the heated chamber at 680 °C. The carbon dioxide produced was analysed with a CO_2 detector. The CO_2 concentration was directly proportional to the organic carbon concentration in the sample (Clesciri et. al., 1998).

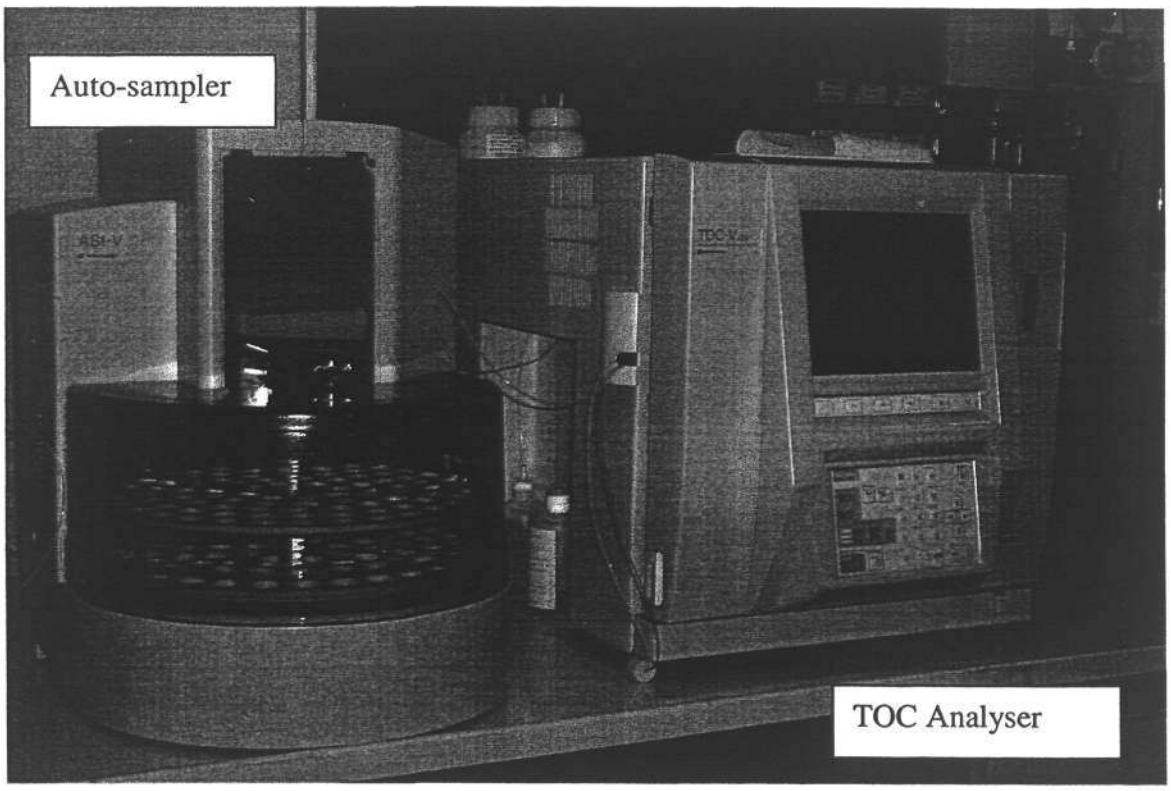

Figure 3.4 Photo of TOC analyser and auto-sampler

3.3.7 Dissolved Inorganic Carbon (DIC)

The Shimadzu TOC-V CSH TOC analyser and Shimadzu ASI-V auto-sampler (Figure 3.4) were used for DIC measurement with a 7-point calibration performed weekly. Each DIC sample was analyzed in triplicates. Standards solution of calcium carbonate and calcium bicarbonate were also analysed as calibration check during each analysis to ensure the validity of results. When samples were injected into the analyser, it was being sent to a reaction chamber filled with 0.25 M phosphoric acid. The inorganic carbon would react with the acid to form CO_2. The carbon dioxide produced was thus

analysed with a CO_2 detector. The CO_2 concentration was directly proportional to the organic carbon concentration in the sample (Clesciri et. al., 1998).

3.3.8 Major Cations and Heavy Metals analysis

Analysis of samples for the four major cations was done using the ICP spectroscopy. Samples of 40 ml were transferred into 40 ml glass valves. All samples were adjusted to pH 2 with concentrated nitric acid and stored in 4°C prior to analysis. Calibration solutions of 1 mg/L, 5 mg/L, 10 mg/L and 100 mg/L were used for major cations, whereas, 0.1 mg/L, 0/5 mg/L and 1 mg/L were used for trace heavy metals analysis. Dilution was necessary for major cation analysis as groundwater's sodium ion concentration might exceed the calibration range (Clesciri et. al., 1998). The detection limit of individual cation was shown in **Table 3.1**.

Table 3.1 Method detection limit of ICP

Cation	***Cation***	***Method Detection Limit (mg/L)***
Aluminium	Al	0.002
Arsenic	As	0.02
Barium	Ba	0.001
Calcium	Ca	0.001
Chromium	Cr	0.001
Copper	Cu	0.001
Iron	Fe	0.001
Lead	Pb	0.004
Magnesium	Mg	0.003
Manganese	Mn	0.001
Nickel	Ni	0.001
Potassium	K	0.003
Selenium	Se	0.020
Sodium	Na	0.005
Zinc	Zn	0.002

3.3.9 Chloride

The FIA Spectrometer was used to analyse chloride concentration. Eight points calibration was done in the range of 10 mg/L – 1,000 mg/L. The calibration curve followed a 2nd order polynomial. Combined colour reagent of mercuric thiocyanate and ferric nitrate reagent would form the coloured ferric thiocyanate, of which the absorbance at 480nm was proportional to the chloride concentration (Diamond, 1995).

3.3.10 Sulphate

The FIA Spectrometer was used for sulphate measurement. Nine points calibration was done in the range of 3 mg/L – 300 mg/L. Sulphate in the samples was precipitated with barium chloride. The precipitation scattered light at 420 nm to produce a signal proportional to sulphate concentration. The precipitate was suspended as a colloid with gelatine and polyvinyl alcohol. The calibration curve followed a 3rd order polynomial (Diamond, 1996; Clesciri et. al., 1998).

3.3.11 Nitrate

The FIA Spectrometer was used. Eight points calibration was done in the range of 0.5 mg/L – 50 mg/L. The calibration curve followed a 2nd order polynomial. Nitrate in the samples was quantitatively reduced to nitrite by passage of the sample through a copperised cadmium column. The reduced nitrate plus the original nitrite were then determined by diazotising with sulphanilamide followed by coupling with N-(1-naphthyl) ethylenediamine dihydrochloride. The resulting water soluble dye has a magenta colour which was absorbed at 520 nm (Diamond, 1997; Clesciri et. al., 1998).

3.3.12 Ultraviolet Absorbance (UVA) at 254 nm

UVA at 254 nm was a gross measurement of humic-like constituents with an aromatic character (both humic and fulvic acids)(David M. Quanrud et al, 1996). Bingman stated that humic acids were a complex mixture of partially "decomposed" and otherwise transformed organic materials. Organic compounds having aromatic or conjugated unsaturated bonding structures were primarily responsible for UV absorption in the range of 200-300 nm (Michail & Idelovitch, 1981). Humics generally resist biodegradation but because of their hydrophobicity, may be more amenable to removal by sorption.

UVA was measured at 25 °C using a Perkin-Elmer Lambda Bio 20 spectrophotometer in a 1 cm path-length quartz glass cuvette. The instrument was zeroed using a potassium/sodium phosphate mixture (0.03/0.02 M) and checked with a standard of known absorbance. All samples were analysed within 7 days of collection and values were reported in cm^{-1}.

3.4 Batch Leaching Test

Batch studies were conducted to examine the extent of leaching that took place between SE, UF, RO, rain water and Changi sands collected from the surface, 5 m below ground and 8 m below ground. Batch studies would give an upper bound value of leaching or sorption as the water to solid ratio is much higher than in situ conditions. In addition, the geochemical effect takes place much faster due to continuous agitation to the mixture. All batch tests were conducted over duration of 7 days to allow it to reach equilibrium. The 7-day period to approach equilibrium was based on earlier kinetic studies in which a series of 20 known solid to water ratio batch samples were prepared and continuously mixed with a mechanical shaker. One sample bottle was taken at a time within close interval of 30min, 1^{st} , 2^{nd} , 4^{th} , 8^{th} and the 24^{th} hour for the first day of experiment, and follow by one sample per day up to the 10^{th} day. The concentration of Ca, Mg, and Cl in the leachate was compared over the duration of mixing. It was found that the leachate was saturated as early as on the 4^{th} hour. Nevertheless, 7 days was selected as it represents a more conservative approach to ensure complete dissolution/leaching effect. The brief description of the batch leaching test is reported in the following paragraph.

The sand from the Changi site was oven dried at 103 °C for 24 hours and sieved through a 2 mm sieve. For each batch test sample, 60 g of the sand was placed in a 600 ml glass bottle and filled to the top with one of the waters to be treated. Mixing was then carried out regularly over the duration of the test. Control bottles were also prepared by filling the bottles with the respective waters, but without the sand. These were subjected to the same experimental conditions over the 7 day period. At the end of

7 days, water samples were extracted from the batch tests for analysis. Temperature, pH, and conductivity were measured immediately upon extraction from the supernatant of the batch tests. All samples were filtered through 0.45μm filter and stored at 4°C prior to analysis and all tests were carried out within two weeks of extraction. The parameters analysed included DIC, major cations (Na^+, K^+, Ca^{2+}, Mg^{2+}), and major anions (Cl^-, SO_4^{2-}, NO_3^-).

3.5 Column Setup

3.5.1 Packing of Column

The test column was packed by partitioning it into multiple sections of equal volume. Equal weight of sand was packed into each section to the desired porosity. A steel rod was used to compact each sand layer by tapping for at least 30 times. Care was taken to ensure the distance between the sand discharge point and packed sand level was no larger than 5 cm. This was to prevent segregation of the fill materials. After packing, the column was wrapped with aluminium foil to prevent over exposure to sunlight and which could encourage algae growth.

3.5.2 Water Tightness Test

The column was saturated with water from bottom to top in order to purge out the trapped air. Water was kept in the column for at least three days to observe for possible leakages. Any leakage was mended and sealed until no further leakage developed. Pumping or hydraulic driven flow was carried out to simulate operating conditions for another week. The targeted influent was used to acclimatise the column.

3.5.3 Hydraulic Conductivity Test

During the trial run, hydraulic conductivity test was carried out. By varying the flow rate, either by adjusting the pumping rate or the level of the constant head tank downstream, the head differences were read from the manometer ports. The flow rate was measured using a weighing method, by collecting effluent over a period of time. At least two sets of results were obtained to compute the hydraulic conductivity. With known flow rate (Q in m^3/day), head difference (h in m), column length (L in m) and

surface loading area (A in m^2), the hydraulic conductivity was obtained using the Darcy's equation as shown in **Equation 3.5**.

$$Q\left(m^3/day\right) = k\frac{h}{L}A \qquad (3.5)$$

3.6 Short term Geochemistry Column with RO Injection

The short term column test was to investigate the geochemical effect of RO injection during the very first pore volume. As shown in **Figure 3.5**, a 0.107 m diameter, 0.517 m length acrylic column was set up for this test. Two manometer ports were fixed at both ends of the column. The flow rate through the system was governed by two constant head tank located up stream and downstream. Adjusting the downstream tank level, which also served as the flow through cell, would cause a change in the flow rate. The flow through cell could give in line measurement of temperature, pH, EC, ORP and chloride concentration with an ion selective electrode (ISE) as shown in **Figure 3.6**.

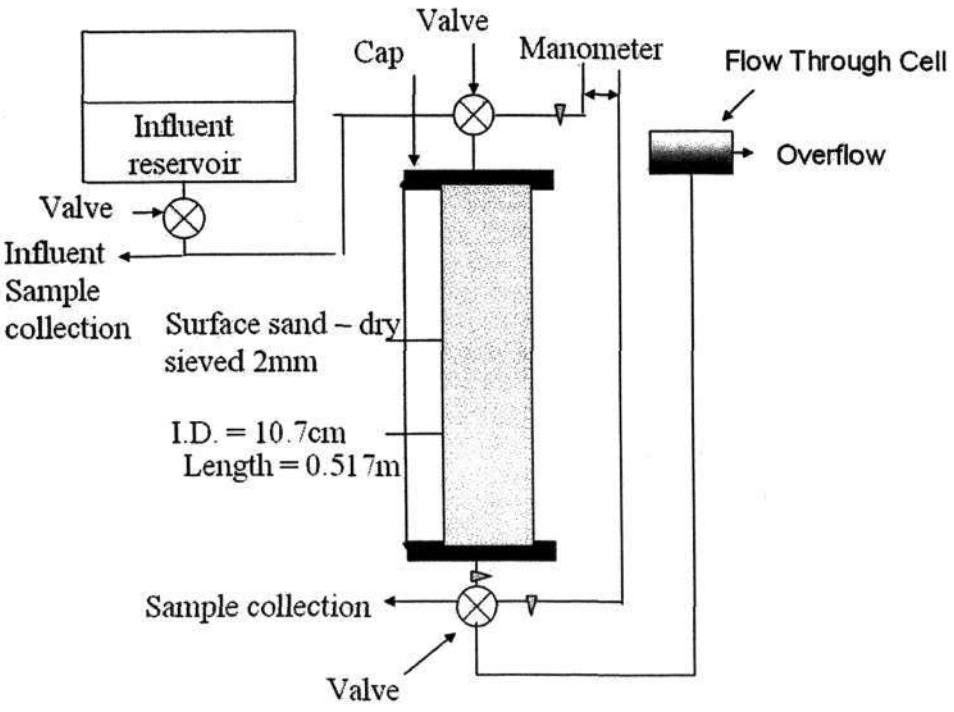

Figure 3.5 Schematic diagram of short term geochemistry column

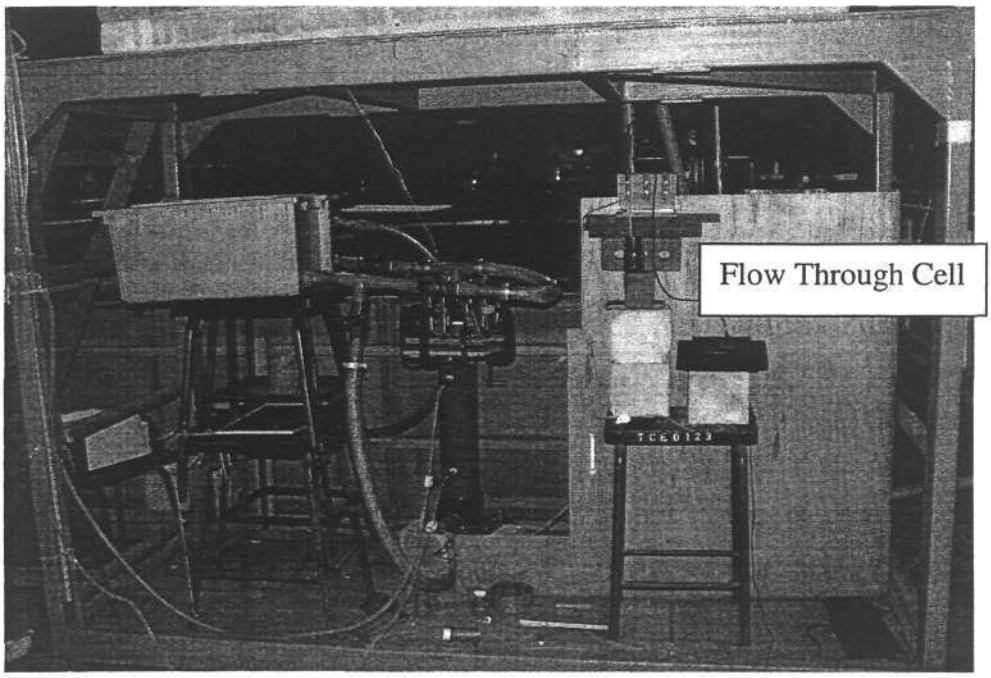

Figure 3.6 Photo of short term geochemistry column

3.7 Field RO Injection Studies

Field RO injection was conducted to better understand the geochemical transformations when high grade water was used to recharge the aquifer, as processes such as ion exchange and precipitation, etc., might lead to clogging and create detrimental impacts on the hydraulic performance of the aquifer.

The experiment was conducted by injecting slugs of RO treated waste water (RO), to study geochemical transformations during injection and the relative permeability of the different zones within the fill material. The RO water used was high grade water produced after secondary treated waste water had been purified using ultra-filtration and reverse osmosis. In total, about $40m^3$ of RO was injected through fully screened well (FSW) 1 (**Figure. 3.7**) into the top 5m of the saturated zone at Corner 2 as shown in Figure 1.4. The bottom 2m of the screened well was packed off, as the salinity of the groundwater at that depth is considerably higher than that of the groundwater in the upper 5 m of the aquifer. The amount of RO injected was approximately six pore volumes, assuming a 2m diameter cylinder of 5m thick fill material, having a porosity

of 0.4. Sampling was carried out from a continuous multi-channelled tubing (CMT), located 1 m away from the screened well, at regular intervals. In addition, samples were also collected from two different depths in the injection well. The samples were tested for electrical conductivity (EC), temperature and pH in the field, and brought back to the laboratory for further analysis.

The injections were carried out at a constant rate of 30L/min. The expected arrival time of RO at the CMT was about 210min. The flow rate was monitored using a flow meter and confirmed by level measurements in the RO water supply tank. The CMT ports 1-5 lied within the injection zone while ports 6 and 7 were outside the injection zone. For the CMT ports that lied within the injection zone, port 1 was located within the silty sand layer which had a lower permeability and the other ports were located within the more permeable zones (Chua et. al., 2004).

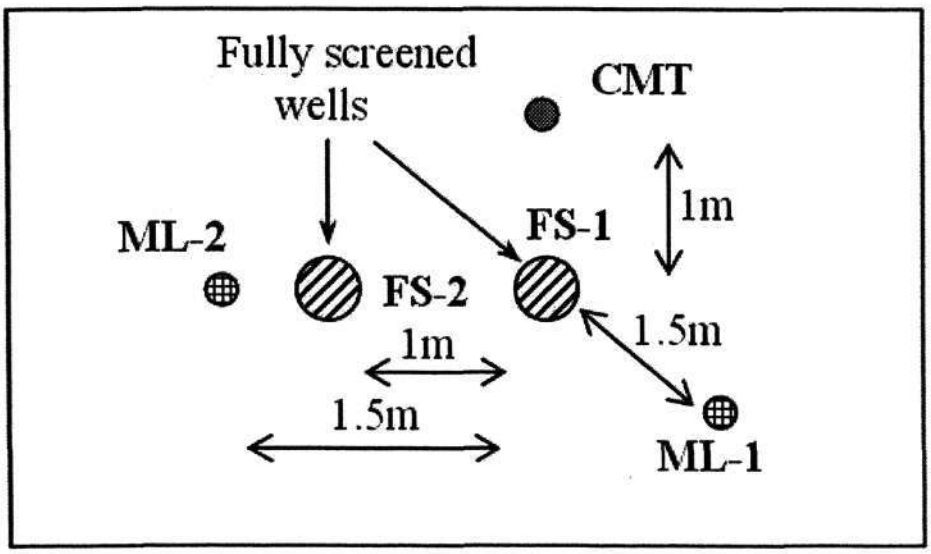

Figure 3.7 Schematic diagram of the location of pumping wells and sampling wells

3.8 Medium term Geochemistry Column Studies

A total of four 0.065 m diameter, 0.75 m length acrylic column were fabricated for the medium term geochemistry studies. This study is to investigate the geochemical effects during ASR operations using three types of recharge water, namely, SE, UF and RO.

The fourth column was re-circulated with native groundwater collected from corner 2 of the NTU test plot in Changi. At least 350 PV of influent was passed through these columns.

The experimental set up is as shown in **Figure 3.8** and **Figure 3.9**. The flow was driven by a pumping system with a top-down flow pattern. Five manometer ports were fixed at 18.75 cm intervals along the column. The ports were connected to a manometer board where head differences could be measured. On the other side of the column, there were three sampling ports. Syringe and needle were used to collect samples from these intermediate points on the column. The sampling port has a perforated rod that extends to half the diameter of the column in order to collect samples that were representative at that particular depth. At both ends of the column, samples could be collected via the sampling valve. All connections and tubings used in the set up were either stainless steel or Teflon®.

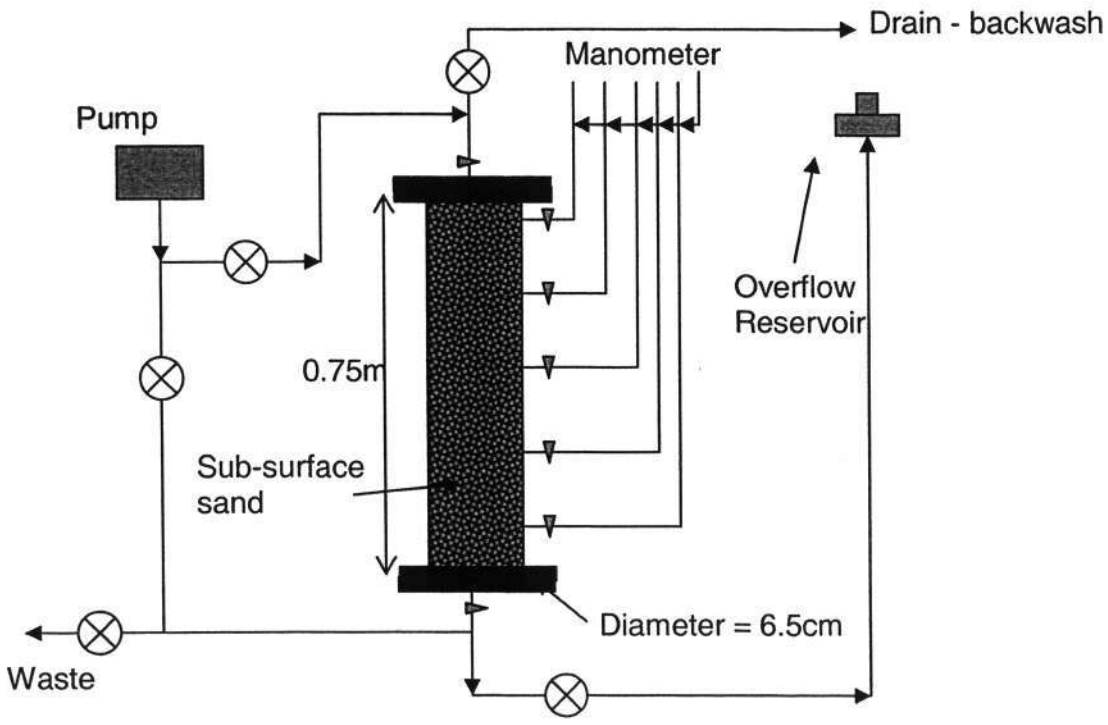

Figure 3.8 Schematic diagram of medium term geochemistry column

Flow rate measurement was done by weighing method, where the weight of effluent was taken over a period of time. The flow rate was verified against an in line flow meter connected to the effluent end of the column.

The hydraulic retention time, dispersivity coefficient and effective porosity were obtained through a tracer test. Chloride was used as a tracer and in-line EC measurement was used to detect the tracer breakthrough.

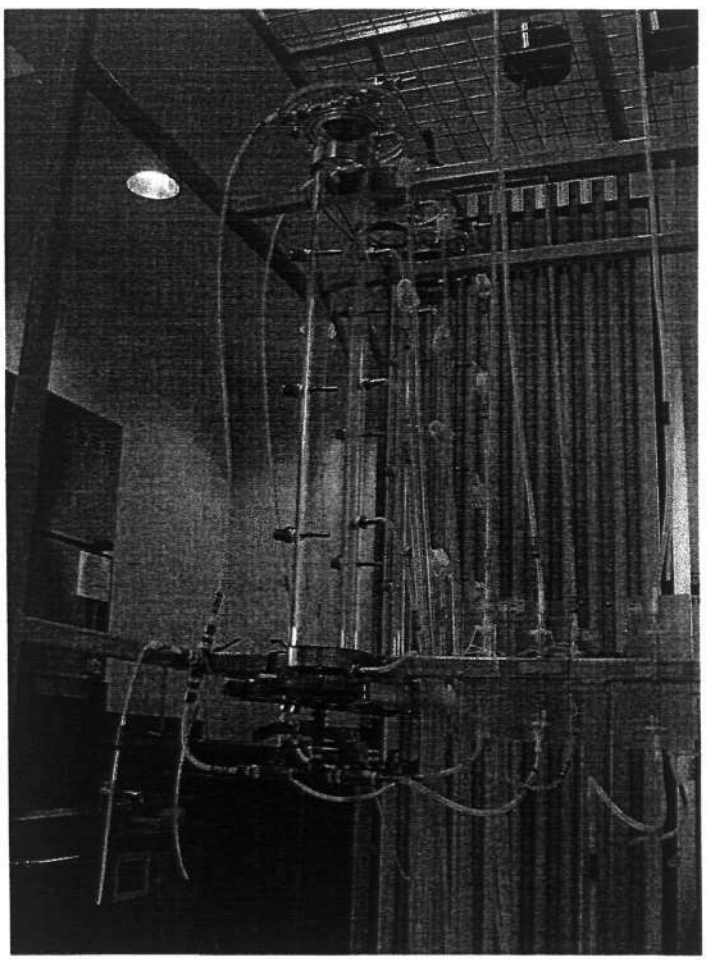

Figure 3.9 Photo of geochemistry column before sand packing

Samples were collected twice a day from the effluent and once from the influent. The water fed to the column was supplied on a daily basis. As the SE was relatively more turbid than UF and RO, the SE feed was continuously stirred with a magnetic stirrer.

Samples were analysed for temperature, pH, EC, DO, ORP, major cation, trace heavy metals, major anions, DOC, DIC and UVA-254nm.

4 RESULTS & DISCUSSIONS

4.1 Background

This project is to study the potential geochemical transformations during ASR operations at the Changi reclaimed land. Mineralogy studies had shown that quartz and carbonate mineral made up 90% of the sand assemblage. Results obtained from batch, column and field studies suggested that carbonate dissolution was the dominant geochemical effect. Ion exchange reactions were found to be more significant in the field study, but not in the laboratory experiments. One possible reason is that the field condition is more heterogeneous than expected. The findings are reported in the following sections.

4.2 Mineralogy

4.2.1 Physical Characteristics

Sand samples were collected from 4.8-6.5 m, 6.5-8.0 m 8.0-9.0 m and 10m below ground surface at corner 2 of NTU's test plot for geophysical analysis. Each of the samples underwent triplicate testing of sieve analysis, hydrometer test and specific gravity test. The grain size distribution curves of the three samples are shown in **Figure 4.1**. Fines content obtained through wet sieving accounted for only 2.9 % of the sand samples obtained from 4.8-6.5 m. Specific gravity was quite consistent among these three samples with an average of 2.65. $D_{50,}$ which represents the minimum diameter of the sand particles of which 50% of it would be passing through this sieve size, and is an indication of samples' uniformity, was found to be 0.34, 0.43 and 0.79 respectively.

The computation of hydraulic conductivity using pore size distribution had been well described in the literature. The Hazen method and empirical formula proposed by Alvamani and Zekai were used to estimate the hydraulic conductivity. The results are compared with slug test results conducted at corner 2 of the test plot in **Table 4.1**.

Table 4.1 Comparison of hydraulic conductivity value obtained from grain size distribution and slug test

	Hydraulic Conductivity (m/day)		
	Hazen Method	Alvamani & Zekai	Slug Test
4.8 to 6.5m	12.48	16.97	31.8
6.5 to 8.0 m	17.28	17.42	39.4
8.0 to 9.0 m	29.2	30.53	-

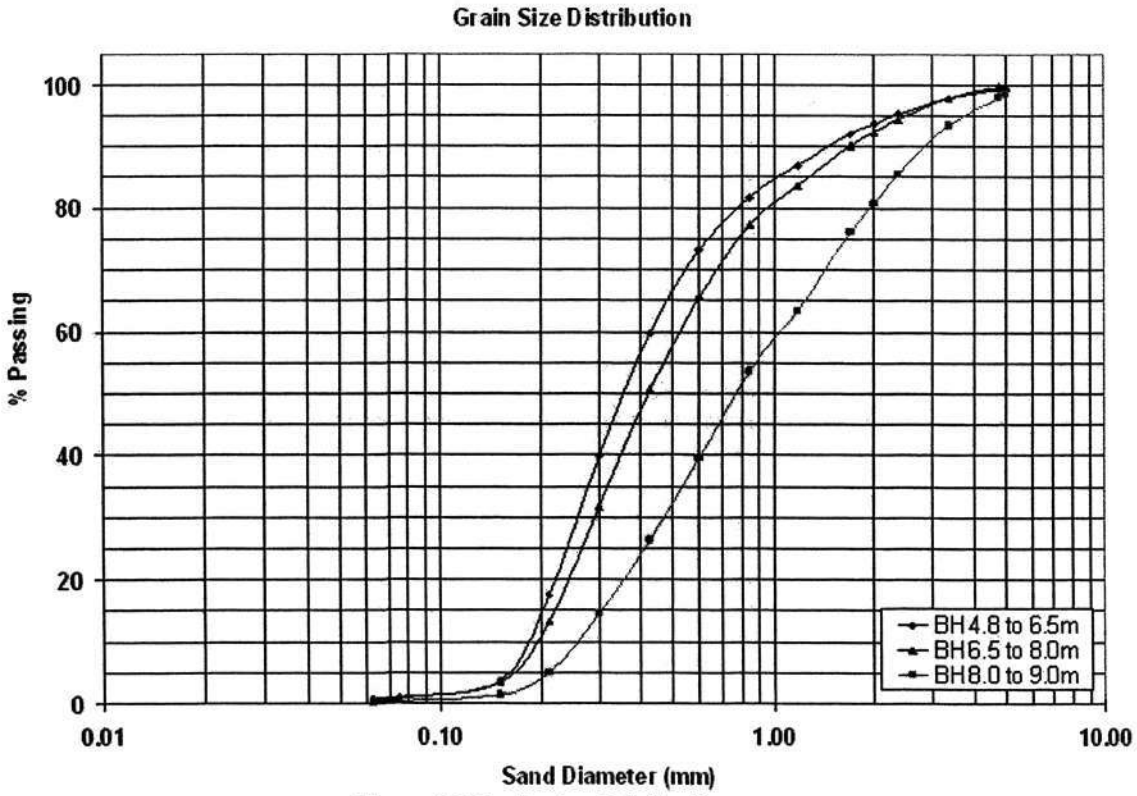

Figure 4.1 Grain size distributions

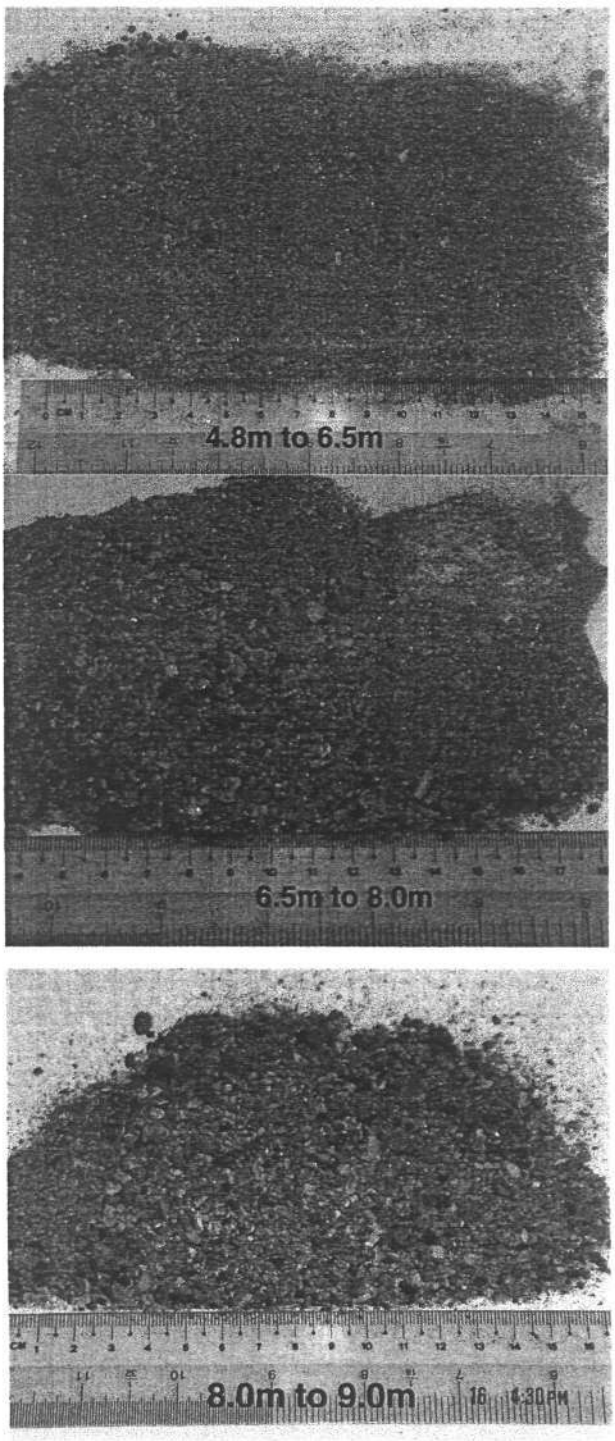

Figure 4.2 Photos of sand samples from different depth

4.2.2 Chemical Characteristics

The sand samples collected from the Changi reclaimed land were characterised using the tests described in the Chapter 3. The main objective was to gain an understanding of the aquifer material in terms of its composition. This was necessary for predicting the performance of the sand during ASR operations.

The main source of the Changi fill sand was from regional sea beds and consisted of coastal sands and sea shells. The mineralogy results presented in **Table 4.2** show significant amounts of Ca, Mg and carbonate, suggesting that the quartz sand contained significant amounts of calcite and/or magnesium calcite. **Table 4.2** also summarises the results for the aqueous chemistry of major ions and trace elements.

Organic content was low at 0.7%, in which organic carbon content was 0.3%. The organic carbon content was found to be on the same level in comparison with a similar calcareous aquifer in Adelaide (Pavelic et al., 2001). A low organic carbon content could be an indication of low sorptive capacity and hence negligible retardation as shown by Roberts et al. (1982), Fram et al. (2003) and Rivett et al. (2001).

The Carbonate content was relatively high at 14.63 g CO_3^{2-}/100 g sand, indicating that carbonate-based minerals would be of significant concentrations in the mineral phase. At the same time, it was also observed that calcium ion was notably more abundant than other metal ions in the mineral phase. This suggested that calcite ($CaCO_3$) might be the dominant mineral phase in the Changi fill material. Organic content was low at 0.7%, in which organic carbon content was 0.3%. The organic carbon content was found to be on the same level in comparison with a similar calcareous aquifer in Adelaide (Pavelic et al., 2001). This information was significant because calcite was one of the most reactive minerals in groundwater chemistry and thus was expected to readily dissolve during artificial recharge.

Iron and Aluminium were the next most abundant heavy metals in the mineral assemblage. The result confirmed the initial assumption that the vast amount of visible black particles were ferromagnetic minerals.

Table 4.2 Soil characterisation results for subsurface sand

Soil Parameters	Sub surface sand
Soil pH	9.72 (0.06)
Temperature (°C)	21.3
Carbonate Content (%)	14.63 (1.20)
Organic Content (%)	0.5876 (0.3085)
Metal Digestion (%)	
Ca	5.1595 (0.6271)
Mg	0.2230 (0.0026)
Na	0.0642 (0.0016)
K	0.0329 (0.0006)
Al	0.0823 (0.0068)
Fe	0.6933 (0.0194)
Mn	0.0300 (0.0003)
Ba	0.0028 (0.0011)
Cr	0.00117 (0.00002)
Cu	N.D.
Pb	0.00033 (0.00004)
Ni	0.00015 (0.00001)
Ag	N.D.
Cd	N.D.
Se	0.00006 (0.00001)
As	0.00091 (0.00005)
Zn	0.00089 (0.00014)
Cation Exchange Capacity, CEC ($cmol_c kg$)	0.0070 (0.0011)
Anion Exchange Capacity, AEC (cmol/kg)	8.0931 (0.1393)

Note: Carbonate content, organic content and metal ions reported as % mass of soil. For all parameters, the average values and standard deviations (in parentheses) are reported.
N.D. = not detected by instrument

Sodium and potassium did not show up in great amounts. The vast majority of sodium and potassium ions in the water samples owed their origin to the sea. Halite composition in the sand accounted to less than 0.1% by weight.

Low concentrations in chromium, lead, manganese, nickel and zinc were detected in the metal digestion of the subsurface sand. Cadmium, silver and copper were below the detection limits. The results indicated that the surface sand was not contaminated with heavy metals and hence suitable for water recharge and reuse.

The mineralogy tests results showed that the anion exchange capacity was much higher than the cation exchange capacity. The cation and anion exchange capacities in soil material were essential for developing a preliminary understanding on how the geochemistry of recharge water might vary over time, especially when more aggressive highly treated effluents were used for recharge. The low cation exchange capacity (~ 7 $x10^{-3}$ cmol/kg) indicated that the sand was highly limited in retaining cations against leaching. The high anion exchange capacity (≈ 8 cmol/kg) indicated that there would be significant retention of anions. Finally, the cation exchange capacity (CEC) also had implications on solute transport because a low CEC indicated a low retardation factor since R ∝ CEC (Parkhurst and Appelo, 1999). Solutes therefore were expected to move through the sand matrix with least dispersion without being significantly retarded by sorption mechanisms.

4.2.3 XRD

Three sand samples were collected from 3.0 to 4.0m, 4.8 to 6.5m and 8.0 to 9.0m depth at corner 2 and were analysed for XRD. FULLPAT was used to quantify the mineral composition in the sand. The results obtained are shown in **Table 4.3**, **Table 4.4** and **Table 4.5** respectively. The results shown were the averages of at least 12 replicates.

The results were quite conclusive that the main compositions were quartz and carbonate related minerals in which quartz made up at least 60% by weight of the

minerals. Carbonate minerals were basically calcium and magnesium carbonate or their complexes.

Table 4.3 XRD results for 3.0 to 4.0m, unit in % by mass

Contents	Mean	Standard deviation
Quartz	55.7	2.77
Halite	0.2	0.12
Aragonite	8.6	2.69
Calcite	3.8	1.23
Pyrite	0.7	0.74
Magnesium Calcite Syn $(Mg_{0.06}Ca_{0.94})(CO_3)$	6.3	1.42
Calcite, Magnesian $(Mg_{0.1}Ca_{0.9})(CO_3)$	5.1	2.40
Calcite, Magnesian $(Mg_{0.64}Ca_{0.36})(CO_3)$	6.0	1.95
Gypsum	1.2	0.87
Hematite	1.7	0.72
Magnetite	1.7	2.29
Kaolinite	9.3	1.94

The composition of the mineral at each depth generally agreed well with the hydraulic conductivity values shown in **Table 4.1**. The lowest clay content in the 8.0 to 9.0m (**Table 4.5**) sample corresponded to the highest hydraulic conductivity. Unfortunately, the XRD analysis for 6.5 to 8.0m was not performed and comparison could not be done. The hydraulic conductivity obtained at this layer through slug test was 19.7 m/day, was much lower than that of the coarse sand layer. The low conductivity value corresponded well with the relatively high clay content as shown in **Table 4.3**.

The XRD results also indicated that the amount of chloride, sulphate and sulphide in the sand matrix were insignificant. The result confirmed the findings from acid digestion tests.

Table 4.4 XRD results for 4.8 to 6.5m, unit in % by mass

Contents	Mean	Standard deviation
Quartz	63.8	8.40
Halite	0.1	0.00
Aragonite	14.2	4.80
Calcite	2.3	0.27
Pyrite	0.5	0.41
Magnesium Calcite Syn $(Mg_{0.06}Ca_{0.94})(CO_3)$	4.8	2.71
Calcite, Magnesian $(Mg_{0.1}Ca_{0.9})(CO_3)$	5.6	1.76
Calcite, Magnesian $(Mg_{0.64}Ca_{0.36})(CO_3)$	4.5	1.04
Gypsum	0.9	1.16
Hematite	0.9	0.64
Magnetite	0.7	0.55
Kaolinite	1.9	0.93

Table 4.5 XRD results for 8.0 to 9.0m, unit in % by mass

Contents	Mean	Standard deviation
Quartz	69.8	6.92
Halite	0.1	0.06
Aragonite	10.7	6.16
Calcite	3.0	1.70
Pyrite	1.6	0.80
Magnesium Calcite Syn $(Mg_{0.06}Ca_{0.94})(CO_3)$	4.9	3.17
Calcite, Magnesian $(Mg_{0.1}Ca_{0.9})(CO_3)$	3.7	2.74
Calcite, Magnesian $(Mg_{0.64}Ca_{0.36})(CO_3)$	3.6	2.21
Gypsum	2.6	1.87

4.2.4 SEM

SEM studies were conducted to examine the structure of the minerals in the sand with emphasis given to calcareous minerals. Calcareous minerals originated from the sea and were made up mainly of shell fragments and remains of living organism. The existence of these materials was both an advantage and disadvantage. The advantage was that these minerals were highly porous and hence would increase the storage capacity of the aquifer. **Figure 4.3** shows a porous shell fragment obtained from a sand sample. **Figure 4.4** shows the enlarge image of a shell fragment. The disadvantage was that these calcareous minerals could be a source of carbonate dissolution and thus caused potential soil problem, e.g. local soil collapsing or clogging downstream due to precipitation of the dissolved mineral

As discussed in the previous section, there were tiny black particles in the sand matrix. Several particles were selected and scanned for its images. **Figure 4.5** shows an image of these particles. The particles could be metal oxides of iron and aluminium.

Figure 4.3 SEM image of sea shell's fragment (x11 magnification)

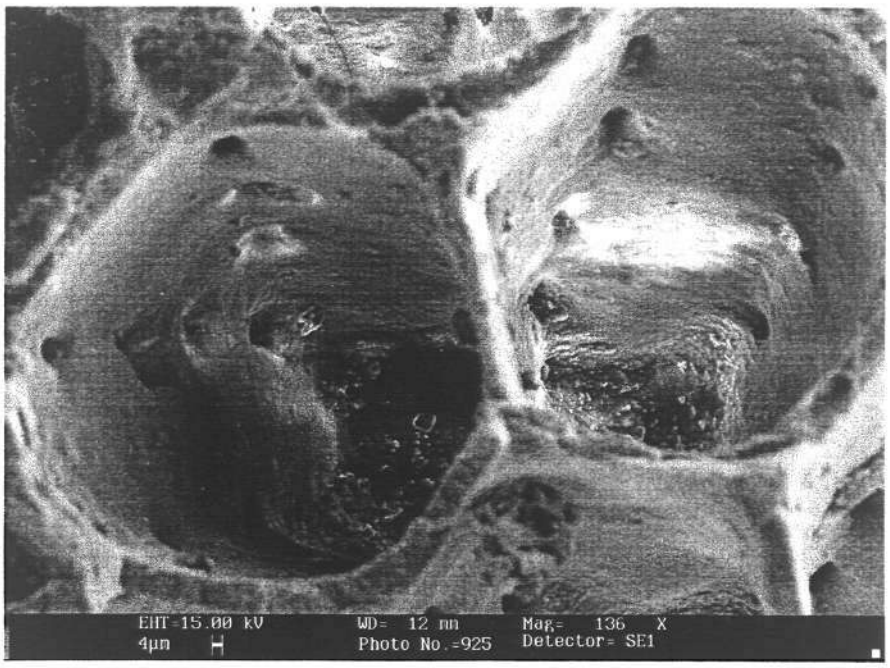

Figure 4.4 SEM image on the enlarged (x136 magnification)

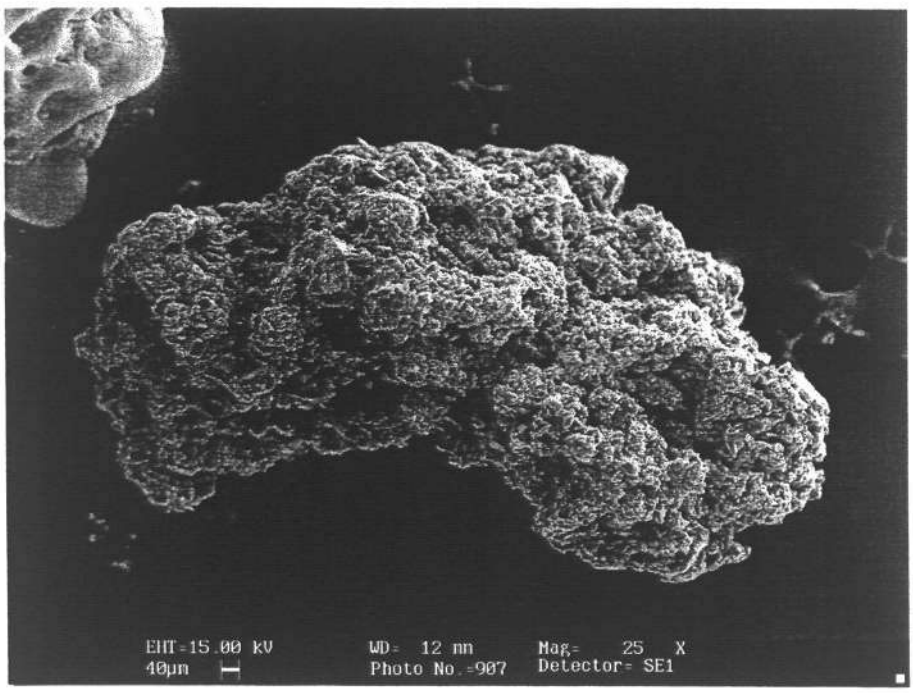

Figure 4.5 SEM image of iron oxides (x25 magnification)

4.3 Characterisation of Recharge Water

Water characterisation of the Bedok NEWater plant effluents and rain water were carried out periodically especially during the laboratory column studies when water samples were collected every fortnight. The rain water was collected from the Changi reclaimed land site using a 304 stainless steel bucket. The water samples collected were characterised as discussed in Chapter 3.

The quality of rain water, NEWater and RO water were generally very good and were well within the USEPA Drinking Water Standards as shown in **Table 4.6** and **Table 4.7**. The tabulated data were the average water quality during April to June 2004. One concern was the high sulphate content in rain water, which was an indication of "acid" rain occurring. Nonetheless, the sulphate was likely to have originated from sea spray rather than industrial pollution as the site was closer to the sea. From the results, groundwater contamination should not be a concern if NEWater or RO effluent were used as recharge water.

Table 4.6 Water characterisation of Bedok NEWater plant effluent and rain water

Water Quality Parameters	*EPA Water Quality Standard (MCL)*	*NEWater*	*Reverse Osmosis*	*Ultra Filtration*	*Rain Water*	*Secondary Effluent*
Tubidity (NTU)	0.3	0.2	0.3	0.2	0.3	1.8
Colour (Hazen units)	15	0.0	0.7	6.6	0.7	12.8
Conductivity (μS/cm)	1600	45.7	48.1	728.7	54.7	1066.8
pH Value	7.4 – 9.8	9.2	7.8	7.4	9.0	8.0
Total Dissolved Solids (mg/L)	1000	13.0	8.3	374.8	17.3	1201.0
Total Organic Carbon (mg/L)	N/A	0.36	0.42	4.47	1.60	7.52
Total Alkalinity ($CaCO_3$) (mg/L)	13 – 120	11.0	9.8	5.4	7.4	78.0
Total Hardness ($CaCO_3$) (mg/L)	10 – 142	1.1	0.97	62.2	16.9	97.0
Total Suspended Solids (mg/L)	N/A	0.4	0.1	0.9	1.1	3.6
Total Inorganic Carbon (mg/L)	N/A	2.5	2.2	10.1	1.7	15.5
Ultra Violet Absorbance (cm^{-1})	N/A	0.01	0.01	0.09	0.01	0.16
Anions (mg/L)						
Chloride (Cl)	500	17.5	18.0	121.0	16.9	183.4
Nitrate (N)	10	0.92	1.11	5.79	N.D.	7.44
Sulphate (SO_4)	500	2.7	2.3	55.4	11.4	83.2

Table 4.7 Metal ions analysis of Bedok NEWater plant effluent and rain water

Water Quality Parameters	*EPA Water Quality Standard (MCL)*	*NEWater*	*Reverse Osmosis*	*Ultra Filtration*	*Rain Water*	*Secondary Effluent*
			Metals (mg/L)			
Aluminium (Al) (0.0006)	1	0.06	0.05	0.05	0.12	0.12
Barium (Ba) (0.001)	1	0.01	0.03	0.03	0.15	0.16
Cadmium (Cd) (0,001)	N/A	N.D.	N.D.	N.D.	N.D.	N.D.
Calcium (Ca) (0.001)	(4 – 31)	0.40	0.36	15.60	5.97	24.12
Copper (Cu) (0.001)	1.3	N.D.	0.01	0.2	0.02	0.01
Chromium (Cr) (0.001)	0.05	N.D.	0.01	0.01	0.01	0.01
Iron (Fe) (0.001)	0.	0.03	0.03	0.07	0.08	0.12
Lead (Pb) (0.006)	0.15	N.D.	N.D.	N.D.	N.D.	N.D.
Manganese (Mn) (0.001)	N/A	N.D.	N.D.	0.28	N.D.	0.04
Magnesium (Mg) (0.003)	(0.5 – 11)	0.02	0.02	5.65	0.49	8.93
Nickel (Ni) (0.001)	N/A	N.D.	N.D.	0.02	N.D.	0.02
Potassium (K) (0.003)	(0.5 – 1)	0.59	0.67	12.84	0.27	19.96
Selenium (Se) (0.020)	0.05	0.02	0.02	0.02	0.03	0.04
Silver (Ag) (0.001)	N/A	N.D.	N.D.	N.D.	N.D.	N.D.
Sodium (Na) (0.005)	(3 – 22)	7.50	7.46	94.86	2.19	137.73
Zinc (Zn) (0.001)	5	N.D.	0.01	0.03	0.19	0.03

The UF and SE effluents were generally of good quality except for potassium and sodium concentrations. However, these two parameters were usually not a major health concern in potable water. The TDS in the SE effluent exceeded the EPA standards of 1,000 mg/L, but was comparable to the native groundwater quality as shown in **Table 1.1**.

For heavy metals, the method detection limits were tabulated as the bracketed values beside the water quality parameters in **Table 4.7**. The Barium concentration in the SE was considerably higher than the other waters as well as in the groundwater, but was well within the stipulated MCL.

As a result, all four types of waters were acceptable for injection into the aquifer without risks of causing groundwater contamination.

4.4 Batch Leaching Studies

Batch studies were conducted on surface sand and subsurface sand collected from 5m and 8m below ground surface. The fines portion of each of these sands (passing through 2mm U.S. Standard #10 sieve) were used for the batch experiments as this fraction is the most geochemically reactive (Masscheleyn et al., 1991; Allard, 1995). Five types of recharge water were used as leachant, giving a total of 15 combinations. Results on the surface sand (Chan, 2004) and the 8m subsurface sand (Lim, 2004) had been reported. In this study, the results on the 5m subsurface sand would be presented as sand collected from this depth was used to pack the column.

The results showed that carbonate dissolution was the dominant geochemical effect during mineral-solution interaction. The control sample with no sand was used as the blank. The sorption or dissolution of individual ions was then computed by subtracting the original concentrations in the blank. **Figure 4.6** shows the effect of sorption or dissolution of major cations after 7 days of contact time. The increase in concentrations for calcium and magnesium ions indicated dissolution. The effect in RO was most significant as calcium concentration increased from below detection limit to 8.059 mg/L. The ranking in terms of decreasing aggressiveness was RO, NEWater, rain water, UF and SE.

These results suggested that the extent of dissolution effect was sensitive to the pH and ionic strength. The lower the pH, the more likelihood the carbonated minerals would dissolute. The dissolution process would continue until the recharge effluent was saturated with the particular mineral. This was confirmed by the saturation indices of calcite and aragonite approaching equilibrium. The ionic strength was crucial as it had a direct relationship with the solubility product of the mineral. In a pure water phase, the solubility product was represented by the product of the molar concentration of its dissociated ions. In an environmental matrix, the solubility product was represented by the product of the activities of its dissociated ions, in which the activity was affected by

the ionic strength as shown in section 2.2.4. In general, a higher ionic strength would decrease the solubility product of the targeted mineral.

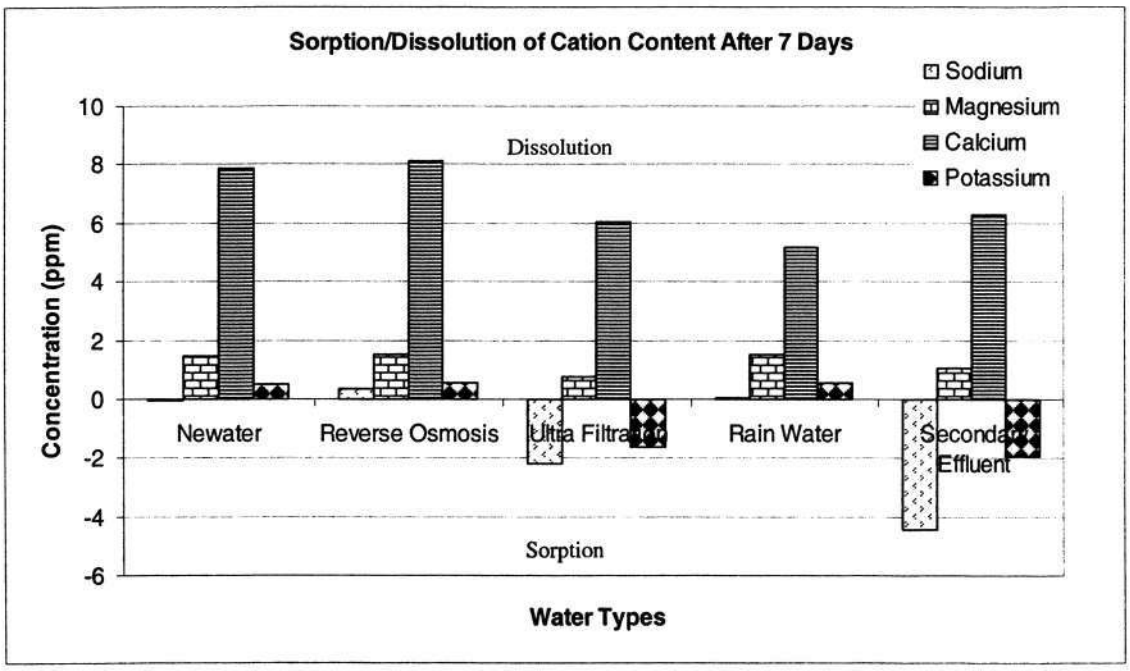

Figure 4.6 Sorption/dissolution of major cation during batch test

Another interesting observation was the loss of sodium and potassium ions in UF and SE batch samples. Sorption was a possible explanation for this, but sorption of monovalent metal elements in sand was not well-documented in the literature. Another possible reason was ion exchange, in which divalent ions were released to the recharge effluent in exchange for monovalent ion as shown in section 2.3.11.

Table 4.8 compared the batch test results with the drinking water quality of Anaheim, California. Anaheim Public Utilities, which governs the Orange County water reclamation project, was one of the pioneers in operating an operating ASR scheme. High quality tertially treated water was recharged to the ground before being recovered as potable water. As a result, it would be interesting to compare the quality of the batch effluent to that of Anaheim. The values tabulated next to the Anaheim's water quality data were results obtained through batch studies after seven days of contact time. The highlighted values represented quality inferior to that of Anaheim, whereas the non-

highlighted values indicated better quality for that particular parameter. The bracketed values below the batch results denoted the changes in the respective parameters during the batch leaching experiments.

For NEWater, RO and rain water, most of the parameters considered were better than those of Anaheim with the exception of aluminium, chromium and selenium. Rain water posed a concern with it high barium concentration. Barium originated from rain water itself as its concentration was also persistently high in the control samples. Its source was air-borne as the samples were collected during precipitation into the container without contact with the ground.

The major cations appeared to be more dominant in the UF and SE batch tests, in which sodium, potassium and chloride were considerably higher than those of Anaheim. This is not unexpected as it was comparing treated wastewater with tertiary treated effluent.

Batch test results could provide an indication of the possible outcomes if actual ASR operations were carried out. With a higher water to soil ratio and greater interaction between minerals and recharge water, the batch studies would represent the maximum leachable contaminant level.

Table 4.8 Comparison of Batch test results with drinking water quality from Anaheim, CA., U.S.

Water Quality	*Anaheim, CA, U.S.*	*NEWater*	*Reverse*	*Ultra*	*Rain*	*Second.*
Parameters	**Wells**		**Osmosis**	**Filtration**	**Water**	**Effluent**
Conductivity (μS/cm)	672 - 1120	86	88	691	94	1044
		(38.58)	(45.3)	(5.67)	(42.68)	(0.17)
pH Value	7.3 - 8.2	9.27	7.35	8.70	9.21	8.28
		-(0.12)	-(0.04)	(0.30)	(0.13)	(0.50)
Dissolved Organic Carbon (mg/L)	Not Available	1.04	1.18	5.45	2.19	8.11
		(0.543)	(0.909)	(0.962)	(0.706)	-(0.112)
Total Alkalinity (CaCO3) (mg/L)	125 - 233	30.34	29.69	52.77	27.50	79.37
		(19.20)	(18.69)	(10.61)	(18.61)	(14.70)

Total Hardness (CaCO3) (mg/L)	254 - 457	26.96	26.93	109.70	35.42	153.94
		(21.86)	(22.45)	(8.41)	(15.24)	(7.74)
Total Inorganic Carbon (mg/L)	Not Available	6.55	6.31	12.39	5.99	19.07
		(4.39)	(4.16)	(2.33)	(4.10)	(3.07)
B) Anions (mg/L)						
Chloride (Cl)	41 - 107	17.68	18.04	121.23	16.94	184.28
		(0.20)	(0.07)	(0.20)	(0.07)	(0.87)
Nitrate (NO_3)	5.76 - 28.79	1.51	1.13	5.77	N.D.	7.51
	1.3 - 6.5	(0.59)	(0.01)	-(0.02)	(0.00)	(0.07)
Sulphate (SO_4)	93 - 207	4.37	4.05	55.36	12.34	86.84
		(1.67)	(1.76)	-(0.01)	(0.96)	(3.69)
C) Cations (mg/L)						
Aluminium (Al)	<0.0067	0.087	0.096	<0.006	0.151	0.080
		(0.032)	(0.047)	-(0.051)	(0.032)	-(0.038)
Barium (Ba)	<0.124	0.034	0.034	0.013	0.175	0.149
		(0.026)	(0.001)	-(0.020)	(0.027)	-(0.014)
Cadmium (Cd)	Not Available	<0.001	<0.001	<0.001	<0.001	<0.001
		N/A	N/A	N/A	N/A	N/A
Calcium (Ca)	71 - 137	8.087	8.059	24.361	11.917	32.538
		(7.886)	(8.059)	(6.029)	(5.182)	(6.285)
Copper (Cu)	<0.18	0.008	0.018	0.023	0.005	0.010
		(0.005)	(0.009)	(0.001)	-(0.010)	(0.004)
Chromium (Cr)	<0.0043	0.006	0.008	0.009	0.004	0.007
		(0.002)	(0.001)	(0.0)	-(0.003)	-(0.002)
Iron (Fe)	< 0.107	0.064	0.077	0.024	0.098	0.095
		(0.038)	(0.049)	-(0.042)	(0.019)	-(0.024)
Lead (Pb)	Not Available	<0.006	<0.006	<0.006	<0.006	<0.006
		N/A	N/A	N/A	N/A	N/A
Manganese (Mn)	Not Available	0.004	0.003	0.015	0.002	0.026
		(0.002)	(0.001)	-(0.013)	-(0.001)	-(0.013)
Magnesium (Mg)	15 - 28	1.149	1.159	7.595	1.811	11.155
		(1.470)	(1.497)	(0.769)	(1.521)	(1.084)
Nickel (Ni)	Not Available	0.002	0.002	0.011	0.003	0.016
		(0.0)	-(0.001)	-(0.005)	-(0.002)	-(0.008)
Potassium (K)	3.4 - 8.5	1.638	1.649	11.858	1.367	17.640
		(0.520)	(0.530)	-(1.618)	(0.554)	-(1.938)
Selenium (Se)	<0.0071	<0.020	0.023	0.027	0.021	0.035
		N/A	(0.001)	(0.003)	-(0.009)	-(0.001)
Silver (Ag)	Not Available	<0.001	<0.001	<0.001	<0.001	<0.001
		N/A	N/A	N/A	N/A	N/A
Sodium (Na)	41 - 102	7.573	7.389	100.560	3.164	140.141

Zinc (Zn)	<0.20	-(0.078) 0.007 (0.003)	(0.367) 0.011 (0.0)	-(2.177) 0.039 (0.014)	(0.054) 0.002 -(0.189)	-(4.435) 0.019 -(0.010)

4.5 Short Term Column Studies

4.5.1 Experimental Setup

A short term column study was carried out to investigate the geochemical transformations during the first few pore volumes of artificial recharge. The geochemistry effects were thought to be greatest during this stage, as the minerals would be depleted at the latter stages due to "flushing out" effect.

A 0.517m length and 0.107m internal diameter acrylic column was set up to conduct the experiments as discussed in section 3.5. **Table 4.9** tabulates some hydraulic characteristics of the column.

Table 4.9 Basic hydraulic properties for short term column

Parameters	*Findings*
Length of Column, (m)	0.517
Internal Diameter, (m)	0.107
Flow Rate, (ml/min)	2.61 ± 0.083
Pore Volume, (ml)	1851.9
Hydraulic Conductivity, (m/day)	14.30
Porosity	0.3984

The hydraulic conductivity was determined as discussed in section 3.5.3. As the manometers were fixed at 0.3 m apart, the flow length, L, was thus fixed. The head difference between the ports was read directly from the manometers. Pairs of readings of flow rates and head differences were collected for computation of the hydraulic conductivity. The results are plotted in **Figure 4.7** with the flow rate ranging from 0.43 to 6.24ml/s. The results show that the column behave linearly within the range of flow rates tested. As a result, it would be prudent to operate the column at a flow rate within the linear range. The hydraulic conductivity was found to be 0.000166 m/s or 14.3 m/day.

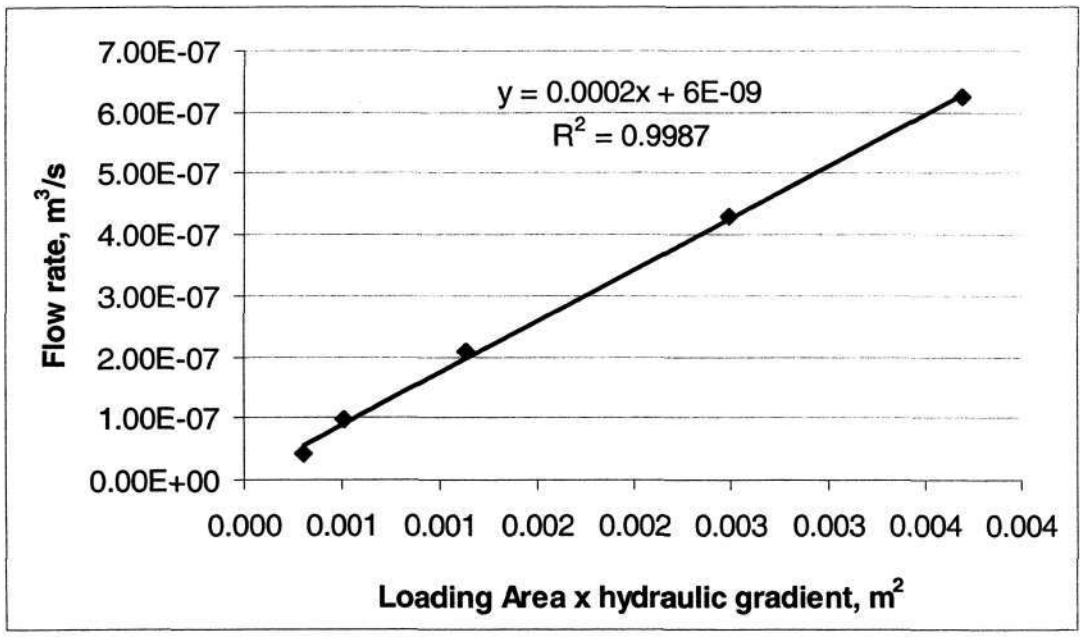

Figure 4.7 Results on hydraulic conductivity test, flow rate v.s. area x hydraulic gradient

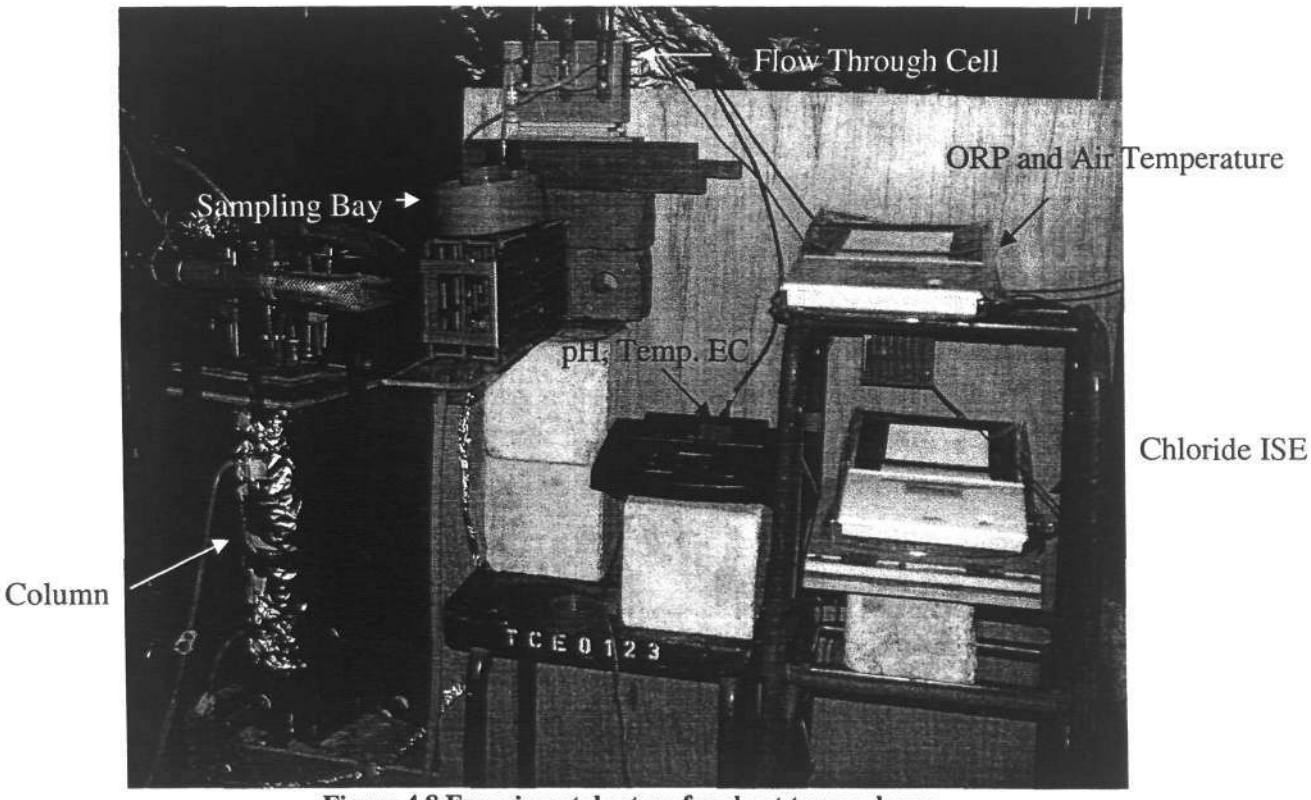

Figure 4.8 Experimental set up for short term column

The column was first saturated with native groundwater collected from Corner 2 of the test plot. RO water was then recharged to the column for 53 hours at a flow rate of 2.61 ± 0.08 ml/min. In-line measurement of pH, temperature, EC, ORP, chloride ISE was carried out using the in-line flow through cell. The RO influent was also measured for its pH, temperature and conductivity. The air temperature was recorded using a separate temperature probe. Water samples were collected hourly immediately after the flow through cell. The time lag in the tubing leading to the sampling bay was determined to be insignificant compared to the hydraulic retention time of the column. The experimental set up is shown in **Figure 4.8**.

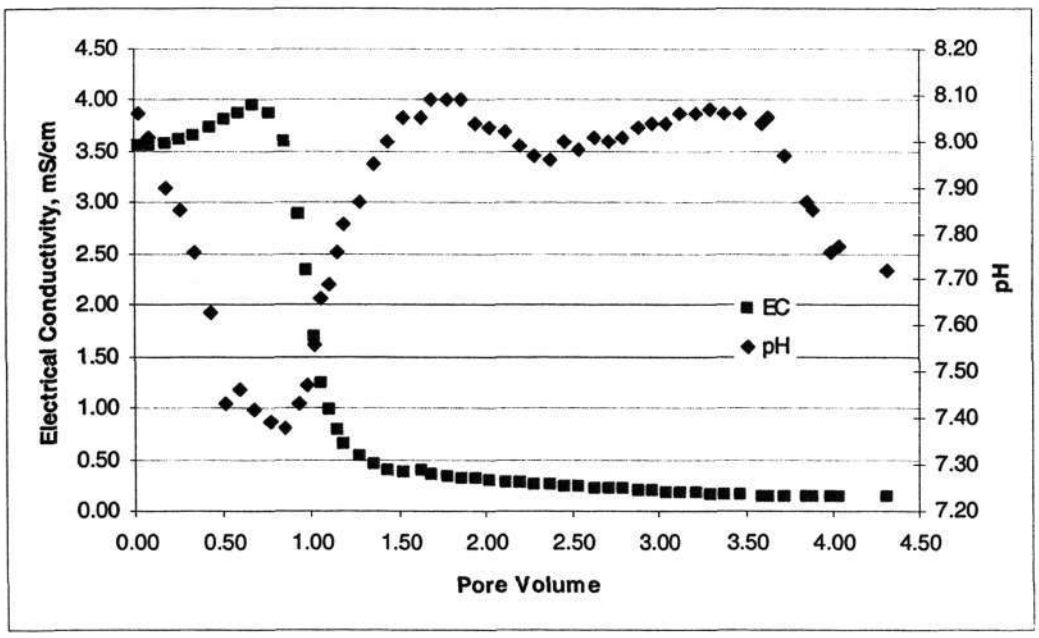

Figure 4.9 Relationship of pH against EC against pore volume

4.5.2 Results and Discussions

Results of pH and EC for the column effluent are plotted in Figure 4.9. At one pore volume, a sharp drop in EC was accompanied by an increase in pH. This observation indicated that carbonate dissolution had taken place as soon as RO flowed through the sand column, as the presence of carbonate species would increase the pH values. However, there were several uncertainties associated with this plot. Firstly, the drop in

pH within the first PV could probably be due to short circuiting of RO which had a lower pH. Secondly, the instability in the effluent pH in the region of 1.5-4.0 PV was probably due to temperature variations. The temperature fluctuation was within 5 °C within a 24 hours span. The temperature variations are plotted against pH in **Figure 4.10**. It could be seen clearly that a drop in temperature increases the pH, and vice versa.

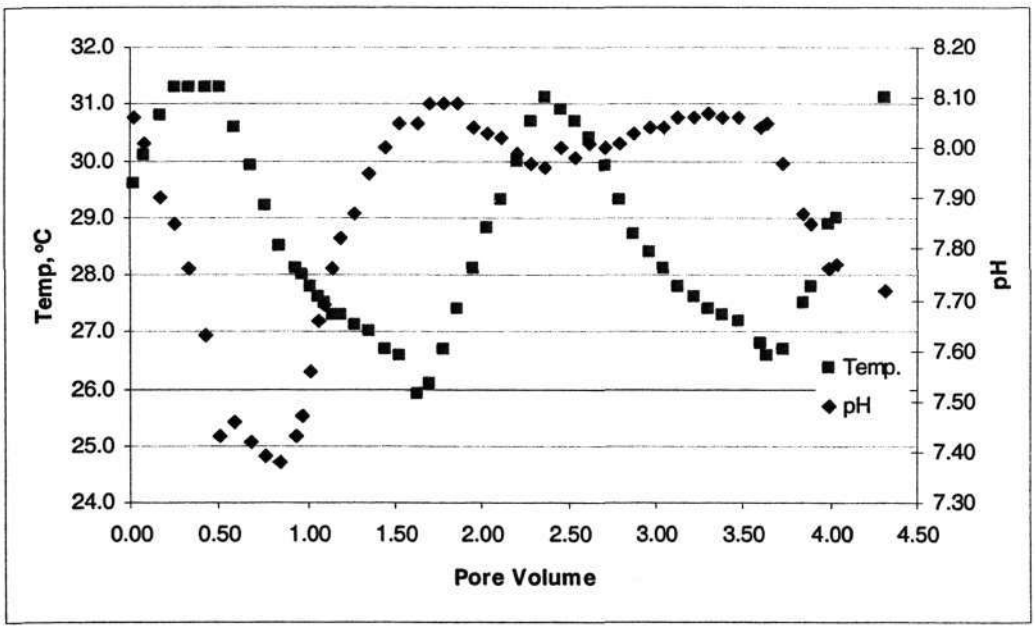

Figure 4.10 Effect of Temperature on pH measurement

Samples collected were analysed for the major cations and anions. Ion balance was performed and 73% of the samples analysed had an ion balance of less than 10% error. In order to identify the individual geochemical effect, several approaches had been adopted. The relative composition of sodium ion and the sum of calcium and magnesium ion (Ca + Mg) were compared in **Figure 4.11**. The values were normalised against the total cation for ease of comparison. The changes in composition between Na and (Ca + Mg) were correlated. The curve of Na/Total Cation was a mirror image of (Ca + Mg)/Total Cation. It was expected as these three cations represented more than 95% of the total cations.

At the point of breakthrough, the sodium composition increased, whereas (Ca + Mg) decreased. This indicated the occurrence of ion exchange. Under a situation with no

ions rich medium, e.g. clay, silt etc, carbonate dissolution should be the dominant effect, in which the (Ca + Mg) composition will increase while the sodium concentration remains virtually unchanged, as halite source was not found in the sand. However, if silty material did exist, it would tend to attract ions with a higher positive charge, since silty material was negatively charge in nature. As a result, sodium ions were released into the effluent. Ion exchange, which related to aquifer freshening, primarily affects the saturation state for calcite by taking up calcium ions onto the exchanger, which may stimulate further calcite dissolution and acid consumption (Bishop and Lloyd, 1990; Appelo, 1994; Melo et al., 1999). Interestingly the zone of high pH in the transition zone (**Figure 4.10**) corresponds to the zone of sodium enrichment and (Ca + Mg) depletion (**Figure 4.11**), supporting the coupling of ion exchange and calcite dissolution. Therefore, it was concluded that ion exchange would be a concern during the initial stage of artificial recharge. Carbonate dissolution also could not be neglected, as ion exchange was actually induced by dissolution effect, in which calcium, magnesium, etc, were released into the effluent.

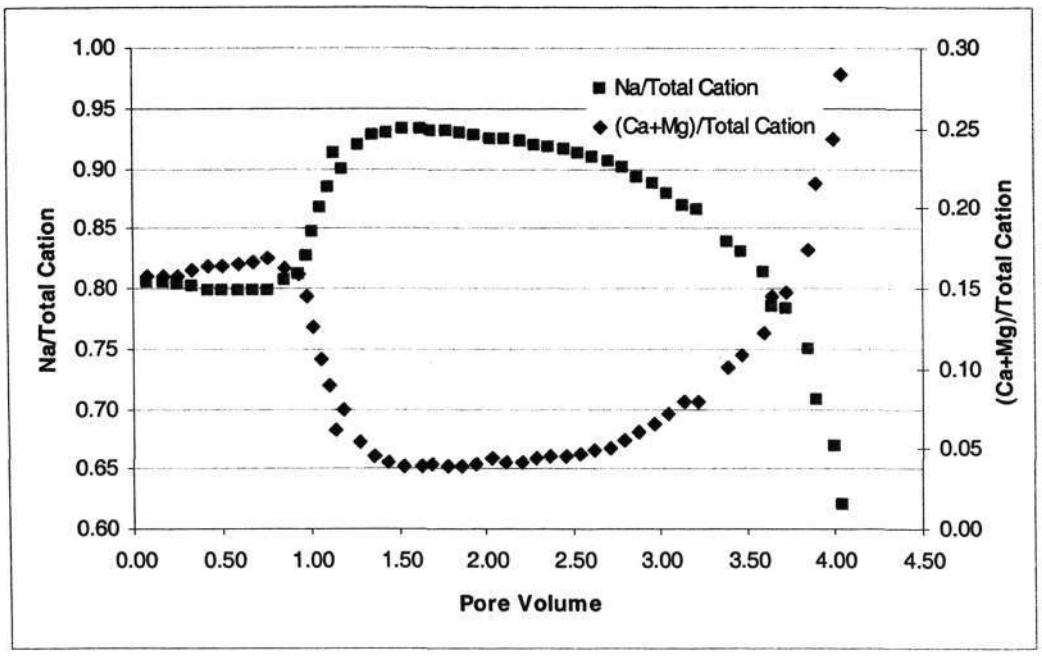

Figure 4.11 Relationship of Na/Total Cation and (Ca + Mg)/Total Cation against pore volume

Figure 4.11 shows that the ion exchange process peaked at around 1.5 PV. The trend was then reversed with a decrease in sodium composition accompanied by an increase in (Ca + Mg) composition. This phenomenon signified the fading of ion exchange reaction, in which the limited amount of silty materials had reached its sorption capacity. The (Ca + Mg) composition continued to increase exponentially until the experiment ceased at 4 PV. The six folds increase was probably due to the "washing out" of all sodium ions in original groundwater and sand as sodium concentration in RO was insignificant.

Sodium adsorption ration (SAR) and exchangeable sodium ratio (ESR) were better gauges to quantify the extent of ion exchange reactions. These relationships were plotted in **Figure 4.12**. Both SAR and ESR were relatively high until around 2 PV. The 15% threshold for ESR was plotted as a red line. ESR values above the threshold indicated a potential problem of clay swelling, which would cause the hydraulic conductivity to decrease. One interesting finding was that at the time when ESR values fell below the 15% threshold, it coincided with the change in trend in Na and (Ca + Mg) composition. This showed that the rate of ion exchange reactions decreased tremendously after only 4 PV of exchanges. However, it may not be possible to claim that this situation would arise if similar recharge water was passed through the aquifer at Changi. The size of the column and hence the mineral reservoir, was a major constraint. Although, the minerals could be "washed out" after 4 PVs in the laboratory column, it would take a much longer time if not forever for Changi aquifer to reach chemical equilibria state.

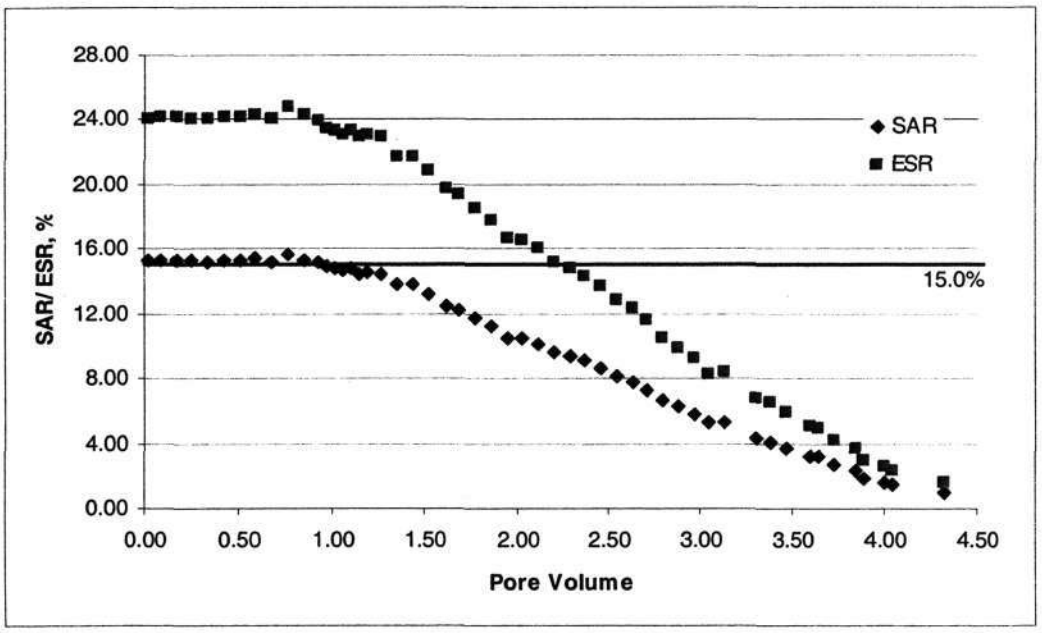

Figure 4.12 Plot of SAR/ESR against pore volume (the red line indicated a threshold for clay swelling)

This study provides some indications on how the Changi aquifer would react during artificial recharge. Ion exchange could be a dominant geochemical effect in the short term, whereas carbonate dissolution would be a long term effect. The next study would be to look into the long term effects of ASR with different types of recharge water. RO being the cleanest among the Bedok plant's effluent, would not be a good candidate due to the high cost of treatment as well as its aggressiveness.

A tracer test was carried out after the RO injection test. The objective was to investigate the hydraulic performance of the column as well to identify the most suitable tracer to be used in future laboratory and field scale studies. Multiple tracers tracer study had been carried to some extent of success in literature with a mixture of conservative and reactive tracers (Pavelic et al., 2005). Therefore, four types of tracers were used concurrently, i.e. chloride, nitrate, fluorescein and EC. Chloride, being the most conservative was used as a benchmark. However, the effectiveness of chloride tracer at the Changi reclaimed land was affected by the high chloride background concentration.

Table 4.10 Tracer test results

Parameters		*Results*
Tracer Flow Rate (mL/min)		5.318
Chaser Flow Rate (mL/min)		4.701
Hydraulic Retention Time (hours)		6.250
Coefficient of Hydrodynamic Dispersion	EC	3.0×10^{-7}
	Chloride	2.2×10^{-7}
	Fluorescein	2.2×10^{-7}
Dynamic Dispersivity, α_l	EC	0.03132
	Chloride	0.02294
	Fluorescein	0.02294
Tracer Recover (% by mass)	Chloride (%)	101.0776
	Nitrate (%)	108.5857
	Fluorescein (%)	84.9481

The test was carried out by injecting a composite solution of 500 mg/L of chloride concentration; 100mg/L of nitrate concentration and 100 μg/L of fluorescein Acid Yellow 73. The composite tracer was injected for 17.8 hours at a flow rate of 5.32 ml/min, followed by RO water for 22.8 hours at a flow rate of 4.70 ml/min. The results from the tracer test are shown in **Table 4.10** and **Figure 4.13**.

The 50% breakthrough time agreed well with the computed pore volume based on porosity. The hydraulic retention time was found to be 6.250 hours. The dynamic dispersivity was computed by fitting the breakthrough curve (BTC) with the following set of equations (**Equation 4.1-4.3**):

$$D_l = \alpha_l \bar{v} + D^* \qquad \textbf{(4.1)}$$

where D_l =coefficient of hydrodynamic dispersion

α_l = dynamic dispersivity

D^* = coefficient of molecular diffusion

$$\frac{C}{C_o} = \frac{1}{2}\left[erfc\left(\frac{l-\bar{v}t}{2\sqrt{D_l t}}\right) + \exp\left(\frac{\bar{v}l}{D_l}\right) erfc\left(\frac{l+\bar{v}t}{2\sqrt{D_l t}}\right)\right] \quad \textbf{(4.2)}$$

where C: effluent concentration

C_0: initial concentration

l: flow length

$\bar{v}$: flow rate in m/s

t: elapsed time in s

For an infinitely long column, **Equation 4.2** would be simplified to:

$$\frac{C}{C_o} = \frac{1}{2}\left[erfc\left(\frac{1-\bar{v}t}{2\sqrt{D_l t}}\right)\right] \quad \textbf{(4.3)}$$

Assuming D^*=1.0x10^{-9} m^2/s, and $\bar{v}$ and t were obtained from the experiment, a set of D_l could be selected to compute $\frac{C}{C_o}$. The computed values were compared with the BTC until a match was found. The dynamic dispersivity could then be estimated. The results shown in **Table 4.10** suggest that both chloride and fluorescein performed equally well as a tracer. One shortcoming of fluorescein would be the lower mass recovery rate. Approximately 15 % of fluorescein was lost probably due to sorption as the control samples indicated that photodegradation was minimal. All four tracers were found to be suitable candidates for laboratory tracer test. Fluorescein and nitrate could be considered for the field studies since chloride could not be used.

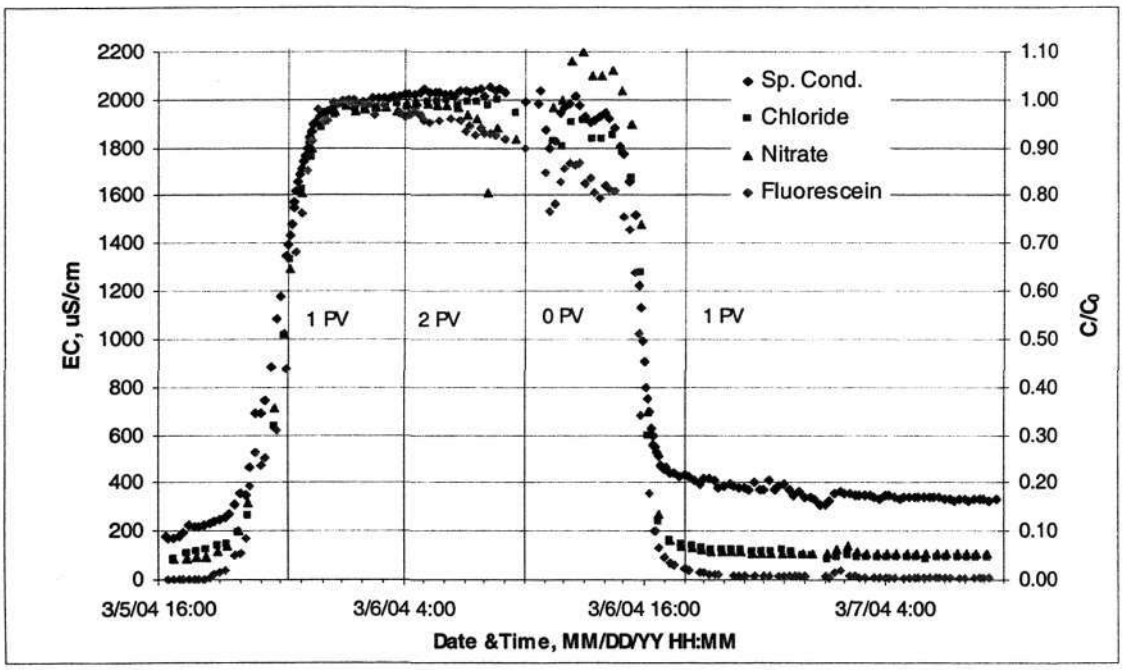

Figure 4.13 Tracer test results using four types of tracer

4.6 Field RO Injection Studies

4.6.1 Site Characteristic

A 500 m x 500 m field experimental test plot was set up at the Changi reclaimed land. Reclamation works for this part of the reclaimed land were completed in 2000. The present study commenced soon after completion of soil consolidation works, removal of surcharge material and sand densification. The ground surface has an elevation of about +3.77 m (MSL). Drilling contractors were engaged to install two fully screened wells and piezometers, collect soil samples, and carry out cone penetration tests (CPT) at each of the four corners of the experimental test plot. Cone Penetrometer testing was also performed at the centre of the test plot. The CPT results at corner 2 are shown in **Figure 4.15**.

The screened wells were installed by the rotary wash method, with groundwater used as the drilling fluid. The screens used are 100 mm internal diameter Boode B.V. (Netherlands) lengthwise slotted, PVC screens with slots size of 0.4 mm. A 125 mm

outer diameter steel casing was advanced during drilling. When the desired depth was reached, the PVC screened wells were inserted into the steel casing. The annulus between the screen and the casing was filled with surface sand before the casing was extracted. Gravel packs were not used. In addition, three multilevel monitoring wells (CMT, ML1 and ML2) were installed close to the fully-screened wells at one corner (designated as Corner 2) of the experimental site. The CMT had 7 sampling ports while ML1 and ML2 had 15 sampling ports each. The relative locations of the fully-screened wells and the multilevel wells were shown in **Figure 4.14**. The relative depth of the sampling ports for CMT was shown in **Figure 4.14**, in which port 1 to 5 were in the fresh water zone and port 6 and 7 were in the saline zone. The saline zone was packed off with a packer inflated with nitrogen gas.

4.6.2 Materials and instrumentations

Sieve analyses were performed on the soil samples obtained from various depths at Corner 2. More than 90% of the fill material was made up of fine-medium sand (particle size < 2.0mm). The silt content was generally less than 2% and the coarse sand and shell contents were not more than 10%. It was found that the fine contents in the sands decreased with depth. This was presumably caused by the segregation of the particles during hydraulic filling. The average specific gravity was found to be 2.67. The sand was classified as poorly graded sand (SP) in accordance with the Unified Soil Classification System. The values of the mean particle size, d_{50} (mm), uniformity coefficient, C_u, and the coefficient of gradation, C_g, for a composite sample (i.e., a composite of all depth-discrete soil samples) obtained from Corner 2 were 0.42 ± 0.10, 2.78 ± 0.73 and 0.91 ± 0.12 respectively.

Results from a CPT test obtained at Corner 2 are shown in Figure 4.15. Soil classification was based on the methodology of Lunne *et al.* (1997). The results showed a shallow silty sand zone underlain by a zone of compacted sand. Those sediments were, in turn, underlain by a loose sand layer in the deeper portion of the sand fill. The

loose sand layer was consistent with reclamation works by hydraulic filling and the upper medium sand zone was attributed to sand densification works (Chua *et al.*, 1997).

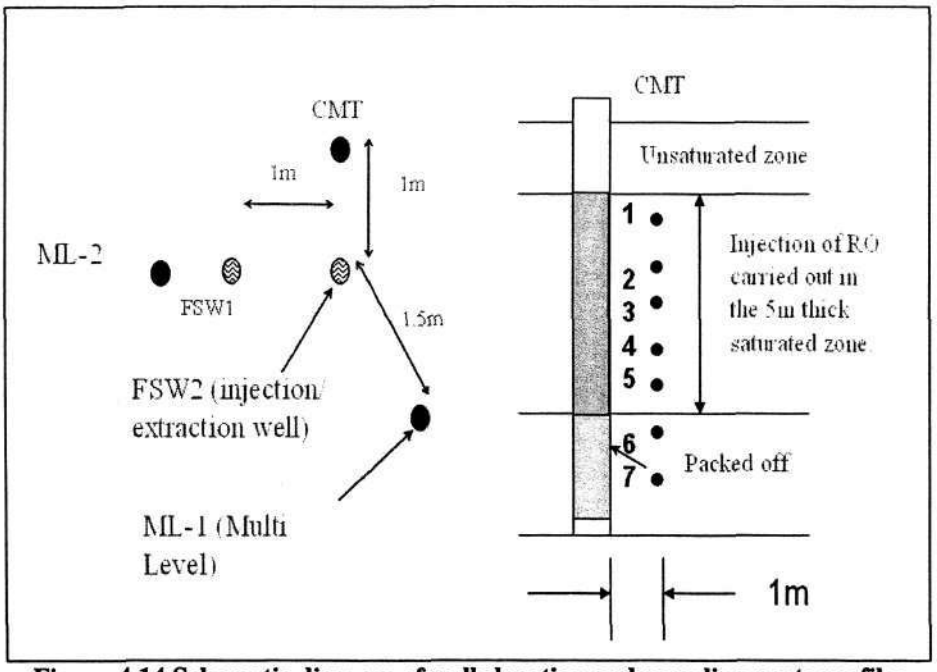

Figure 4.14 Schematic diagram of wells location and sampling ports profiles

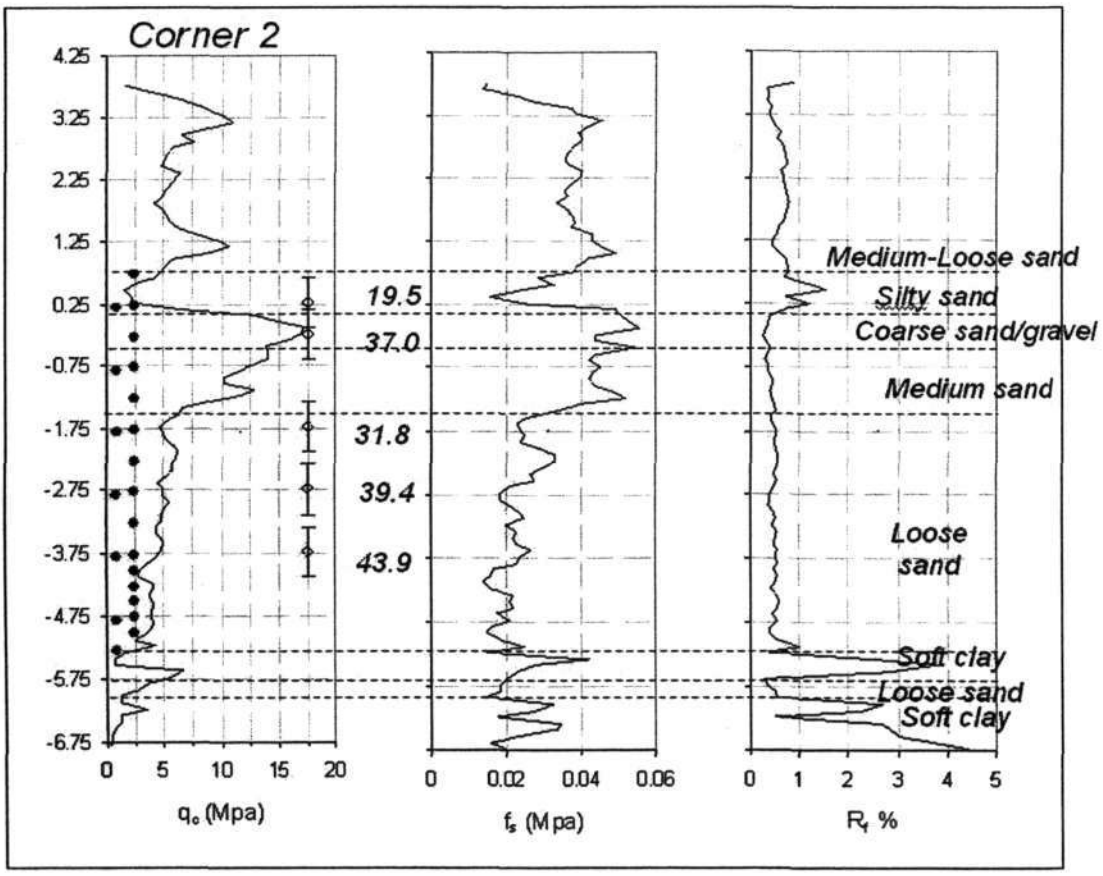

Figure 4.15 CPT result at Corner 2 at NTU test plot

The position of sampling ports were shown in **Figure 4.15**. CMT sampling ports were depicted as the red dots, whereas the blue dots represented the sampling ports of ML2. The hydraulic conductivity values obtained through slug test were also shown. The values represented the average values corresponding to the respective length of slugs indicated by the error bars.

4.6.3 Methodology

The experiment was conducted by injecting slugs of RO treated waste water (RO) to study the geochemical transformations during injection and the relative permeability of the different zones within the fill material. The RO used was high grade water produced after secondary effluent (SE) had been purified by ultra-filtration and reverse osmosis process.

In total, about 40m^3 of RO was injected into the top 5 m of the saturated zone at Corner 2 through FSW1 (**Figure 4.14**). The bottom 2 m of the screened well was packed off, as the salinity of the groundwater at this depth was considerably higher than that of the groundwater in the upper portions of the aquifer. The amount of RO injected was approximately six pore volumes, assuming a 2 m diameter cylinder of 5 m thick fill material, with a porosity of 0.4. Sampling was carried out from the CMT located 1 m away from the screened well, at regular time intervals. In addition, samples were also collected from two different depths in the injection well. The samples were tested for electrical conductivity (EC), temperature and pH in the field, and also brought back to the laboratory for more detailed analysis. The RO slugs were injected on 3rd September, 4th September and 5th September 2003. The time interval between the 1st and 2nd, and 2nd and 3rd injections were 16 hours and 9 hours, respectively. The injection schedule was given in **Table 4.11**.

The injections were carried out at a constant rate of 30 L/min. The expected arrival time of RO at the CMT was estimate at 210 min. The flow rate was monitored using a flow meter and confirmed by level measurements in the RO water supply tank. CMT ports 1-5 lied within the injection zone while ports 6 and 7 were outside the injection zone. For the CMT ports that were within the injection zone, port 1 was located within the lower permeability, silty sand layer, while the other ports were located within the more permeable zone.

Table 4.11 RO injection schedule

Flow (L/min)	*Injection times*								*Total Vol. Injected (m^3)*
	1st injection			2nd injection			3rd injection		
	Duration (hrs)	Vol. (m^3)	Interval (hr)	Duration (hrs)	Vol. (m^3)	Interval (hr)	Duration (hrs)	Vol. (m^3)	
30	5.5	9.9	16	6.25	11.25	9	9.5	17.1	38.25

4.6.4 Results and Discussion

The relative locations of the CMT sampling ports and the change in EC recorded at selected sampling ports are shown in **Figure 4.16**. Results for sampling ports 5 and 6 were similar to that of sampling port 4, and were hence not plotted.

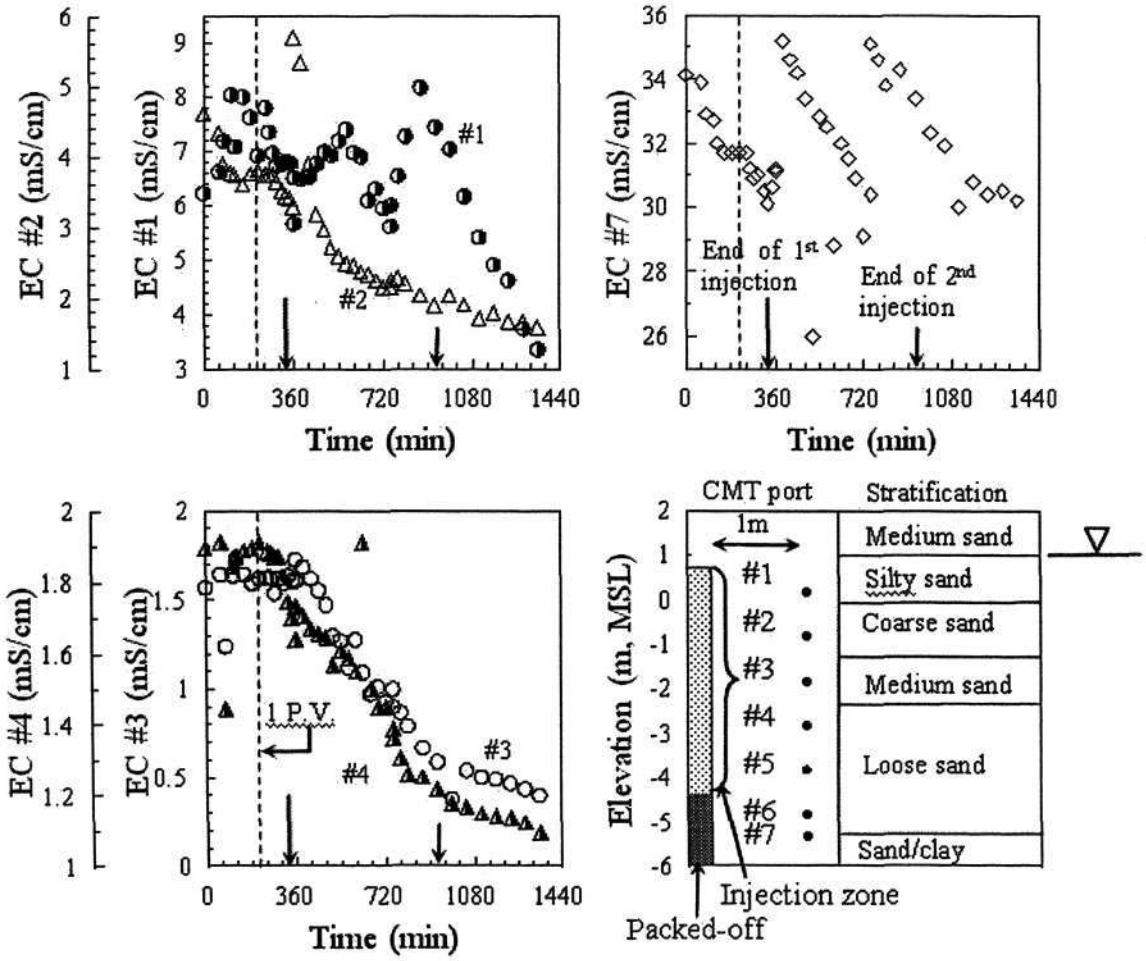

Figure 4.16 Variation of EC during injection. Groundwater elevation is at elev. 3.77 m MSL. Original seabed elevation at -6.3 m MSL. The 1st pore volume is indicated by a dashed vertical line

The data were presented in a continuous sequence, i.e. the first recorded EC value after the commencement of tracer injection was plotted directly after the last recorded EC reading, prior to the cessation of injection on the previous day. Some spikes in the measured EC values were observed in **Figure 4.16**, corresponding to the earliest samples collected after cessation of the previous day's injection. The spiking was likely to be caused by background flow. In spite of this discrepancy, the EC associated with the

later injections matched up well with the previous day's EC measurements, allowing a continuous trend to be established. The samples collected during the spiking period were excluded from further analysis. **Figure 4.16** showed that the RO arrival time at sampling ports 2, 3 and 4 agreed well with the expected arrival time of about 210 min. Similar arrival times were obtained for sampling ports 5 and 6. The EC of samples collected from sampling port 1 (located within the silty sand layer) showed an unusual trend. The installation of the CMT by rotary drilling was complicated by the presence of cohesive material. This technique worked well in an unconsolidated media, because the ground material collapsed onto the CMT when the casing, used to support the sand media during the installation process, was removed. The presence of a silty sand layer obviously impeded this process, with the possibility of the formation of an annulus of more permeable material, surrounding the CMT, at port 1. This would then give rise to preferential flow paths around port 1 of the CMT, and hence the possibility of getting erroneous results during sampling. Finally, although sampling port 7 was situated furthest away from the injection zone, and located in a highly saline zone (EC approximately 32 mS/cm), a decrease in EC was observed during injection. The EC however recovered to the previous day's initial EC value, presumably as a result of steep concentration gradients present at the deeper portions of the aquifer during injection.

A geochemical analysis was conducted on the samples collected during the experiment. The variation of EC and pH with time, obtained from a representative sampling port (sampling port 4) was shown in **Figure 4.17**. The decrease in EC, as the original groundwater was displaced by RO during injection, was accompanied by an increase in pH, presumably a result of carbonate mineral dissolution.

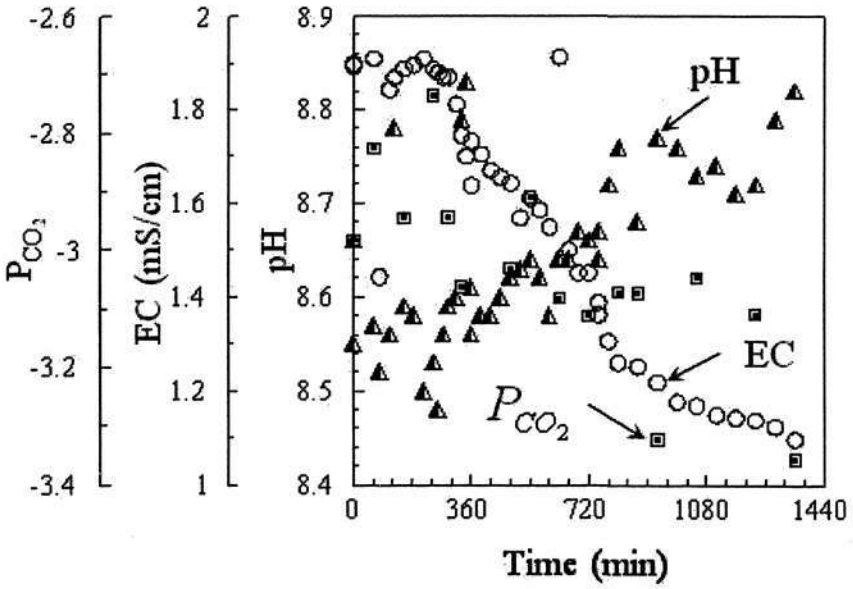

Figure 4.17 Breakthrough of RO measured at sampling ports of CMT and changes in pH and P_{CO_2} during RO injection

The samples collected from the CMT during RO injection were analyzed for the major cations (K^+, Mg^{2+}, Na^+ and Ca^{2+}) and alkalinity. Bicarbonate and carbonate concentrations were calculated from alkalinity and pH measurements. In addition, the partial pressure of carbon dioxide, P_{co_2}, was calculated from the solubility product of carbonic acid. In these calculations, the mass action constants were corrected for temperature using the Van Hoff's equation and activities were corrected for ionic strength, *I*, using the Davies equation.

The increase in pH with a corresponding decrease in P_{co_2}, gave further indication of calcite dissolution according to:

$$CaCO_3 + CO_2 \rightarrow Ca^{2+} + 2HCO_3^-$$

However, an inspection of the data for Ca^{2+} concentration showed a decrease rather than an increase in Ca^{2+} as one might expect from calcite dissolution (**Figure 4.18**). The possibility of ion exchange was therefore investigated. The proportions of Na^+ and

(Ca^{2+}+Mg^{2+}) were compared in **Figure 4.18**. The increase in Na^{+} and the concomitant decrease in (Ca^{2+}+Mg^{2+}) gave strong indication of ion exchange given by:

$$Na - X + Ca^{2+} \leftrightarrow Ca - X + 2Na^{+}$$

This phenomenon was identical to that of Guo and Wang (2004) in Datong Basin, China, in which the geochemical transformation of rainwater/groundwater interaction was investigated. Soil samples obtained from the subsurface indicated the presence of clay pockets, providing confirmation of the possibility for ion exchange to occur. The data were further analyzed to obtain the SAR and ESR and shown in **Figure 4.19**.

The figure shows that the SAR remained high (> 10) even after the end of injection, by which time ionic strength had reached fresh water levels (i.e. $I \approx 0.015$). The corresponding exchangeable sodium ratio, ESR remained above the critical value of 15%. The high ESR values indicated possible swelling of clay, which would lead to a decrease in the hydraulic conductivity.

In essence, results from the field experiment showed that carbonate dissolution, and possibly ion exchange, could be the dominant geochemical processes that might be expected during subsurface storage of RO. RO contained very little dissolved ions and was therefore considered to be aggressive. Further analysis of the clays in the subsurface and laboratory column experiments were planned to further quantify these processes, as part of an overall study to characterise the site for water storage.

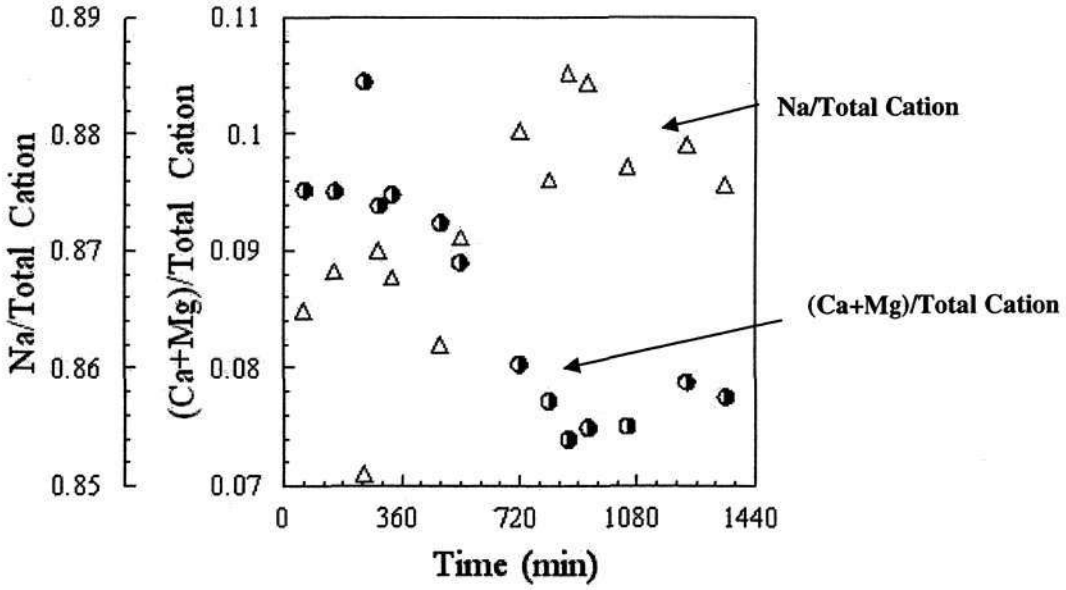

Figure 4.18 Decrease in (Ca+Mg)/Total Cation accompanied by a concomitant increase in Na/Total Cations

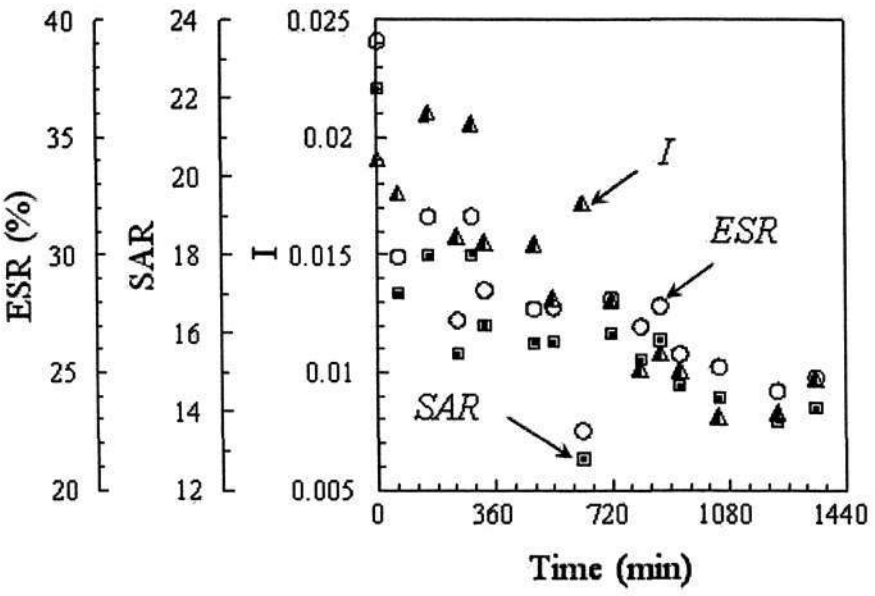

Figure 4.19 Variation of ionic strength (I), ESR and SAR during RO injection

4.7 Medium Term Geochemistry Column Studies

4.7.1 Background

The laboratory and the field RO injection tests suggested that geochemistry effects were an important issue when assessing the feasibility of the ASR scheme. However, these studies were restricted by the number of exchanges of pore volumes passing through the sand column. In both tests, detailed analysis was only conducted for the first exchange of pore volume. The primary objective of this study was to investigate the medium to long term geochemical transformations during ASR operations. Dissolution and ion exchange reactions would be examined, as well as the potential of heavy metal contamination due to leaching. In addition, the same sets of columns are used to verify the effectiveness of SAT in the saturated zone with a hydraulic retention time (HRT) of approximately 7 hours. This study was to complement the results obtained from other SAT column experiments which focused on SAT effects in both the vadose zone (0.50 day HRT) and the saturated zone (30 days HRT).

4.7.2 Methodology

Three types of high quality treated wastewaters were used as recharge waters to the columns, namely RO, UF and SE. An additional column was recirculated with native groundwater in order to simulate natural aquifer condition in which the groundwater was in equilibrium with the environment. The dimensions of the column were as summarised in **Table 4.12**. To identify the individual columns, the column with SE as recharge water would be denoted as the SE column. Similarly, the UF column and RO column would have UF and RO as recharge waters respectively. The groundwater recirculated column would be referred to as the control column as it basically represented the natural aquifer condition without artificial recharge.

Table 4.12 Specifications of the medium term column

Column Design	*Unit*	*Characteristics*
Length	m	0.75
Diameter	m	0.065
Volume	L	2.489
Porosity		0.328±0.005

The column studies commenced on 28th September 2004 and ended on 24th January 2005. The experiments spanned over 118 days as shown in **Table 4.13**. Samples were collected twice a day, once in the morning and the other in late afternoon. The chosen time coincided with one PV of approximately 8 hours. Therefore the morning influent sample and the afternoon effluent sample could be compared directly.

Table 4.13 Geochemistry column operating schedule and sampling scheme

Geochemistry Column Studies	
Start date	28th September 2004
End Date	24th January 2005
Experiment duration	118 days
Sampling schedule	Twice per day 0900 and 1530 daily
Sample size	100 ml

The samples collected were similarly analysed as for the short term column study but in greater details. Chemical balance was analysed for each and every sample together with 11 other trace metal ions. DOC and UVA-254nm were also analysed to look into the SAT potential under saturated condition. A list of parameters tested is tabulated in **Table 4.14.**

Table 4.14 List of water quality parameters tested for the medium term column studies

Water Quality Parameters	
General Water Quality	Temperature, pH, EC, dissolved oxygen, ORP, turbidity
Major cations	Sodium, potassium, calcium, magnesium
Major anions	Chloride, sulphate, nitrate, carbonate, bicarbonate
Tracer heavy metals	Aluminium, arsenic, barium, copper, chromium, iron, lead, manganese, nickel, selenium, zinc

4.7.3 Results and Discussions

The general hydraulic characteristics of these columns were shown in **Table 4.15**. The flow rate was the average value based on daily flow rate measurements using a weighing method. Porosity was obtained during the sand packing process as discussed in Chapter 3. In the same table, two PV was formulated based on different methodology. The PV based on porosity was a theoretical value as air pockets, dead volume, preferential flow path etc. were not accounted in this calculation. As a result, a tracer test was carried on each column to find out the effective hydraulic retention time (HRT) and hence the corrected PV. 500-1000 ml of the respective feed, spiked with 500 mg/L of chloride was used as tracer and fed into the column. The EC value at the effluent point was recorded every 5 minutes and a 20 ml sample was collected every one hour for chloride analysis.

Table 4.15 Hydraulic characteristic of each column

Parameters	*unit*	*SE*	*UF*	*RO*	*Control*
Flow rate	ml/min	2.30±0.48	2.23±0.24	2.34±0.48	2.69±0.44
Porosity		0.33	0.32	0.33	0.33
Pore Volume (based on porosity)	L	0.821	0.796	0.821	0.821
No. of PV (based on porosity)		532	481	480	546
Hydraulic Retention Time (based on tracer study)	minute hour	397 6.62	366 6.10	449 7.48	536 8.33
Corrected Pore Volume (based on tracer study)	L	0.913 (11.2%)	0.816 (0.03%)	1.051 (28.0%)	1.300 (58.3%)
No. of PV (based on tracer study)		478	469	375	345
Dynamic Dispersivity	m		0.000731		

The $0.5\frac{C}{C_0}$ point was adopted as the point of breakthrough similar to the tracer test in the short term column. As shown in **Table 4.15**, the corrected PV was all higher than that estimated from porosity. The bracketed values under the corrected PV were the percentage increase in PV. The dynamic dispersivity was also computed using the formulae in section 4.5. The computed dynamic dispersivity values were the same as the dimension of the column and the packing of the sand were apparently the dominant factor.

Figure 4.20 shows the breakthrough curves for the four tracer tests. The plateau length varied as the size of the injection plume was not the same. The UF column's tracer study was the first to be carried out and it showed that four hours of tracer injection (equivalent to approximately 535 ml) was insufficient. The average time taken for the entire breakthrough process to occur (i.e. from $C = 0$ to $C = 1.0$) was 4.2 hours. As a result, all subsequent trace tests were injected with at least 8 hours of tracer.

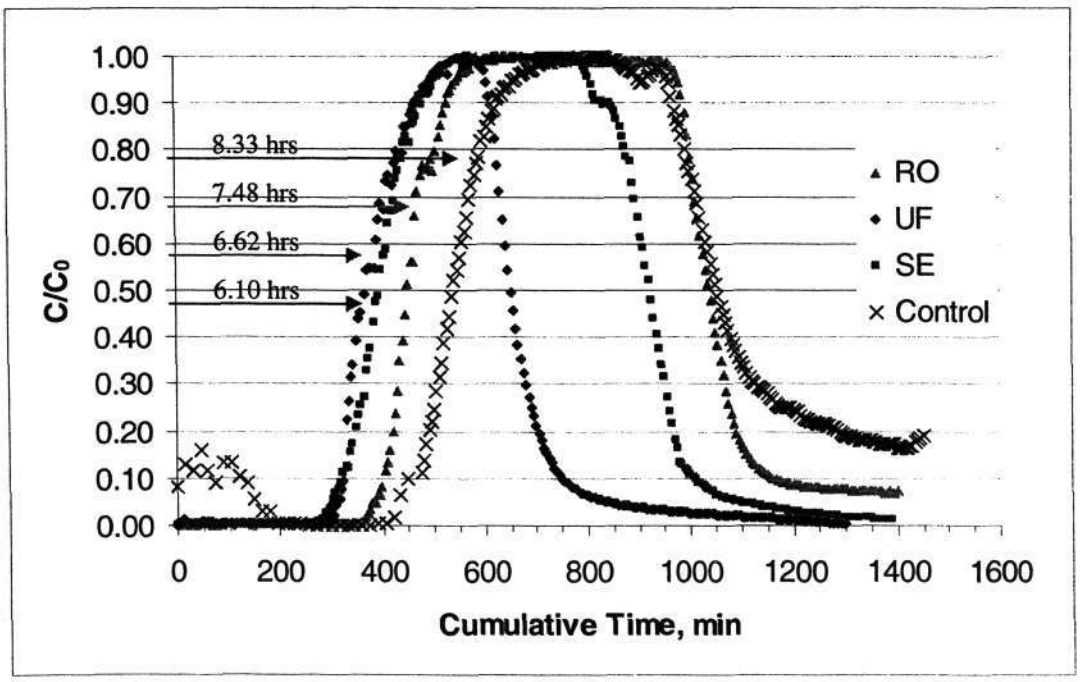

Figure 4.20 Breakthrough curve of tracer studies

The corrected PVs were comparable for the SE, UF and RO columns but the tracer arrival time of the control column was almost 60 % slower than the expected time. One

possible reason could be the groundwater used to prepare the tracer may have a different ionic strength compared with the groundwater used for recirculation. The density difference would cause local mixing in the column and hence delayed the tracer arrival time. Nonetheless, the corrected PVs were used to compute the HRT and all PVs in the subsequent sections referred to the corrected PVs.

Since the PV for each column was now known, the four columns could be compared on a common axis in terms of the cumulative number of exchanges of PV. Comparisons in terms of the cumulative PV would be more representative and convenient as this eliminated two variables, namely flow rate and retention time.

Figure 4.21 compares the pH changes between the influent and effluent of each column. It showed that the pH values of the effluent, with the exception of the control column, were higher than the influent by 1.0-1.5 pH value, as the feeds gained alkalinity along the sand packed column. This translated to about 10-30 times increase in the concentration of the hydroxide ions ($[OH^-]$) in the effluent given the pH value is the representation of negative logarithm of the hydrogen ions. The rise in pH indicated the possibility of carbonate dissolution during ASR. As discussed in section 4.5, the pH changes were accompanied by a drop in the partial pressure of carbon dioxide and an increase in the concentration of dissolved inorganic carbon as shown in **Figure 4.22** and **Figure 4.23**.

These results were consistent with all the previous findings. Besides reassuring the quality of the experiment, it also provides further indications of the implications during the implementation of the ASR scheme on this sand medium.

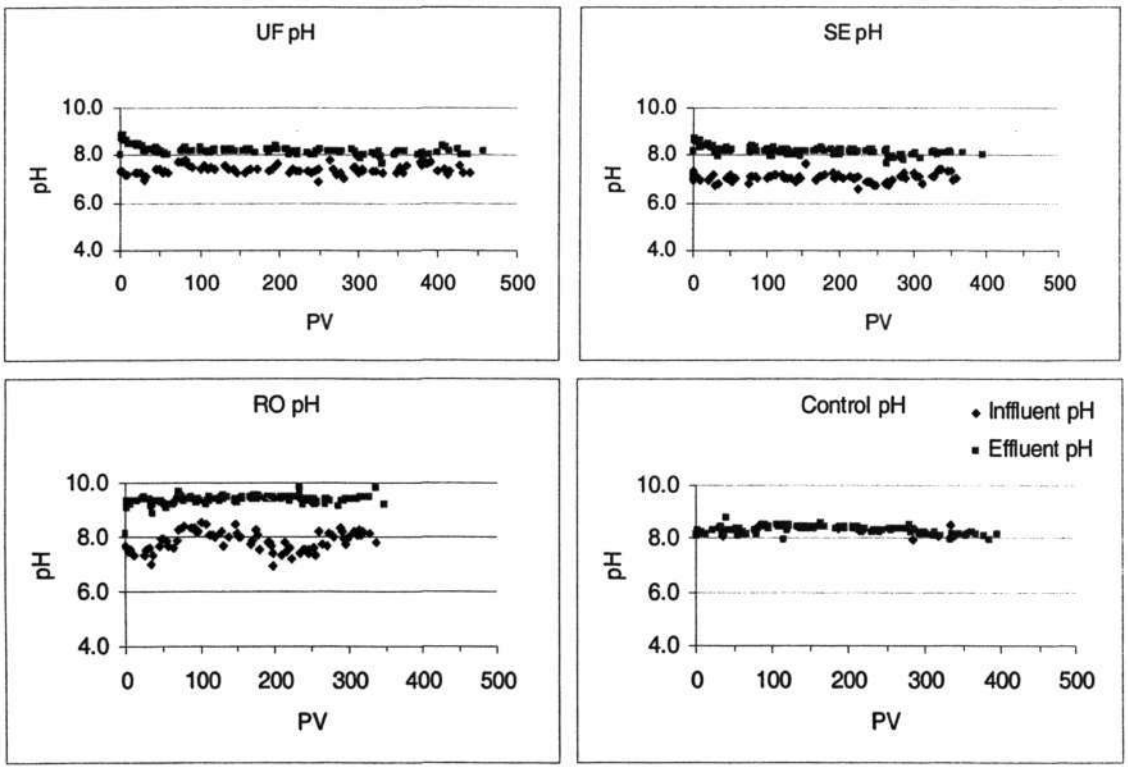

Figure 4.21 pH data for each geochemistry columns

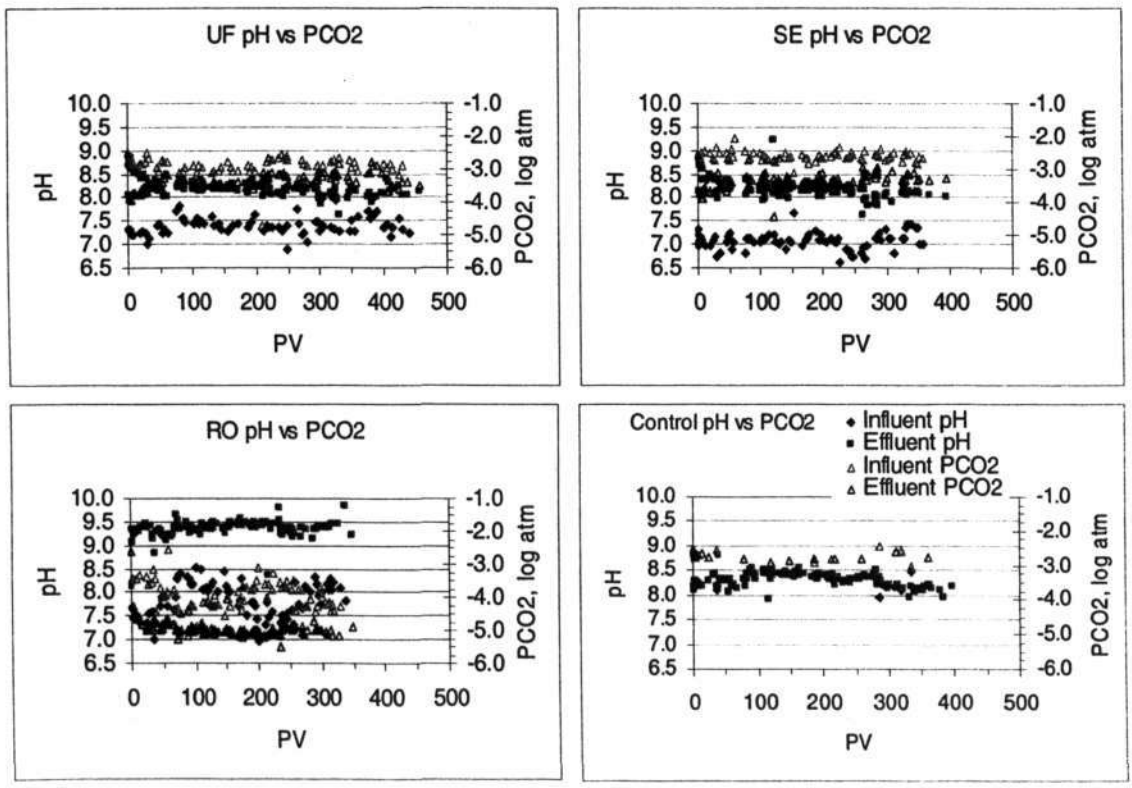

Figure 4.22 pH v.s. partial pressure of carbon dioxide for each geochemistry columns

Firstly, the buffering capacity of this sand medium was persistent throughout the experiment. From **Figure 4.21**, there was some fluctuation in the influent's pH for the RO column. The reason could be due to insensitive response of pH electrode at the region near to neutral or due to the nature of the influent solution itself. However, the effluent's pH was always consistent regardless of what was entering the column. This observation applied to the UF and SE columns as well. In addition, analysis of the effluent samples indicated that all the effluents were saturated against calcite, aragonite and dolomite as shown in **Table 4.16**, giving further insights to the buffering capacity of the sand media. The saturation indices of the three calcium related minerals were computed based on equation 2.24. The near unity values indicated that the calcium based minerals were in equilibrium state after passing through the columns.

Table 4.16 Saturation indices of three calcium related minerals from the effluents of each geochemistry columns

Column	*Calcite*	*Aragonite*	*Dolomite*
UF	1.0057	1.301	1.0305
SE	0.9494	0.9724	1.0067
RO	1.0513	1.0768	1.0886
Control	0.9208	0.9431	0.9008

Note: SI > 1 : over saturation
SI < 1 : under saturation
SI = 1 : in equilibrium or saturated

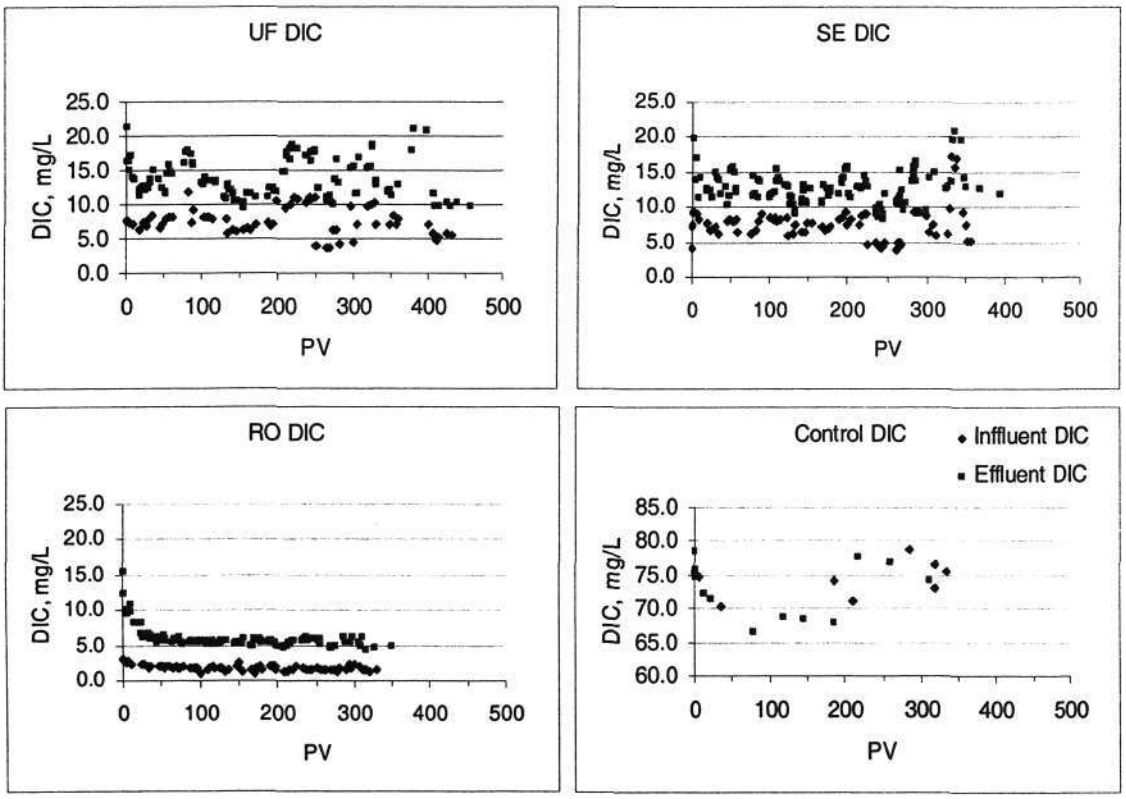

Figure 4.23 DIC data for each geochemistry columns

Therefore, it is confirmed that the sand matrix is of calcareous origin. Several important ratios that were reported in the literature could provide further implication based on the available information. **Table 4.17** shows the influent and effluent Ca/Mg and Ca/Cl ratio of each geochemistry column. Ca/Mg ratio gives an indication whether the formation of the sand matrix is of calcite/aragonite origin or dolomite base. A value near to 1 indicates dolomite origin and a value larger than one would mean a high possibility of calcite/aragonite formations. The influent ratio of the control column was much lower than 1, which agreed well with the origin of the aquifer. The high concentration of Mg should be due to the seawater remaining in the aquifer as well as sea spray. Overall, the Ca/Mg ratio for the other three column were higher than one, and hence it can be concluded that calcite or aragonite should be the major calcium minerals in the aquifer.

The Ca/Cl ratio gives an indication of the extent of seawater intrusion and in this case, provides an insight on the history of transformation of the aquifer upon reclamation. A

value less than 0.10 would signify the need to prevent sea water intrusion. In this experiment, the Ca/Cl ratio in the control column, 0.37, considered as low, remained basically unchanged after 345 PVs. This was expected under laboratory controlled conditions as no chloride ions were taken in or out of the system. The actual condition on site is expected to improve with time under natural rainfall recharge. However, with the three types of recharge water tested, the Ca/Cl ratio increased at the end of the experiment. Therefore, the ASR scheme on site could help speed up the process of "cleaning" up the medium to brackish groundwater in the aquifer with minimum geochemical effect.

Table 4.17 Ca/Mg and Ca/Cl ratio influent and effluent for each geochemistry columns

Column	*Ca/Mg*	*Ca/Cl*
SE	Influent: 1.97 ± 0.61	Influent: 1.97 ± 0.61
	Effluent: 2.87 ± 0.68	Effluent: 2.87 ± 0.68
UF	Influent: 1.72 ± 0.50	Influent: 0.24 ± 0.07
	Effluent: 2.64 ± 0.44	Effluent: 0.32 ± 0.05
RO	Influent: +∞	Influent: 1.97 ± 0.61
	Effluent: 6.24 ± 1.64	Effluent: 2.87 ± 0.68
Control	Influent: 0.37 ± 0.00	Influent: 0.19 ± 0.01
	Effluent: 0.37 ± 0.03	Effluent: 0.19 ± 0.02

Note: Ca/Mg ratio of RO is infinitely large as the Mg is below detection limit

Although, the enormous buffering capacity could be advantageous as the operator of the ASR scheme could minimise the cost of conditioning the extracted water, which is a standard process in water treatment plant, it would be a concern in the long run as continuous carbonate dissolution would eventually "wash out" the carbonaceous compound in the sand, thus affecting the structural integrity of the reclaimed land, lead to the collapses of the sand column. Also, precipitation process downstream of the recharge well due to over saturation could lead to localised clogging which would not be desirable. This could result in a more porous sand medium upstream and less porous medium downstream of the recharge well.

Nonetheless, it would take a long time before such a situation could happen. On the basis of an average of 400 exchanges of PV that had been run on each of the geochemistry columns, based on the assumption of at least 30 days of HRT in an operating ASR scheme, this would be equivalent to 33 years of continuous ASR operation. As there was no indication of a substantial change in the PV or flow rate in the laboratory column, there was no evidence that dissolution would create additional voids in the sand column, or that the accompanying precipitation process would cause clogging after 400 PVs. As a result, it could be concluded that carbonate dissolution effects, though dominant, would have little influences on the feasibility of the ASR scheme in short to medium term.

As shown by the tests on the short term column and at the Changi field, ion exchange reactions were equally important as compared with carbonate dissolution. Therefore, a similar approach was carried out to investigate the extent of ion exchange in the laboratory controlled columns. The major indicators would be the sodium concentration and the combination of calcium and magnesium concentration, which effectively contribute to the hardness of the groundwater. The ratio of Na/Total Cation and (Ca+Mg)/Total Cation were plotted for each of the geochemistry column in **Fig 4.24** and **Fig 4.25**. The ratio was computed in terms of milli-equivalent per litre such that there could be compared under the same axis. However the results obtained were different from the results in Sections 4.5 and 4.6. The Na/Total Cation ratio decreased accompanied by an increase in (Ca+Mg)/Total Cation ratio contradicting the findings in Section 4.6. The results confirmed the occurrence of carbonate dissolution but show no hint of the occurrence of ion exchange reactions.

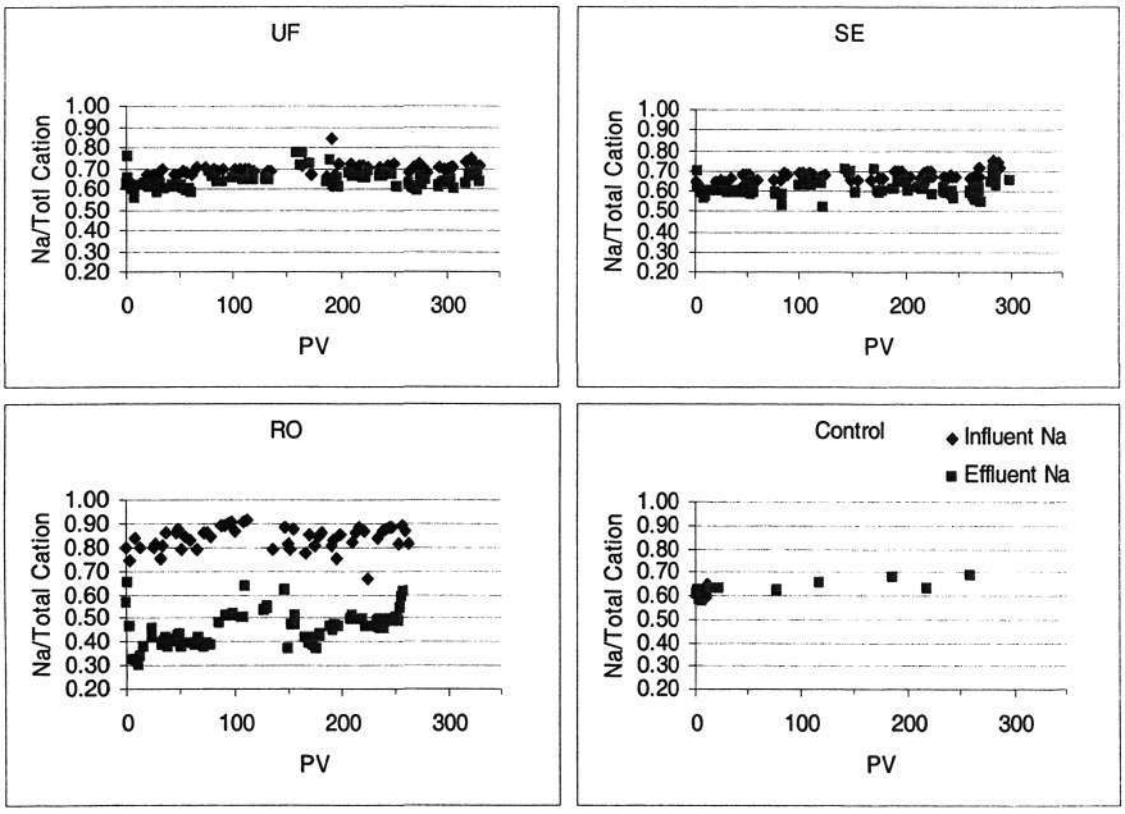

Figure 4.24 Na/Total Cation for each of the geochemistry columns

Sodium Adsorption Ratio (ASR) and Exchangeable Sodium Ratio (ESR) were computed to trace the existence of the ion exchange reactions. SAR is a measure of the proportion of Na^+ present, with respect to the other major ions, and has been used to account for the ion exchange process. When the Na^+ concentration is high, it tends to adsorb onto the clay minerals, displacing calcium and magnesium ions. For a SAR value greater than 6 to 9, the recharge water could be expected to cause a permeability problem on the shrinking and swelling types of clayey soils. In the case of ESR, it is used to predict the possibility of clay swelling when it is in excess of 15%.The SAR and ESR for the influent and effluent of each geochemistry column were shown in **Fig 4.26** and **Fig 4.27**.

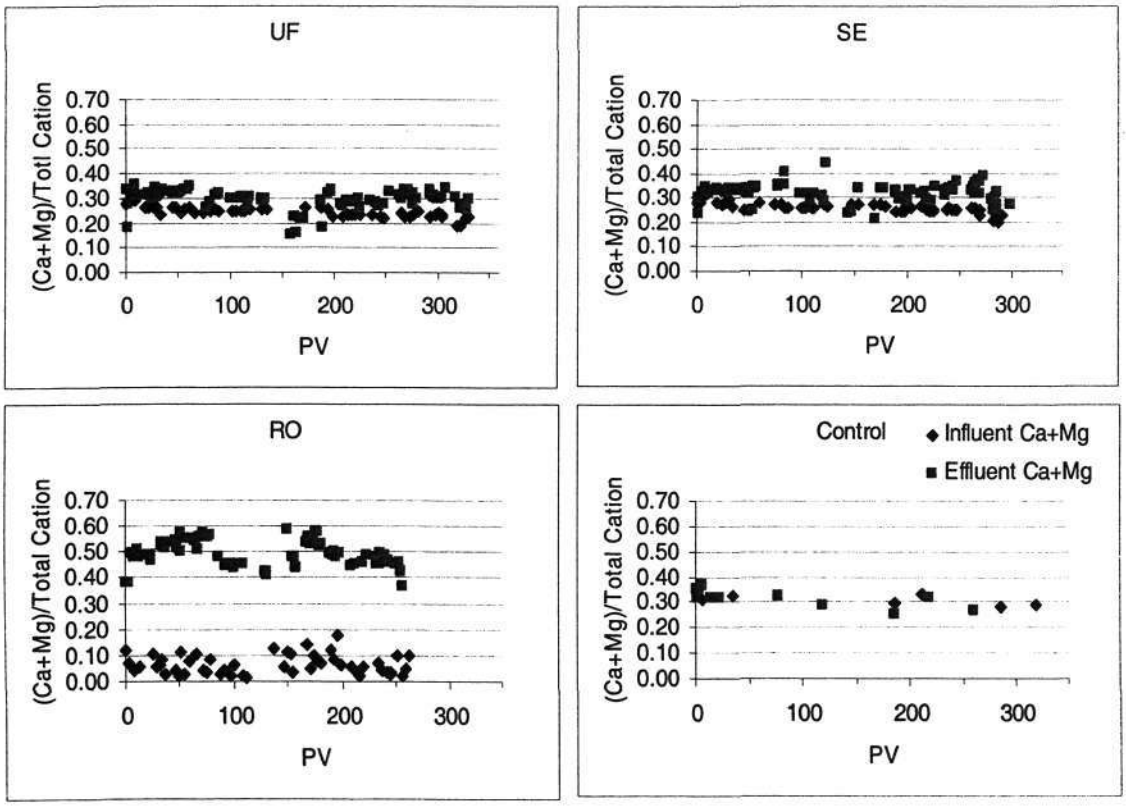

Figure 4.25 (Ca+Mg)/Total Cation for each of the geochemistry columns

Observation of the SAR and ESR ratio did not yield concrete findings on the occurrence of ion exchange reactions. The effluents from each column were all below the limits deemed to trigger the occurrence of the ion exchange reaction. Although, it was certain that ion exchange reaction did occur during the ASR operation, no scientific proof was apparent from the colleted data. There were several possibilities that could lead to this situation.

First of all, the column was filled with medium to course sand of minimum fines. High surface area clayey material which exist in insignificant amount would provide limited sites for ion exchange effect to take place. Secondly, unlike the previous experiments, samples were collected over a longer period of time. The first data point made available was after 2.33 PV had passed through the column. From the short term column study, ion exchange effect ceased to exist after only 1.5 PV. This could have led to data being lost due to insufficient data collected in the earlier stage, preferably collected within the

first PV. However, since the test was designed to observe the long term effect of the ASR, it was practically impossible to collect sample consecutively as the resulting samples size would be overwhelming.

Therefore, we could conclude that the column study was not efficient for the analysis of long term ion exchange reactions. The test should only be restricted to short term studies of less than 2 PV, due to the limited size of ions reservoir in such clean sand. Otherwise, a batch test would be an alternative to account for the total leachable ions in the sand. Nonetheless, a pilot scale field study should be carried out to verify the laboratory findings before any planning of full scale operation. The results here, though consistent due to its homogeneity of artificial filling material, could be totally different at another test site.

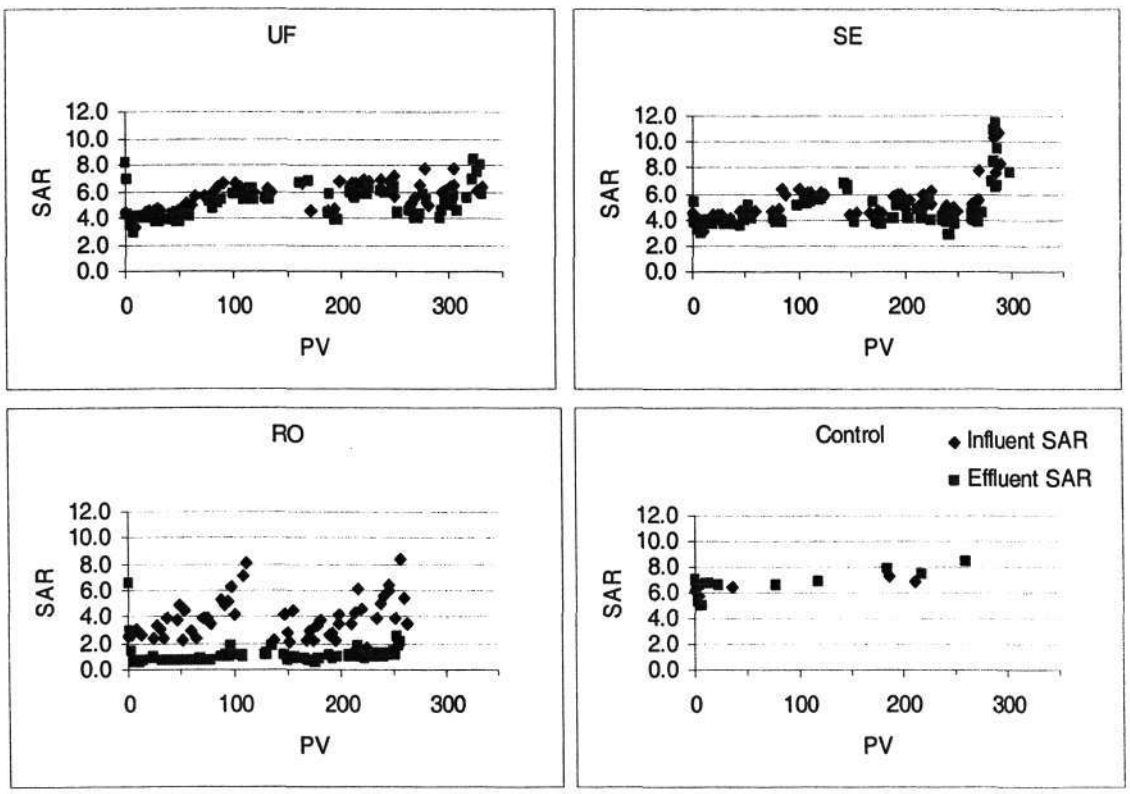

Figure 4.26 SAR for each of the geochemistry columns

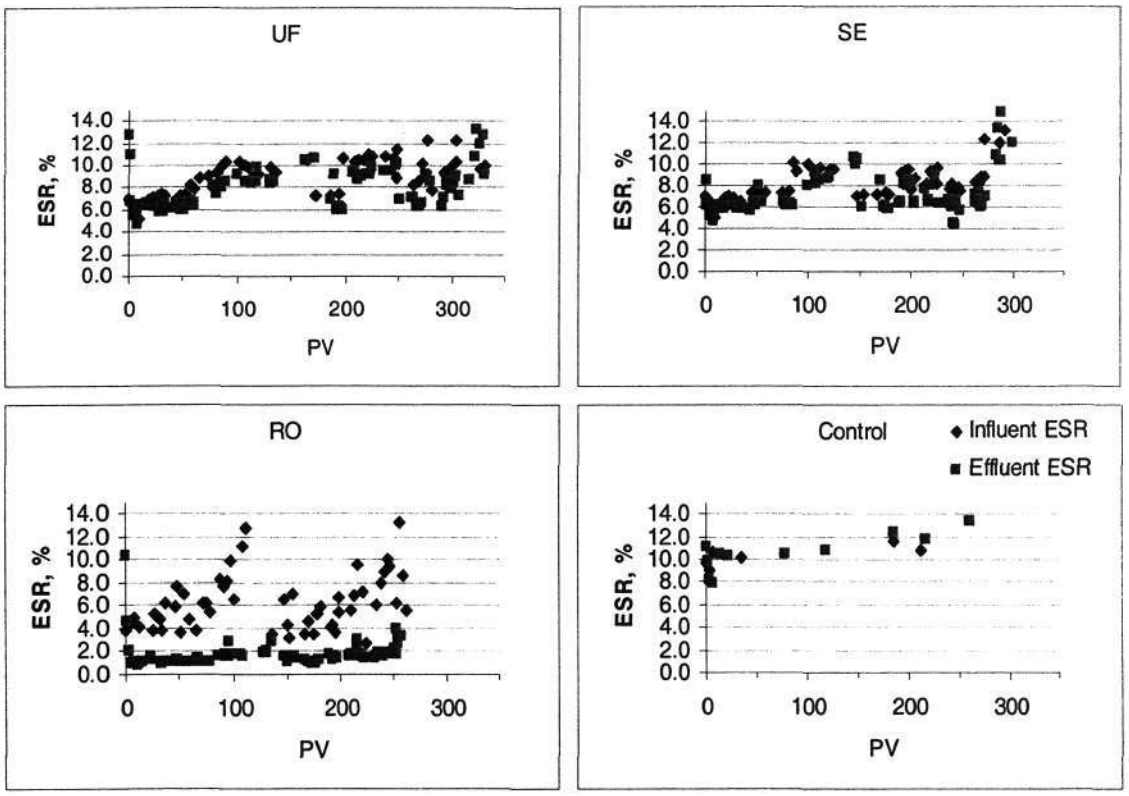

Figure 4.27 ESR for each of the geochemistry columns

The parameters discussed in the previous section illustrated the geochemistry effect that each of the recharge water would have on the artificial sand filling. It would be useful to look into the changes in chemical composition of the influent and effluent during the course of recharging. **Table 4.18** tabulated the results of all major cations and anions with respect to the number of PV passing through the RO column. The results for RO column were shown for its aggressiveness and thus should reveal more scientific findings than the UF and SE columns.

Table 4.18 shows the changes in the composition of major ions at 6, 12, 100 and 255 PV. Three values were given for each ion. The first line represented the increase in concentration after the recharge water had passed through the column. The second line showed the initial concentration of the respective ion in the influent, whereas the third line was the change in percentage by concentration.

Table 4.18 Changes in major ions composition for RO column at various stae of recharge

		6PV	*12PV*	*100PV*	*255PV*
Na^+	Increase in conc.	-2.479	-2.452	-3.621	-3.950
	Original Conc.	(8.965)	(7.726)	(14.568)	(17.452)
	% Change	-27.7%	31.7%	-24.9%	-22.6%
Mg^{2+}	Increase in conc.	+3.218	+2.726	+1.495	+1.482
	Original Conc.	< D.L.	< D.L.	(0.094)	< D. L.
	% Change	+∞	+∞	1590%	+∞
Ca^{2+}	Increase in conc.	+3.100	+3.068	+4.553	+8.921
	Original Conc.	(0.266)	(0.313)	(0.786)	(0.327)
	% Change	1165%	980%	577%	2728%
K^+	Increase in conc.	+4.984	+3.966	+0.177	+0.603
	Original Conc.	(1.451)	(1.710)	(1.375)	(2.540)
	% Change	343%	232%	12.9%	23.7%
Cl^-	Increase in conc.	-1.103	0.413	-0.979	-0.591
	Original Conc.	(5.513)	(5.471)	(15.257)	(13.149)
	% Change	-20.0%	7.5%	-6.4%	-4.5%
SO_4^{2-}	Increase in conc.	+3.422	+1.568	< D.L.	+1.256
	Original Conc.	(0.044)	< D.L.	< D.L.	< D.L.
	% Change	7777%	+∞	N/A	+∞
HCO_3^-	Increase in conc.	+33.367	+33.977	+17.141	+18.178
	Original Conc.	(13.847)	(10.736)	(8.784)	(7.137)
	% Change	214%	316%	195%	255%
NO_3^-	Increase in conc.	+0.031	-0.699	-0.48	+0.921
	Original Conc.	(1.450)	(1.480)	(1.672)	(1.163)
	% Change	2.1%	-47.2%	-28.7%	79.2%

Note: < D.L. is below detection limit

From the table, calcium and magnesium ions increased significantly during the experiment. The original influent was scarce in magnesium and sulphate, but they leached out from the sand column consistently throughout the test. The concentrations

for both Mg^{2+} and SO_4^{2-} in meq/L together with that of Ca^{2+} and HCO_3^- could add up quite well, indicating the dissolution of calcite, dolomite and gypsum. The nitrate concentration was found to be decreasing in the effluent. This could be an indicator for the SAT taking place.

Heavy metal analysis was also done to look into the sorption and desorption capacity of the sand column during artificial recharge. It was observed that desorption of heavy metals did take place in the initial stage especially for aluminium (Al), Iron (Fe) and manganese (Mn). However, the effluent concentrations fell after 20 PV of recharge water had passed through the UF, SE and RO columns. This was probably due to the effect of "washing out" as the heavy ions pool in the sand column was limited.

Table 4.19 reported the average trace metals concentration both in the influent and effluent for each of the geochemistry columns over the entire duration of the experiment. The trace metals presented included: Al, Arsenic (As), Copper (Cu), Fe, Mn, Selenium (Se) and Zinc (Zn). Other trace metals such as Barium (Ba), Chromium (Cr), Nickel (Ni) and Lead (Pb) were found to be below the detection limit of the ICP. The bracketed values in column 2 show the sample sizes for the statistical analysis. As the sample size was relatively large and the influent quality was fluctuating. The results presented did not reflect the changes occurring within the time domain, but represent the overall mass balance of the trace metals passing through the column.

The results in **Table 4.19** showed that adsorption or desorption of heavy metals should not be a major concern. The effect is insignificant probably due to the relatively clean sand column which provides minimum sites for exchanges as well as limited pools of heavy metals for desorption to occur. Al, Fe and Mn were the more prominent heavy metal but well within the EPA Drinking Water Standards. The only concern was for arsenic, the concentration detected even for the influent was higher than the regulations. The main reason was probably due to the analytical method used for As detection. The ICP could only measure As concentrations above 0.020 mg/L and the interference for As analysis was abundant. The preferred analytical method for As

determination should be Atomic Adsorption Spectrometry (AAS). However the instrument was down during the time of experiment. As a result, the As results presented should only be used for comparison purposes as the accuracy of the absolute results may not be too high.

Table 4.19 Trace metals concentration in the influent and effluent for each of the geochemistry columns

			Al	*As*	*Cu*	*Fe*	*Mn*	*Se*	*Zn*
UF	Influent	Conc.	0.149	0.043	0.013	0.050	0.029	0.005	0.032
	(78)	St. Dev.	0.168	0.032	0.011	0.018	0.016	0.003	0.020
	Effluent	Conc.	0.133	0.053	0.010	0.036	0.031	0.004	0.023
	(131)	St. Dev.	0.152	0.046	0.009	0.025	0.006	0.004	0.016
SE	Influent	Conc.	0.169	0.048	0.014	0.063	0.034	0.007	0.046
	(78)	St. Dev.	0.159	0.034	0.007	0.021	0.014	0.004	0.013
	Effluent	Conc.	0.160	0.044	0.012	0.038	0.023	0.005	0.024
	(131)	St. Dev.	0.163	0.034	0.008	0.024	0.008	0.003	0.014
RO	Influent	Conc.	0.128	0.045	0.013	0.015	0.005	0.007	0.008
	(78)	St. Dev.	0.155	0.036	0.009	0.005	0.003	0.005	0.005
	Effluent	Conc.	0.136	0.053	0.009	0.019	0.006	0.006	0.008
	(131)	St. Dev.	0.169	0.036	0.008	0.011	0.006	0.004	0007
Control	Influent	Conc.	0.136	0.033	0.010	0.024	0.122	0.006	0.022
	(9)	St. Dev.	0.079	0.018	0.007	0.011	0.003	0.006	0.016

The previous discussions have been revolved around the chemical quality of the effluent, without addressing the potential problem of clogging. **Figure 4.28** shows the turbidity results for the influent and effluent for each of the geochemistry columns. The turbidity was observed to increase significantly at the initial stage, possibly caused by flushing out of the fines in the sand column, but thereafter decreased with time. With the exception of the SE column, the effluent's turbidity results were always higher than the influent, contrary to the expectation that the sand column would act as a sand filter. This could be due to the aggressive nature of both the UF and RO effluents, in which

the dissoluted fines were washed out of the column. In contrast, the SE column showed improvement with time and the turbidity was reduced by 50% at the end of the experiment. The aggressive nature of UF and RO had to be taken into consideration if it was to be selected as the recharge water in Changi reclaimed land.

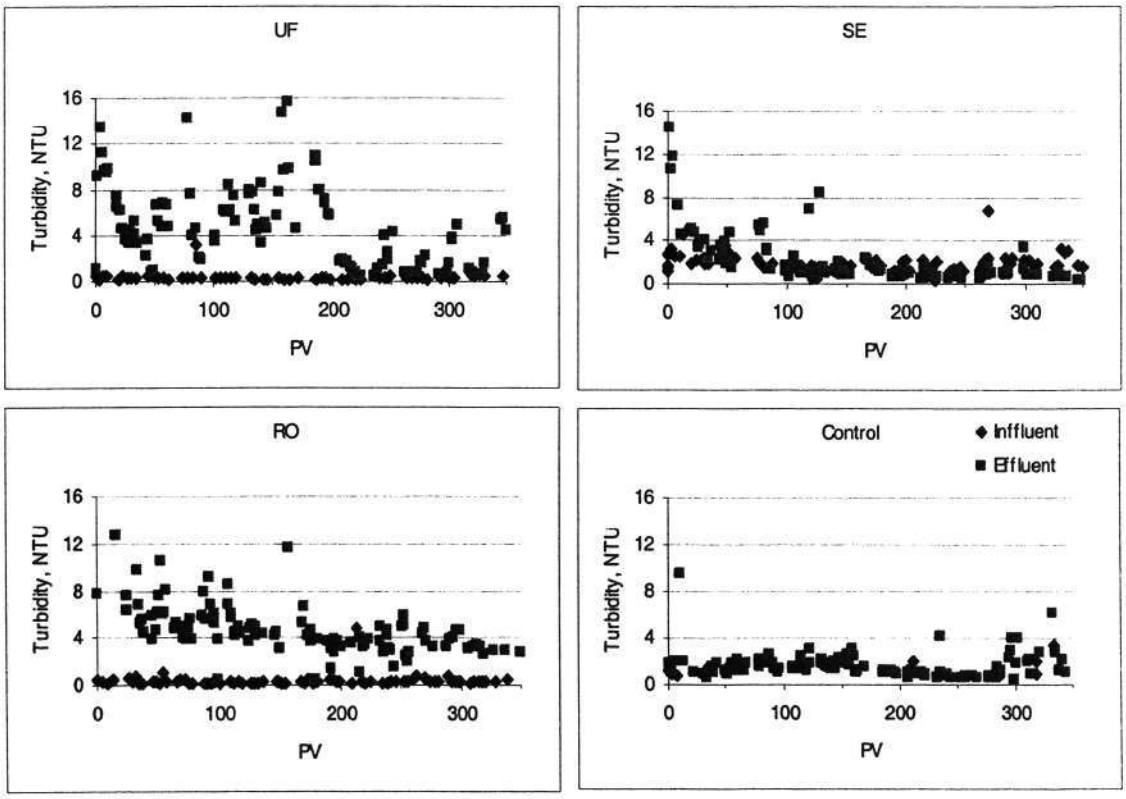

Figure 4.28 Turbidity data for each of the geochemistry columns

There was no significant change in the constantly monitored flow rate also suggesting that the column did not experience serious clogging problem even in the case of SE. However, further experiments should be carried to verify if continuous washing out of fines and dissolute would cause clogging further downstream.

In the following section, the potential of SAT in these short term (6-8 hours retention time) columns could be assess from the test data. **Figure 4.29** shows the results of UVA-254nm for both the influent and effluent of each test column. The results showed an overall reduction in UVA for the UF and SE columns, but otherwise for the RO

column. The UVA for the control column in which groundwater was recirculated did not change against time. There was an initial fluctuation in the UVA data for the first 20 PVs. The reason could be the presence of original groundwater. However, it was more likely due to a delay in the analysis of the samples because the UV-spectrophotometer had broken down during that period of time. From our sensitivity studies, UVA readings were always over estimated if the sample was not analysed within 2 days from the time of sample collection. Therefore, the results for the initial 20 PVs would not be representative.

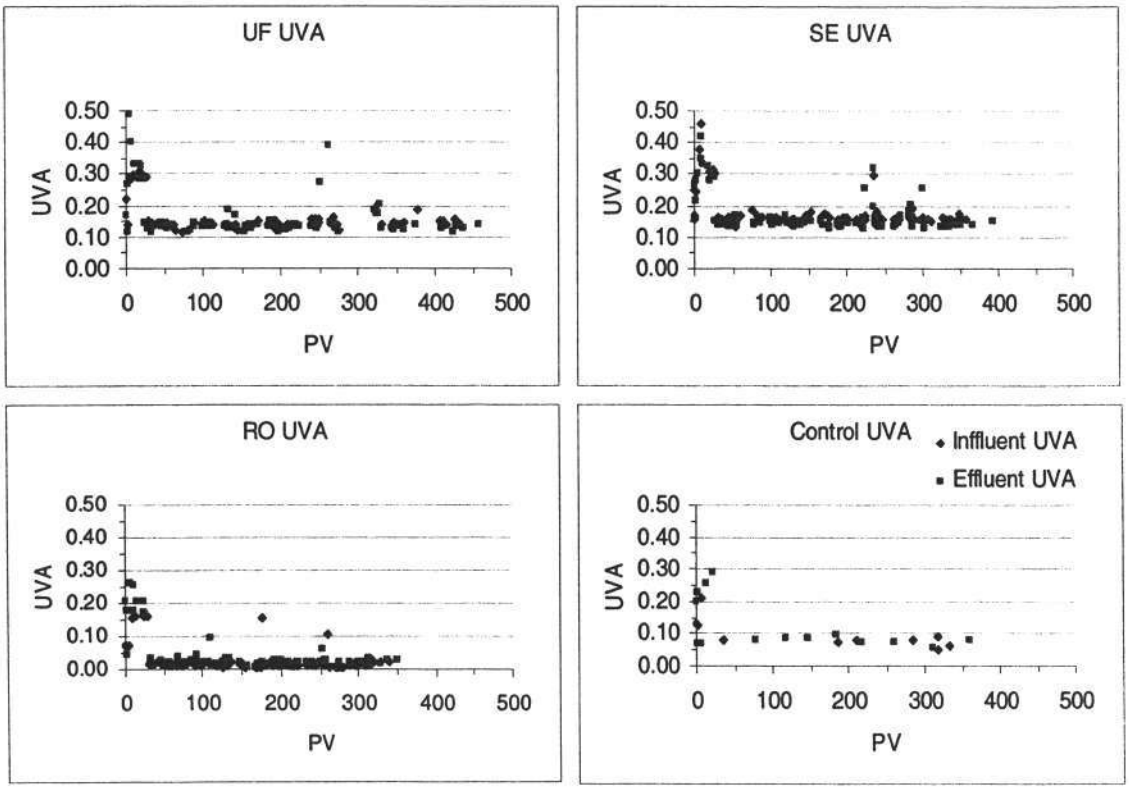

Figure 4.29 UVA-254 nm data for each geochemistry columns

The UVA results were re-plotted in **Figure 4.30** using a different scale. The average removal of UVA was from 10-13 %. The results showed great potential as the HRT was only 6.10 hours for the UF column and 6.62 hours for the SE column. Although the columns were designed for geochemistry analysis in which the emphasis was the number of exchanges of PV instead of the HRT, it had provided an indication of the potential of SAT in a sand medium.

The RO column showed peculiar behaviour as the UVA increased rather than decreased as it was passed through the column. There was no definite explanation for this observation though the readings were quite low in the range of 0.005-0.03 cm^{-1}. This highlighted the fact that RO, being the cleanest and hence the most aggressive, would have greater effects in term of geochemistry, but minimum effects in term of SAT due to its cleanliness. As a result, RO could be considered as a candidate for ASR if storage of water was the main concern.

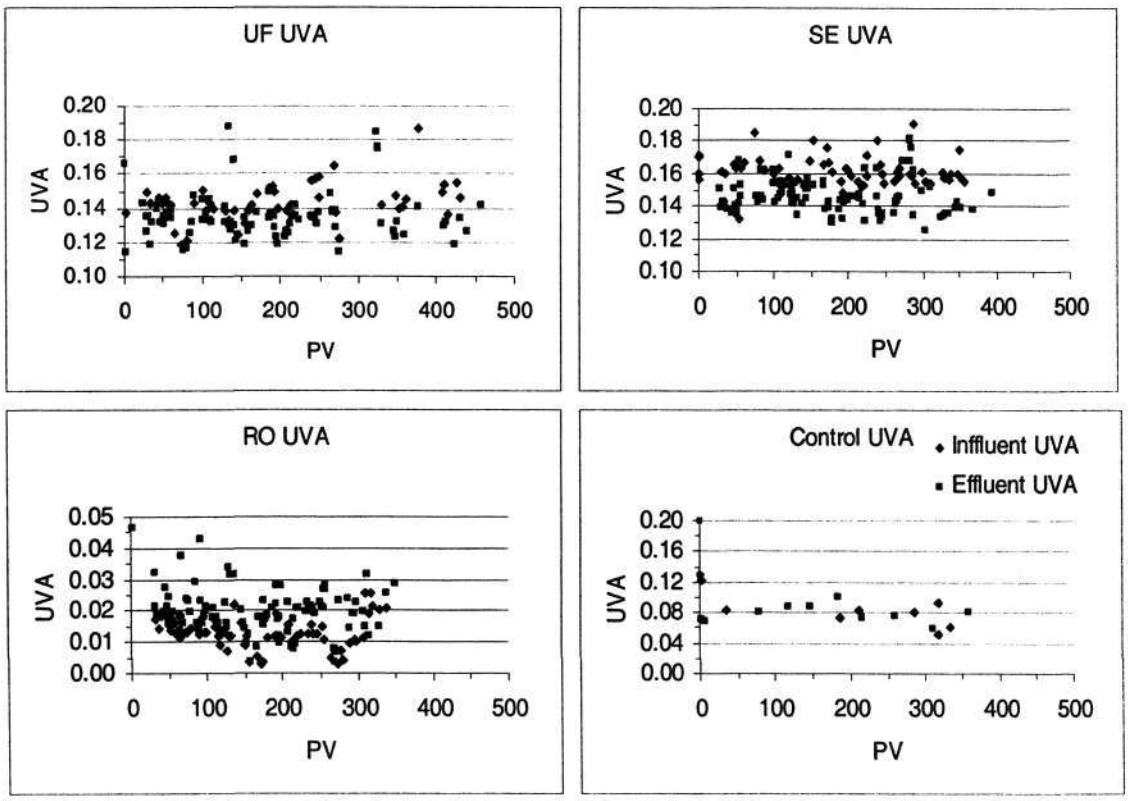

Figure 4.30 UVA at 254 nm data for each geochemistry columns (enlarged scale)

Another important parameter to gauge the effectiveness of SAT was DOC. **Figure 4.31** shows the fate of DOC in these columns. The trend was similar to that of UVA. The RO column again showed no removal of DOC. There was greater removal of DOC compared with UVA in the SE and UF columns. The DOC removal efficiency was about 21 % for SE and about 18 % for UF. There was an indication of acclimatisation taking place for the SE column as the influent and effluent DOCs appeared to be

diverging when plotted against the cumulative PV. However, the experiments was stopped before any clearer trend developed.

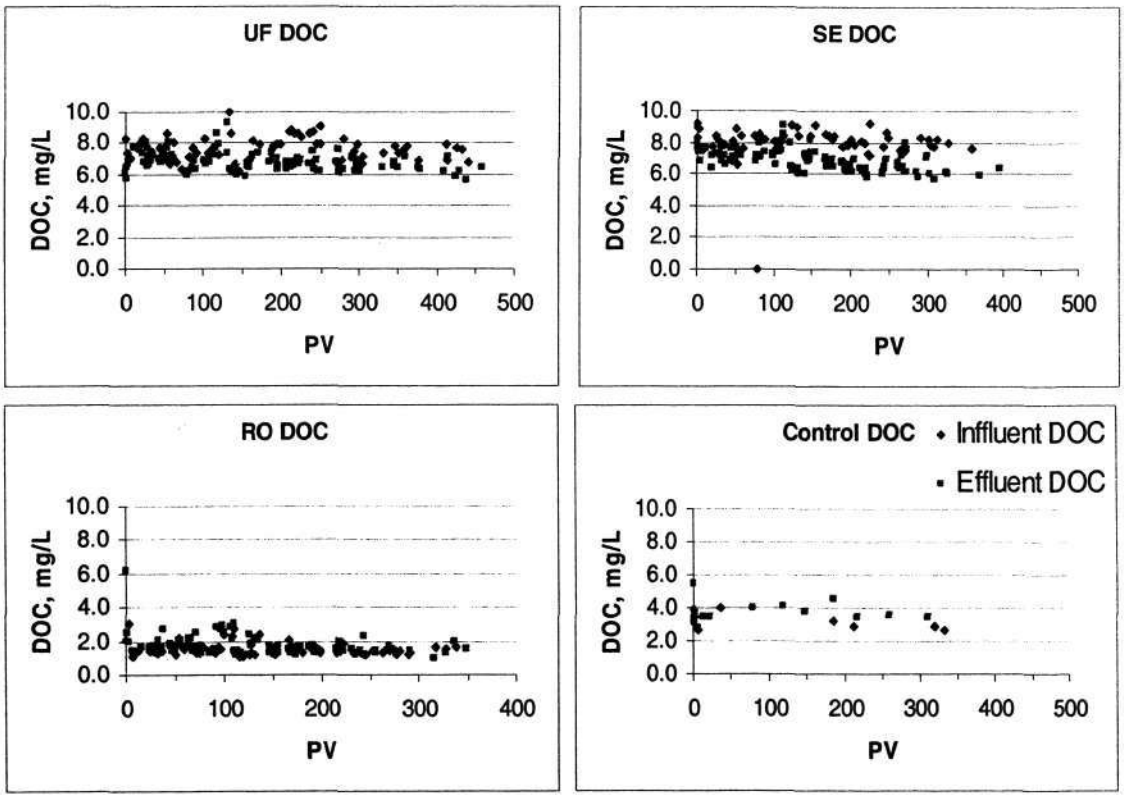

Figure 4.31 DOC data for each geochemistry column

Figure 4.32 shows the specific ultra-violet absorbance (SUVA) against PV. As SUVA is quantified by the ratio of UVA/DOC, the SUVA value of the effluent was found to be higher given the fact that DOC removal was higher than that of UVA. A higher SUVA after treatment signified that removal of the fulvic/humic acid components of the recharge water was not as efficient as the removal of the other hydrocarbons of lesser molecular weight.

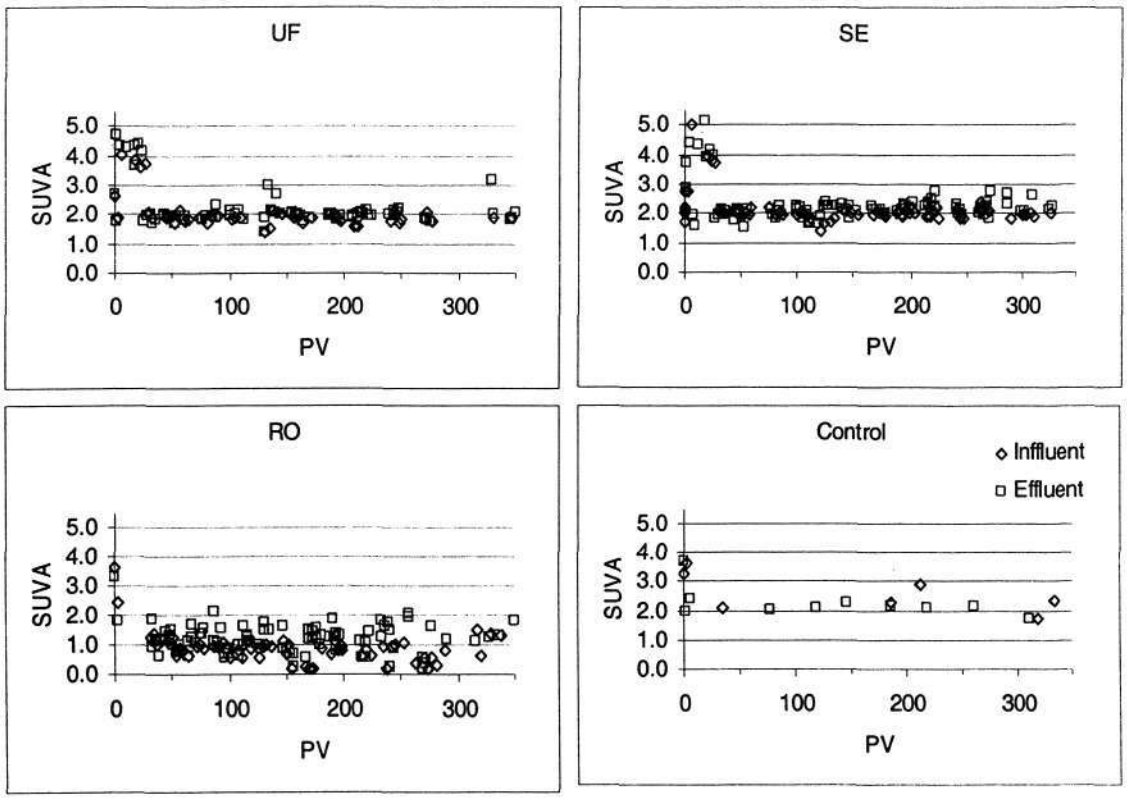

Figure 4.32 SUVA data for each geochemistry columns

5 CONCLUSION AND RECOMMENDATIONS

5.1 Conclusion

A comprehensive set of experiments was carried out to investigate the geochemical effects during ASR operations using several types of recharge water. The quality of the existing groundwater at the Changi reclaimed land, rain water and potential recharge waters were analysed. The mineralogy of the fill material at the reclaimed site was also examined. Batch tests were carried out using sand samples collected from various depths at the site. Short term studies on geochemistry effects during ASR operation with RO water, with focus on the geochemical transformations during the first PV of recharge, were carried out both in laboratory columns and in a field scaled RO injection experiment. Four laboratory columns were also set up to investigate the medium to long term effects of geochemical transformations under continuous recharge using different type of treated waste effluents, including tertiary treated water.

The mineralogy studies indicated that the fill media used for reclamation were medium to coarse sand with 60-65 % quartz and 25-30 % carbonaceous minerals. The nature of the mineral assemblage meant the fill media could be a huge reservoir of carbonate source for dissolution. This was proven to be the case in all the experiments.

The different potential recharge waters investigated in this study were deemed to be suitable for recharging the reclaimed land. The natural rainfall precipitation, RO, UF and SE, met the USEPA Drinking Water Standards for most quality parameters before and after recharge and recovery, with the exception of total dissolved solids for SE.

Batch tests were carried out to investigate the maximum leachability of the sand media from different depths of the site with different types of recharge water. The results were compared with the potable water quality of Anaheim, California, and were found to be comparable. The carbonate derivatives were the dominant ions in the leachant as expected. Several trace metal ions like aluminium, chromium and selenium had

marginally higher concentrations than those of Anaheim, but were still within the permissible limits of USEPA standards.

The short term column study and the field RO injection test showed that both carbonate dissolution and ion exchange were significant geochemical effects when one PV of RO effluent was passing through the sand column. Carbonate dissolution was especially dominant throughout the experiment while ion exchange reaction faded off at around 1.5 PV in the laboratory column. In the field study, ion exchange was still dominant when the experiment ceased. This could be due to the limited exchangeable ions in the laboratory column as the amount of sand was limited by the size of the column. There was no such restriction in the field and ion exchange could be a major concern if the ASR scheme was to be carried out in the field.

Medium term laboratory column studies were also carried out to supplement the results of the short term experiments. Approximately 400 exchanges of PV were passed through each medium term column. The results clearly showed persistent carbonate dissolution. Ion exchange effect was not detected as not enough data were available during the first few PVs. Trace metal contaminants were detected only during the first 10 PV as the columns experienced a "washing out" effect. In conclusion, the limited amount of sand in the column did not allow long term monitoring of ion exchange effects and leaching of heavy metals. In this regard, batch tests could provide better results for such studies.

Clogging was not likely to be a major concern as the medium term columns did not experience a drop in the flow rate. The turbidity of SE decreased significantly as it passed through the sand column, as the sand column had effectively functioned as a sand filtration bed, but periodic flushing out of fines were observed in the UF and RO columns, probably due to the breaking down of the partially dissoluted carbonaceous soil matrix. Therefore, more experiment should be carried out to look into the operational problems if UF or RO was chosen as the recharge water.

The potential for SAT was demonstrated in the medium term column studies in which both the UF and SE columns experienced a removal efficiency of 10 to 13 % for UVA, and 18 to 21 % for DOC. With a retention time of only about 6.10 and 6.62 hours respectively for the UF and SE columns, the removal efficiency was quite encouraging.

5.2 Recommendations

Several modifications could have further improved the quality of the experiments and are recommended in any future studies as follows:

- A longer column should be used to increase the retention time as well as the sand holding capacity. An increase in column length will allow better observation of the potential problem of clogging as most of the dissoluted fines were washed out rather than accumulate further downstream. An increase in sand holding capacity could facilitate the investigation of ion exchange and sorption/desorption effects;
- The recharge water used was rather aggressive and should be conditioned to a pH value of around 8.0. This will help to reduce dissolution and prolong the sustainability of the aquifer;
- Tracer test should be carried out before and after the experiment together, as well as during the course of experiments, in order to observe any change in porosity.
- The head difference along the column should be measured throughout the course of the experiment. This exercise was abandoned in the tests as the pressure head was too high inside the column such that the manometer could not work properly. An investment in pressure gauges could solve this problem
- Scanning electron microscope could be adopted to observe the micropore structure of the sand before and after the experiment. This could help to confirm the occurrence of dissolution and ion exchange effects.
- Analysis of arsenic should be conducted using the atomic adsorption spectrometry (AAS) instead of inductively coupled-plasma spectrometry (ICP);

BIBLIOGRAPHY

Allard, B. (1995), "Groundwater", CRC Press, Atlanta, GA.

Amy, G. L., Wilson, L. G., Conroy, A., Chahabandour, J., Zhai, W. and Siddiqui, M. (1993). "Fate of chlorinated byproducts and nitrogen species during effluent recharge and soil aquifer treatment (SAT)", Water Environ. Res., Vol. 65, pp. 726-734.

Anderson, M. S., Jacobsen, V. N. R. and Postma, D. (2005), "Geochemical processes and solute transport at the seawater/freshwater interface of a sandy aquifer", Geochimica et Cosmogeochimica Acta, Vol. 69(16), pp. 3979-3994.

Appelo, C. A. J. (1994), "Cation and proton exchange, pH variations and carbonate reactions in a freshening aquifer", Water Resourse Research, Vol. 30, pp. 2793-2805.

Appelo, C. A. J. and Postma, D. (1996), "Ion exchange and sorption. in g*eochemistry*", Groundwater and Pollution, pp. 142–201.

ASTM D2487-00. (2000), "Standard Classification of Soils for Engineering Purposes (Unified Soil Classification System)", American National Standards Institution.

Azadpour-Keeley, A., Keeley, J. W., Russell, H. H. and Sewell, G. W. (2001), "Monitored natural attenuation of contaminants in the subsurface: processes", Ground Water Monitoring and Remediation, Vol. 20(2), pp. 97-107.

Baker, L. A., Qureshi, T. and Wyman, M. (1998). "Sources and fate of arsenic in the salt and Verde Rivers, Arizona", Water Resour. Res. Vol. 34, pp. 1543-1552.

Barcelona, M. J., Holm, T. R., Schock, M. R. and George, G.K. (1989), "Spatial and temporal gradients in aquifer oxidation– reduction conditions", Water Resources Research, Vol. 25(5), pp. 991-1003.

Bianchini, G., Pennisi, M., Cioni, M., Cerbai, N. and Kloppmann, W. (2005), "Hydrogechemistry of the high-boron groundwaters of the Cornia aquifer (Tuscany, Italy)", Geothermics, Vol. 34, pp. 297-319.

Bishop, P. K. and Lloyd, J. W. (1990), "Chemical and isotopic evidence for hydrogeochemical processes occurring in the Lincolnshire limestone", Journal of Hydrolpgy, Vol. 121, pp. 293-320.

Bjerg, P. L. and Christensen, T. H. (1992), "Spatial and temporal small-scale variation in groundwater quality of a shallow sandy aquifer", Journal of Hydrology, Vol. 131, pp. 133-149.

Bouwer H., Pyne G. and Goodrich J. (1990), "Recharging groundwater". Civil Eng., June, pp. 63-66.

Bouwer, H., Lance, J. C. and Riggs, M. S. (1974). "High rate land treatment II: water quality and economic aspects of the flushing meadows project", Journal Water Pollut. Control Fed, Vol. 46, pp. 844-859.

Bouwer, H., Rice, R. C. (1984). "Renovation of wastewater at the 23rd avenue rapid infiltration project", Journal Water Pollut. Control Fed, Vol. 56, pp. 76-83.

Brown, D. L. and Silvey, W. D. (1977), "Artificial Recharge to a Freshwater-Sensitive Brackish-Water Sand Aquifer, Norfolk, Virginia", U.S. Geological Survey Professional Paper, No. 939.

Brun, A. and Engesaard, P. (2002), "Modelling of transport and biogeochemical processes in pollution plumes: literature review and model development", Journal of Hydrology, Vol. 256(3-4), pp. 211-227.

BS ISO 10390:1994(E), (1994), "Soil Quality – Determination of pH", British Standards ISO.

BS ISO 10693:1995(E), (1995), "Soil Quality – Determination of carbonate content – Volumetric method", British Standards ISO.

BS ISO 10694:1995(E), (1995), "Soil Quality – Determination of organic and total carbon after dry combustion (elementary analysis)", British Standards ISO.

BS ISO 11464:1994(E), (1994), "Soil Quality – Pretreatment of samples for physico-chemical analyses", British Standards ISO.

BS ISO 11466:1995(E), (1995), "Soil quality - Extraction of trace elements soluble in aqua regia", British Standards ISO.

BS ISO 13536:1995(E), (1995), "Soil quality - Determination of the potential cation exchange capacity and exchangeable cations using barium chloride solution buffered at pH = 8.1", British Standards ISO.

Carlyle, H. F., Tellam, J. H. and Parker, K. E. (2003), "The use of laboratory determined ion exchange parameters in the predictive modelling of field-scale major cation migration in groundwater over a 40-year period", Journal of Contaminant Hydrology, Vol. 68, pp. 55– 81.

Chae, G., Kim, S., Yun, S., Kim, K., Kim, S., Choi, B., Kim, H. and Rhee, V. W. (2004), "Hydrogeochemistry of alluvial groundwater in a agricultural area: a implication for groundwater contamination susceptibitlity", Chemispheres, Vol. 55, pp. 369-378.

Chan, H. C. (2004), "Water Quality Transformation During Soil Aquifer Treatment using Changi Fill Material – UF water", Master Thesis, Singapore Stanford Partnership - Graduate studies in Environmental Engineering, Nanyang Technological University.

Chipera, S. J. and Bish, D. L. (2002). "FULLPAT: A Full Pattern Quantitative Analysis Program for X-Ray Diffraction Using Measured and Calculated Patterns", Journal of Appl. Cryst., Vol. 35, pp. 744-749.

Choa, V., Bo, M. W., Arulrajah, A. and Na, Y. M. (1997). "Overview of Densification of Granular Soil by Deep Compaction Methods",. Proceedings of Int. Conf. on Ground Improvement Techniques, 7 – 8 May, 1997, Macau.

Chua, Lloyd H. C. , K. C. Wong, N. Mzila, S. K. TAN, T. T. Lim, J. H. Tay, Lawrence C. C. Koe and James O. L. (2004). "Subsurface injection of RO-treated waste water at a reclaimed land site", Proceedings of the 4th International Symposium on Environmental Hydraulics and the 14th Congress of Asia and Pacific Division, International Association of Hydraulic Engineering and research, vol. 2, pp. 1175-1181.

Cirmo, C. P. and McDonell, J. J. (1997), "Linking hydrologic and biogeochemical controls on nitrogen transport in near-stream zones of temperate-forested catchments: a review", Journal of Hydrology, Vol. 199 (1– 2), pp. 88-120.

Clesciri, L., Greenberg, A. and Eaton, A., (1998), " 4500-No3- I. Cadmium Reduction Flow Injection Method (Proposed)", Standard Method, for the Examination of Water and Waste Water", APHA, AWWA and WEF, 20th ed.

Clesciri, L., Greenberg, A. and Eaton, A., (1998), " 4500-NO_3^- I. Cadmium Reduction Flow Injection Method (Proposed)", Standard Method, for the Examination of Water and Waste Water", APHA, AWWA and WEF, 20th ed.

Clesciri, L., Greenberg, A. and Eaton, A., (1998), "*2520B Electrical Conductivity Method*", Standard Method, for the Examination of Water and Waste Water", APHA, AWWA and WEF, 20th ed.

Clesciri, L., Greenberg, A. and Eaton, A., (1998), "2580B ORP" Standard Method, for the Examination of Water and Waste Water", APHA, AWWA and WEF, 20th ed.

Clesciri, L., Greenberg, A. and Eaton, A., (1998), "3120 B. ICP Method", Standard Method, for the Examination of Water and Waste Water", APHA, AWWA and WEF, 20th ed.

Clesciri, L., Greenberg, A. and Eaton, A., (1998), "*4500-H^+ pH VA*", Standard Method, for the Examination of Water and Waste Water", APHA, AWWA and WEF, 20th ed.

Clesciri, L., Greenberg, A. and Eaton, A., (1998), "4500-O G. Membrane Electrode Method", Standard Method, for the Examination of Water and Waste Water", APHA, AWWA and WEF, 20th ed.

Clesciri, L., Greenberg, A. and Eaton, A., (1998), "4500-SO_4^{2-} G. Methylthymol Blue FIA (Proposed)", Standard Method, for the Examination of Water and Waste Water", APHA, AWWA and WEF, 20th ed.

Clesciri, L., Greenberg, A. and Eaton, A., (1998), "5310 B. High-Temperature Combustion Method", Standard Method, for the Examination of Water and Waste Water", APHA, AWWA and WEF, 20th ed.

Collins, R. and Jenkins, A. (1996). "The impact of agricultural land use on stream chemistry in the Middle Hills of the Himalayas, Nepal", Journal of Hydrology, Vol. 185, pp. 71-86.

Cronin, A. A., Barth, J. A. C., Elliot, T. and Kelin, R. M. (2005), "Recharge velocity and geochemical evolution for the Permo-Triassic Sherwood Sandstone, Northern Ireland", Journal of Hydrology, pp. 1-17.

David, R. Pyne, G. (1995), Groundwater Recharge and Wells- A Guide to Aquifer Storage and Recovery, Lewis Publishers, New York, U.S.

Delgado, A. N., Periago, E. L. and Viqueira, F. D. F. (1997). "Breakthrough of inorganic ions present in cattle slurry: soil column trials", Wat. Res., Vol. 31(11), pp. 2892-2898.

Deutsch, W. J. (1997). Fundamentals and applications to contamination. Lewis Publishers, New York.

Diamond, D. (1995), "Determination of Chloride by Flow injection Analysis Colorimetry (Mercuric Thiocyanate Method)", QuikChem Method 10-117-07-1-I, Lachat Instruments.

Diamond, D. (1996), "Determination of Sulfate by Flow injection Analysis (Turbidimetric Method)", QuikChem Method 10-116-10-1-A, Lachat Instruments.

Diamond, D. (1997), "Determination of Nitrate/Nitrite by Flow injection Analysis Colorimetry", QuikChem Method 10-107-04-1-F, Lachat Instruments.

Drewes, J. E. and Fox, P. (1999). "Fate of natural organic matter (NOM) during groundwater recharge using reclaimed water", Water Sci. Technol., Vol. 40, pp. 241-248.

Drewes, J. E., Fox, P. (1999). "Behavior and characterization of residual organic compounds in wastewater used for indirect potable reuse", Water Sci. Technol., Vol. 40, pp. 391-398.

Edmunds, W. M., Shand, P., Hart, P. and Ward R. S. (2003), "The natural (baseline) quality of groundwater: a UK pilot study", Science of the Total Environmental, Vol. 310, pp. 25-35.

Edwards, M. L. (2002), 2002 Water Quality Report, Anaheim Public Utilities, Anaheim, California.

Elhazabi, M. and Yong, R. N. (2001). "pH influence on sorption characteristics of heavy metal in the vadose zone", Engineering Geology, Vol. 60, pp. 61-68.

Evangelon, V. P. (1998). Environmental soil and water chemistry-Principles and applications. Wiley, New York, U.S.

Farnham, I. H., Johannesson, K. H., Singh, A. K., Hodge, V. F. and Stetzenbach, K. J. (2003), "Factor analytical approaches for evaluating groundwater trace element chemistry data", Analytica Chimica Acta, Vol. 490, pp. 123-138.

Fram, M. S., Bergamaschi, B. A., Goodwin, K. D., Fujii, R., Clark J. F. (2003), "Processes affecting the trihalomethane concentrations associated with the third injection, storage, and recovery test at Lancaster, Antelope Valley, California", March 1998 through April 1999. U.S. Geological Survey Water–Resources Investigations Report 03-4062, Sacramento, California.

Freedman, V.L., Saripalli, K.P., Meyer, P.D. (2003), "Influence of mineral precipitation and dissolution on hydrologic properties of porous media in static and dynamic systems" Applied Geochemistry, 18, pp. 589-606.

Grady, C. P. L. Jr., Harlow, L. J., Reising, R. R. (1972). "Effects of growth rate and influent substrate concentration on effluent quality from chemostats containing bacteria in pure and mixed culture", Biotechnol. And Bioengrg. Vol. 14, pp. 391-410.

Guo, H. and Wang, Y. (2004), "Hydrogeochemical processes in shallow quarternary aquifers from the northern part of the Datong Basin, China", Applied Geochemistry, Vol. 19, pp. 19-27.

Hartog, N., Van Bergen, P. F., De Leeuw, J. W. and Griffioen, J. (2004), "Reactivity of organic matter in aquifer sediments: Geological and geochemical controls", Geochimica et Cosmochimica Acta, Vol. 68, pp. 1281-1292.

Heath, R. C. (1983). "Basic ground water hydrology", United States geological survey water-supply paper 2220.pp.65. USA.

Hem, J. D. (1970). "Study and interpretation of the chemical characteristics of natural water", U.S. Geological Survey Water Supply Paper No.1473, pp.363, Washington, D.C.

Houston, S. L., Houston, W. N. and Spadola, D. J. (1988). "Prediction of field collapse of soils due to wetting", J. Geotech. Eng., Vol. 114, pp. 40-58.

Idelovitch, I. and Michail, M. (1984). "Soil-aquifer treatment-a new approach to an old method of wastewater reuse", Journal Water Pollut. Control Fed, Vol. 56, pp. 936-943.

Johnson, J.S., Baker, L.A., and Fox, P. (1999), "Geochemical Transformations during Artificial Groundwater Recharge: Soil-Water Interactions of Inorganic Constituents" Water Res., Vol. 33, No. 1, pp. 196-206.

Källvenius, G. and Ekberg, C. (2003), "TACK – A Program Coupling Chemical Kinetics with a Two-Dimensional Transport Model in Geochemical Systems" Computers & Geosciences, Vol. 29, pp. 511–521.

Kehew, A. E. (2001), Applied chemical hydrogeology. Prentice Hall.

Klein-BenDavid, O., Gvirtzman, H. and Katz, A. (2005), "Geochemical identification of freshwater sources in brackish groundwater mixtures; the examples of Lake Kinneret (Sea of Galilee), Israel", Chemical Geology, Vol. 214, pp. 45-59.

Krauskopf, K. B. and Bird, D. K. (1995), "Introduction to Geochemistry", 3rd Ed., McGraw-Hill Book Co.

Langford, R., (2004) "Determination of Carbonate Content", Study of Soil in Laboratory, Department of Geological Science, University of Texas.

Langford, R., (2004) "Determination of Organic Content", Study of Soil in Laboratory, Department of Geological Science, University of Texas.

Lim, T. W. (2004), "Geochemical Evaluation of Changi Fill Material for Aquifer Storage and Recover", Master Thesis, Singapore Stanford Partnership - Graduate studies in Environmental Engineering, Nanyang Technological University.

Lunne, T., Robertson, P. K., and Powell, J. J. M. (1997), Cone Penetration Testing in Geotechnical Practice. London: Blackie Academic & Professional.

Maier, W. J. and Conroy, L. E. (1981). "Ultraviolet multiwavelength absorbance measurements for monitoring trace organics in water", Chemistry in water reuse, Cooper WJ (eds), Ann Arbor Science, Ann Arbor, Michigan, Vol. 1, pp. 85-145.

Masscheleyn, P. H., Deluane, R. D. and Patrick W. H. (1991), "Heavy metals in the environment", J. Environ. Qual, Vol. 20, pp. 522-527.

Matthess, G. (1982), The properties of groundwater. Wiley, Canada.

Melo, M. T. C., Marques da Silva, M. A., and Edmunds, W. M. (1999), "Hydrochemistry and flow modelling of the Aveiro Multilayer Cretaceous Aquifer", Phys. Chem. Earth, Vol.24, pp. 331-336.

Mercado, A. (1985), "The use of hydrogeochemical pattern in carbonate sand and sandstone aquifers to identify intrusion and flushing old saline water", Ground Water, Vol. 23, pp. 635–644.

Michail, M. and Idelovitch, E. (1981). "Gross organics measurements for monitoring of wastewater treatment and reuse", Chemistry in water reuse, Cooper WJ (eds), Ann Arbor Science, Ann Arbor, Michigan, (1981), Vol. 1, pp. 35-64.

Mukhopadhyay, A., Al-Awadi, E., Al-Senafy, M. N. and Smith, P. C. (1998), "Laboratory investigations of compatibility of the Dammam Formation Aquifer with desalinated freshwater at a pilot recharge site in Kuwait", Journal of Arid Environments, Vol. 40, pp. 27-42.

Mzila, N. (2003), "Feasibility of Utilizing Reclaimed Land at Changi as a Groundwater Source". Ph.D. Thesis, Nanyang Technological University.

Nadler, A., Magaritz, M., and Mazor, E. (1980), "Chemical reactions of seawater with rocks and freshwater: experimental and field observations on brackish waters in Israel", Geochimica Cosmochimica Acta, Vol. 44, pp.879–886.

Nellor, M. H., Baird, R. B., Smyth, J. R. (1984). "Health effects study final report", County Districts of Los Angeles County, Whittier, CA, March, Vol. 1-22.

Norris, R. (1999), "Overview of papers: historic perspective on the development of the slow-release concept. In: Koenigberg, S., Norris, R. (Eds.), Accelerated bioremediation using slow release compounds: selected Battelle Conference papers, 1993 – 1999", Regenisis Bioremediation Products, San Clemente, CA, pp. xxi–xxviii.

Ortega-Guerrero, A. (2003), "Origin and geochemical evolution of groundwater in a closed basin clayey aquitard, Northen Mexico", Journal of Hydrology, Vol. 284. pp. 26-44.

Parkhurst, D.L. and Appelo, C.A.J. (1999), "User's Guide to PHREEQC (Version 2) - A Computer Program for Speciation, Batch-Reaction, One-Dimensional Transport, and Inverse Geochemical Calculations"

Parkhurst, D.L. and Petkewich, M.D. (2002), "Geochemical Modeling of an Aquifer Storage Recovery Experiment, Charleston, South Carolina" In Proceedings of the U.S. Geological Survey Artificial Recharge Workshop, Sacramento, California, 2-4 April 2002.

Pavelic, P., Dillon, P. J., Martin, R. R., Traegar, B. and Simmons, C. T. (2001), "Multiscale permeability characterisation of a confined carbonate aquifer targeted for aquifer storage and recovery", In: Seiler, K.-P., Wohnlich, S. (Eds.), Proc IAH XXXI Congress: New Approaches to Characterising Groundwater Flow, Swets and Zeitlinger, Lisse, ISBN: 902 651 848 X, pp. 859– 862.

Pavelic, P., Nicholson, B. C., Dillon, P. J. and Barry, K. E. (2005), "Fate of disincfection by-products in groundwater during aquifer storage and recovery with reclaimed water", J. Contam. Hydrol, Vol. 77, pp. 351-373.

Quanrud, D. M., Arnold, R. G., Wilson, L. G. and Conklin, M. H. (1996). "Effect of soil type on water quality improvement during soil aquifer treatment", Water Sci. Technol., Vol. 33, pp. 419-431.

Quanrud, D. M., Arnold, R. G., Wilson, L. G., Gordon, H. J., Graham, D. W. and Amy, G. L. (1996). "Fate of organics during column studies of soil aquifer treatment", Journal of Environ. Engrg., pp. 314-321.

Quanrud, D. M., Carroll, S. M., Gerba, C. P. and Arnold, R. G. (2001). "Virus removal during simulated soil-aquifer treatment", Water Research, Vol. 37, pp. 753-762.

Quanrud, D. M., Hafer, J., Karpisak, M. M., Zhang, J., Lansey, K. E. and Arnold, R. G. (2003). "Fate of organics during soil-aquifer treatment: sustainability of removals in the field", Water Research, Vol. 37, pp. 3401-3411.

Rebhun, M. and Manka, J. (1971). "Classification of organics in secondary effluents", Environ. Sci. and Technol., Vol. 5, pp. 606-609.

Reckhow, D. A. and Singer, P. C. (1984). "The removal of organic halide precursors by ozonation and alum coagulation", Journal Am. Water Works Association, Vol. 76, pp. 151-157.

Rivett, M. O., Feenstra, S., Cherry, J. A. (2001). "A controlled field experiment on groundwater contamination by a multicomponent DNAPL: creation of the

emplaced-source and overview of dissolved plume development", J. Contam. Hydrol. Vol. 49, pp. 111 –149.

Roberts, P. V., Schreiner, J., Hopkins, G. D. (1982), "Field study of organic water quality changes during groundwater recharge in the Palo Alto Baylands", Water Res., Vol. 16, pp. 1025–1035.

Ronen, D., Magaritz, M., Gvirtzman, H. and Garner, W. (1987), "Microscale chemical heterogeneity in groundwater", Journal of Hydrology Vol. 92, pp. 173-178.

Saaltink, M.W., Ayora, C., Stuyfzand, P.J. and Timmer, H. (2003), "Analysis of a Deep Well Recharge Experiment by Calibrating a Reactive Transport Model with Field Data", Journal of Contaminant Hydrology, Vol. 65, pp. 1-18.

Saleh, A., Al-Ruwaih, F. and Shehata, M. (1999), "Hydrogeochemical processes operating within the main aquifer of Kuwait", Journal of Arid Environments, Vol. 19, pp. 195-209.

Schulmeister, M. K., Healey, J. M., Butler Jr., J. J. and McCall, G. W. (2004), "Direct-push geochemical profiling for assessment of inorganic chemical heterogeneity in aquifers", Journal of Contaminant Hydrology, Vol. 69, pp. 215-232.

Singer, P. C. (1999). "Humic substances as precursors for potentially harmful disinfection by-products", Water Sci. Technol., Vol. 40, pp. 25-30.

Singer, P. C., Barry, J. J. III, Palen, G. M. and Scrivner, A. E. (1981). "Trihalomethane formation in North Carolina drinking waters", Journal Am. Water Works Association, Vol. 73, pp. 392-401.

Sivan, O., Yechieli, Y., Herut, B. and Lazar, B. (2005), "Geochemical evolution and timescale of seawater intrusion into the coastal aquifer of Israel", Geochimica et Cosmochimica Acta, Vol. 69(3), pp. 579-592.

Snyder, M., Tailefert, M. and Ruppel, C. (2004), "Redox zonation at the saline-influenced boundaries of a permeable surficial aquifer: effects of physical forcing on the biogeochemical cycling of iron and manganese", Journal of Hydrology, Vol. 296, pp. 164-178.

Stumm, W. (1992). Chemistry of the Solid-water Interface: Processes at the Mineral-Water and Particle-Water Interface in Natural Systems, John Wiley and Sons, Inc., New York.

Tan, S. K., Lloyd, H. C. Chua, Mzila, N., Tay, J. H., Lawrence, C. C. Koe. (2004), "Measurement of hydraulic conductivity in a sand-fill", Proceedings of 6th Int. Conf. on Hydroscience and Engineering (ICHE-2004), May 30-June 3, Brisbane, Australia.

Tesoriero, A. J., Spruill, T. B. and Eimers, J. L. (2004), "Geochemistry of shallow ground water in coastal plain environments in the southeastern United States: implications for aquifer susceptibility", Applied Geochemistry, Vol. 19, pp. 1471-1482.

V. Metz, V., Kienzler, B. and Schu¨ßler, W. (2002), "Geochemical evaluation of different groundwater–host rock systems for radioactive waste disposal", Journal of Contaminant Hydrology, Vol. 61, pp. 265– 279.

Van Breukelen, B.M., Griffioen, J., Röling, W.F.M. and Van Verseveld, H.W. (2004), "Reactive Transport Modelling of Biogeochemical Processes and Carbon Isotope Geochemistry inside a Landfill Leachate Plume", Journal of Contaminant Hydrology, (article in press).

Van Der Lee, J. and De Windt, L. (2001), "Present State and Future Directions of Modeling of Geochemistry in Hydrogeological Systems", Journal of Contaminant Hydrology, Vol. 47, pp. 265-282.

Vanderzalm, J. L., Le Gal La Salle, C., Hutson, J. L. and Dillon, P. J. (2002), "Water quality changes during aquifer storage and recovery at Bolivar, South Australia", In: Dillon, P.J. (Ed.), Management of Aquifer Recharge for Sustainability Proceedings of the 4th International Symposium on Artificial Recharge, Adelaide Sept 22–26, 2002. Swets and Zeitlinger, Lisse, ISBN: 90 5809 527 4, pp. 83– 88.

Whittemore, D. O. (1995), "Geochemical differentiation of oil and gas brine from other saltwater sources contaminating water resources: case studies from Kansas and Oklahoma", Environmental Geosciences, Vol. 2(1), pp. 15-31.

Wiedemeier, T. H., Swanson, M. A., Moutoux, D. E., Gordon, E. K., Wilson, J. T., Wilson, B. H., Kampbell, D. H., Miller, R. N., Hansen, J. E. and Chapelle, F. H. (1995), "Technical protocol for evaluating natural attenuation of chlorinated solvents in ground water", U.S. EPA 600/R-98/128, National Risk Management Research Laboratory, Cincinnati, OH.

Wilson, L. G., Amy, G. L., Gerba, C. P., Gordon, H., Johnson, B. and Miller, J. (1995). "Water quality changes during soil aquifer treatment of tertiary effluent", Water Environ. Res., Vol. 67, pp. 371-376.

Yong, R. N., Yaacoob, W. Z. W., Bently, S. P., Harris, C. and Tan, B. K. (2001). "Partitioning of heavy metals on soil samples from column tests", Engineering Geology, Vol. 60, pp. 307-322.